

Universität Potsdam
Institut für Geoökologie

HYDROLOGIC MODELING OF AN ARCTIC WATERSHED, ALASKA



Diplomarbeit
vorgelegt von Imke Schramm
April 2005

Betreuer: Dr. Julia Boike, Prof. Dr. Axel Bronstert

TABLE OF CONTENTS

Abstract	iii
Zusammenfassung	iv
List of Figures	vi
List of Tables	viii
Acknowledgements	ix
1. Introduction	1
1.1 Background.....	1
1.2 Literature review: previous studies with models.....	6
1.3 Objectives.....	8
2. Study area	9
2.1 Climate.....	10
2.2 Hydrology.....	14
2.3 Geology and soils.....	19
2.4 Vegetation.....	20
3. Data collection	21
3.1 Meteorological Data.....	22
3.2 Hydrological Data.....	24
3.3 Soil Data.....	26
3.4 Snow Data.....	29
4. Modeling	30
4.1 The Digital Elevation Model.....	30
4.2 Model description of TopoFlow.....	34
4.3 Calibration / Parameterization.....	45

5. Results	53
5.1 Observed meteorological variables and hydrological processes.....	55
5.2 Hydrograph Analysis.....	63
5.3 Snowmelt Analysis.....	69
5.4 Water balance.....	71
5.5 Reproduction of hydrological processes in the model.....	76
5.6 Simulation of future climate changes.....	84
6. Summary and conclusions	87
References	I
Appendix A: List of	
Symbols	VIII
Appendix B: Eidesstattliche Erklärung	IX

Abstract

This study presents the application of the hydrological model TopoFlow to the Innavait Creek watershed, a small arctic headwater basin in northern Alaska. This new process-based, spatially distributed model is executed for the years 2001 to 2003. The model is evaluated for its capability to reproduce the different components of the hydrological cycle. Simulations are done for different climate change scenarios to lend insight into the impacts of global change on hydrological processes.

Innavait Creek (~2 km²) is underlain by continuous permafrost and two features characterize the channel network: The stream is beaded, and numerous water tracks are distributed along the hillslopes. These facts, together with the constraint of the subsurface system to the shallow active layer, strongly influence the runoff-response to rain or snowmelt. Climatic conditions vary greatly during the years of this study, providing a good testing of model capabilities. Streamflow is the dominant form of basin water loss (64% of the water budget). In 2001, snowmelt runoff is the dominant runoff event, whereas in 2003, the summer runoff generated by continuous rainfall surpasses the melt discharge. A single and exceptionally high rainfall causes the dominant runoff event in 2002. Water loss due to evapotranspiration achieves considerable amounts, ranging from 28% to 57% of the water budget.

Simulation results indicate that the model performs quantitatively well, and achieves best results in 2002. Measured and predicted cumulative discharges are in a good agreement. The different components of the water cycle are represented in the model, with refinements necessary in the qualitative reproduction of some sub-processes: Snow damming results in later melt discharge than modeled. Nash-Sutcliffe coefficients between 0.3 and 0.9 reveal that the model requires further refinement in the small-scale, short-term reproduction of storage-related processes. The deviations can be attributed to the facts that the beaded stream system, the spatial variability of the active layer depth, and the complex soil moisture distribution are not sufficiently well represented in the model. Furthermore, the model is highly sensitive to the setting of the initial water table.

While various studies document recently observed climate changes, there remains uncertainty of how these changes will impact the hydrological cycle of the Arctic. Depending on the relative increases in temperature and precipitation, this will result in enhanced or diminished runoff and soil moisture. This study suggests that an 8% increase in summer precipitation balances the increased water loss due to evapotranspiration caused by a temperature increase of 2°C.

Zusammenfassung

In der vorliegenden Arbeit wird die Anwendung des hydrologischen Modells TopoFlow im Einzugsgebiet Innavaik Creek (Alaska) vorgestellt. Dieses neue, prozessbasierte und räumlich verteilte Modell wird für die Jahre 2001 bis 2003 angewendet. Das Modell wird nach seiner Fähigkeit beurteilt, die verschiedenen hydrologischen Prozesse nachzubilden. Simulationen werden für unterschiedliche Szenarien des Klimawandels durchgeführt, um Einblick in dessen Einfluss auf die Hydrologie zu gewähren.

Innavaik Creek (~2 km²) liegt im Gebiet des kontinuierlichen Dauerfrostbodens, und zwei Besonderheiten charakterisieren das Flusssystem: Das Fließgewässer besteht aus einer Aneinanderreihung kleinerer Seen, und entlang der Hänge befinden sich zahlreiche mit Büschen bewachsene Abflussbahnen. Diese Faktoren beeinflussen, zusammen mit der Einschränkung des Grundwassersystems auf die flache Auftauschicht, die Abflussantwort auf Regen oder Schneeschmelze. Die jährlich unterschiedlichen klimatischen Bedingungen stellen eine gute Möglichkeit zur Beurteilung des Modells dar. Abfluss ist die wichtigste Form des Wasserverlustes (64% des Wasserbudgets). Im Jahr 2001 ist der Schneeschmelzabfluss das dominierende Abflussereignis, während im Jahr 2003 der Sommerabfluss, hervorgerufen durch kontinuierlichen Regenfall, den Schneeschmelzabfluss übersteigt. Ein einzelnes und ungewöhnlich hohes Regenereignis verursacht das größte Abflussereignis im Jahr 2002. Evapotranspiration erreicht eine beachtliche Höhe von 28% bis 57% des Wasserbudgets.

Das Modell erzielt quantitativ gute Ergebnisse: Kumulierte gemessene und simulierte Abflüsse stimmen gut überein, und die verschiedenen Komponenten des Wasserkreislaufes sind berücksichtigt. Einige Verfeinerungen sind nötig bei der qualitativen Nachbildung von Teilprozessen: Die Dämmung durch Schnee verursacht einen späteren Abfluss als in Modellergebnissen. Nash-Sutcliffe-Koeffizienten von 0,3 bis 0,9 weisen darauf hin, dass die kleinräumige, kurzzeitige Nachbildung speicherbedingter Prozesse verbessert werden kann. Die Abweichungen können der unzureichenden Repräsentation des Flusssystemes, der räumlichen Variabilität der Auftauschicht und der komplexen Bodenfeuchteverteilung zugeschrieben werden. Des Weiteren zeigt das Modell eine hohe Sensitivität gegenüber dem Wasserstand zu Beginn der Simulation.

Während zahlreiche Studien die Veränderungen des Klimas dokumentieren, ist nach wie vor unsicher, wie dieser Wandel den Wasserkreislauf der Arktis beeinflussen wird. Abhängig von den relativen Anstiegen des Niederschlag und der Temperatur werden diese eine Verstärkung oder Abschwächung des Abflusses und der Bodenfeuchte hervorrufen. Simulationsergebnisse

dieser Arbeit legen nahe, dass ein Anstieg von 8% des sommerlichen Niederschlages den Anstieg des Wasserverlustes durch Evapotranspiration, bedingt durch eine Temperaturerhöhung von 2 °C, ausgleicht.

LIST OF FIGURES

Title page	Innavait Creek watershed, December 2001 (source: Larry Hinzman, WERC)	
2.1	Map of Alaska with the location of Innavait Creek.....	9
2.2	Beaded stream system and water tracks.....	15
3.1	Map of Innavait Creek and data collection sites.....	21
3.2	Sceme of the meteorological station Innavait Creek Basin.....	23
3.3	Flume station at Innavait Creek.....	25
3.4	Ablation curves for the Innavait watershed 2001 to 2003.....	29
4.1	Digital Elevation Model of the Innavait Creek watershed.....	32
4.2	Channel network of the Innavait Creek watershed.....	32
4.3	Structure of TopoFlow.....	34
4.4	Processing of the thawing active layer in TopoFlow.....	42
4.5	Simulated ablation using different C_0 -values.....	46
4.6	Simulated ablation using different T_0 -values.....	46
4.7	Simulated evapotranspiration (Priestley-Taylor) using different α_{PT} -values.....	48
4.8	Simulated evapotranspiration (energy balance) using different z_0 -values.....	48
4.9	Evolution of the active layer depth for different α_{TD} values.....	50
4.10	Thaw depth of the active layer 2001 as a model input.....	50
5.1	Water balance components 2001 to 2003.....	55
5.2	Measured discharge at Innavait Flume station 2001 to 2003.....	57
5.3	Cumulative evapotranspiration 2001.....	60
5.4	Cumulative evapotranspiration 2002.....	60
5.5	Cumulative evapotranspiration 2003.....	60
5.6	Daily evapotranspiration rates 2001.....	60
5.7	Daily evapotranspiration rates 2002.....	60
5.8	Daily evapotranspiration rates 2003.....	60
5.9	Measured and simulated hydrograph 2001.....	64
5.10	Measured and simulated hydrograph 2002.....	64
5.11	Measured and simulated hydrograph 2003.....	64
5.12	Measured and simulated cumulative discharge 2001.....	65
5.13	Measured and simulated cumulative discharge 2002.....	65
5.14	Measured and simulated cumulative discharge 2003.....	65
5.15	Measured and simulated snow ablation 2001.....	70
5.16	Measured and simulated snow ablation 2002.....	70
5.17	Measured and simulated snow ablation 2003.....	70

5.18	Simulated cumulative summer discharge 2001 using different maximum depths of thaw.....	78
5.19	Evolution of the water level during the summer simulation 2003 at different locations within the watershed.....	79
5.20	Comparison of observed and simulated water levels during summer 2003 at hillslope and water track sites.....	79
5.21	Simulated cumulative summer discharge 2001 using different initial water table heights.....	80
5.22	Simulated hydrograph using different roughness coefficients (1).....	82
5.23	Simulated hydrograph using different roughness coefficients (2).....	82
5.24	Simulated hydrograph depicting the influence of water tracks.....	83

LIST OF TABLES

3.1 Description of a representative soil profile at the Imnavait watershed.....27

3.2 Summary of the physical properties of soil samples taken at the
Imnavait watershed.....27

3.3 Annual values for the maximum active layer depth at the Imnavait
watershed obtained from CALM grid measurements.....28

4.1 Soil parameters used as model input.....49

4.2 Overland and channel flow parameters used as model input.....51

5.1 Time intervals of snowmelt period and summer period 2001 to 2003.....53

5.2 Monthly averaged meteorological components (air temperature, net radiation,
wind speed, humidity and precipitation).....62

5.3 Annual precipitation (rain and snow) 2001 to 2003.....72

5.4 Components of the annual water budget (runoff, evapotranspiration and
change in storage) 2001 to 2003.....72

5.5 Partitioning of annual precipitation into runoff, evapotranspiration and
change in soil moisture.....74

5.6 Channel flow properties for the simulations depicted in Figures 5.22 and 5.23.....82

5.7 Description of the climate change scenarios used in the model simulations.....85

5.8 Components of the simulated water budget for different climate change scenarios....85

Acknowledgements

I thank my supervisor Dr. Julia Boike for her great scientific and personal support. She always had time and interest for my countless questions, and encouraged me to develop my own ideas. I appreciate her sense of humor and the friendly atmosphere that she created in the institute. Due to her efforts, I was able to spend three months at the University of Alaska, Fairbanks, where Prof. Dr. Larry Hinzman introduced me to the world of arctic hydrology. His enthusiasm for the topic, and his steady interest in my study turned the field and the computer work into a scientific adventure. I thank the various researchers, staff and students at the University of Fairbanks for their support with data and their generous supply of knowledge. Particular recognition is due to Robert Bolton, who helped me many times to understand the details of the model, and Paul Overduin, who spent many hours in preparation of field data. Sincere thanks is due to Prof. Dr. Axel Bronstert, who introduced to me the subject of modeling.

I am deeply grateful for the support of my parents, who made my studies possible. My friends encouraged me, especially near the end of my studies, and helped me with their comments and suggestions. Josh Winestock, who supported me with his patience, his humor, and his corrections in English, merits particular thanks.

1. Introduction

1.1 Background

The arctic system constitutes a unique and important environment with a central role in the dynamics of the earth. The Arctic is inherently a highly dynamic system, yet there is mounting evidence that it is now experiencing an unprecedented degree of environmental change (e.g. IPCC 2001; HINZMAN et al. 2004). Scientists may not agree on the magnitude of change but there is agreement that the earth is changing due to the increase of carbon dioxide in the atmosphere. Research of carbon isotopes suggest that the long term increase in CO₂ in the atmosphere is the result of the burning of fossil fuels. The severity of global warming is still being argued but most scientists agree that the potential impacts may be great (HENGEVELD 1998). Despite sceptical voices, most experts accept the risk of climate change as a serious problem that requires action now.

Many of these changes are linked to the arctic hydrologic cycle and are quite possibly the result of both the direct and indirect impacts of human activities (VÖRÖSMARTY et al. 2001). Understanding the full dimension of arctic change will be a fundamental challenge to the science community in the coming decades. An important aspect of understanding the exchanges of energy between the land and atmosphere is the hydrology. Water represents a large source of energy exchange via transfer of latent and sensible heat. A change in the climate will affect the water balance across the earth.

Permafrost underlies approx. 24% of the exposed land area in the Northern Hemisphere (ROMANOVSKY et al. 2002) making it a significant proportion of the land mass and a crucial component to study and understand. The presence of this permafrost is the primary factor distinguishing arctic from temperate watersheds. Here, the active layer (the layer of soil above the permafrost that thaws in the summer) is shallow, but it plays a crucial role in the hydrology (KANE et al. 2003).

Studies from a variety of disciplines document recent change in the northern high-latitude environment (HINZMAN et al. 2004). Despite the lack of sustained observational time series, and the technical and logistic constraints of researching in the arctic environment,

the qualitative consistency of observed changes make a compelling case that we are seeing large-scale impacts of global processes. The largest temperature increases in recent decades have occurred over Northern Hemisphere land areas from about 40-70 °N. On the basis of proxy sources (e.g. tree rings and varves), OVERPECK et al. (1997) report that arctic temperatures in the 20th century are the highest in the past 400 years. Another study reveals that the Arctic has undergone regional warming rates of 0.5 °C or more per decade over the past century (CHAPMAN et al. 1993). This has induced changes in other hydrometeorological conditions, including an increase in precipitation (SERREZE et al. 2000; WALSH 2000), an intensification of freshwater discharge from major rivers (PETERSON et al. 2002), and an enhancement of evaporative fluxes (SERREZE et al. 2000). Based on available data, annual precipitation, as evaluated for the period 1900-1994, increased over both North America and Eurasia (NICHOLLS et al. 1996). Positive trends are most apparent over Canada north of 55 °N: the annual precipitation as well as snowfall increased up to a 20% during the past 40 years (GROISMAN et al. 1994a). Concurrently, satellite records indicate that Northern Hemisphere annual snow covered area has declined by about 10% since 1972 (GROISMAN et al. 1994b). Studies from Barrow, Alaska, reveal that the annual end of snowmelt shows an increased variability over the last 60 years, with a trend toward markedly earlier snow free season. Furthermore, snow starts to accumulate later in autumn which causes an extended growing season (HINZMAN et al. 2004). Studies have proven generally negative cumulative mass balances for small glaciers over the Arctic as a whole, Canada, Svalbard and Alaska. The Arctic appears to account for about 20% of the estimated 7.4 mm global sea level rise since 1961 due to melt of small glaciers (SERREZE et al. 2000). The impacts of a warming climate on the hydrological processes in the northern regions are already becoming apparent (HINZMAN et al. 2004): Analysis of US Geological Survey (USGS) data from nine stream monitoring stations with long-term records in central northern Alaska reveal statistically significant trends of river runoff: basins with a substantial glacial component consistently display increasing trends of runoff, presumably due to increases in glacier melt; river basins lacking large glaciers tend to show decreasing runoff, probably because evapotranspiration rates have increased faster than increasing precipitation. HINZMAN et al. (2004) point out that the primary control on hydrological

processes is dictated by the presence or absence of permafrost, but is also influenced by the thickness of the active layer and the total thickness of the underlying permafrost. Thus, as permafrost degrades, the interaction of surface and sub-permafrost ground water processes becomes more important. OSTERKAMP et al. (2000) report that extensive areas of thermokarst terrain (marked subsidence of the surface resulting from thawing of ice-rich permafrost) are now developing in the boreal forests of Alaska as a result of climatic change. Thermokarst can occur with warming even in very cold climates, such as the North Slope of Alaska, because the massive body of permafrost ice is very close to the ground surface (HINZMAN et al. 2004). To date, there has been no conclusive evidence of increases in active layer thickness, but the rate of active layer freezing has been slower on the North Slope of Alaska (KANE et al. 2001a). Permafrost temperature increases are reported for Alaska, but not consistent. The USGS has measured permafrost temperatures from deep drill holes in northern Alaska since the late 1940s. Based on data through the mid 1980s, permafrost in this region generally warmed about 2-4 °C (SERREZE et al. 2000). HINZMAN et al. (1992b) report that temperature profiles within the permafrost of the Alaskan North Slope reveal significant warming over the last century. Modeling results show that changes in below ground temperatures can be influenced as much by temporal variations of the snow cover as by changes in the near-surface air temperatures (STIEGLITZ et al. 2003). Concludingly, ASHFORD et al. (2001) show that there is a clear perception among residents of the North American Arctic that the climate of the region has changed in living memory. The basic observations of warmer temperatures, longer growing season, and thinner cover of sea ice have been observed repeatedly by indigenous people throughout the North American Arctic, even before the trends became statistically detectable in local instrument records (KRUPNIK 2002).

General circulation models (GCMs) predict that the effects of anthropogenic greenhouse warming will be amplified in the northern high latitudes due to feedbacks in which variations in snow and sea ice extent, the stability of the lower troposphere and thawing of permafrost play key roles (SERREZE et al. 2000). The majority of snow-covered lands lie north of 50 °N. Through the temperature-albedo feedback mechanism, changes in snow cover are expected to contribute to polar amplification of externally-driven climate

warming. Changes in the high-latitude terrestrial hydrologic budget, including the amount and seasonality of precipitation, evapotranspiration, snow water equivalent, the timing of snow melt, and runoff may influence terrestrial ecosystems (SERREZE et al. 2000).

The exact evaluation of changes in the meteorological conditions is seen to be difficult, but model simulations trend towards the following scenario: Projected warming is greatest for late autumn and winter, largely because of the delayed onset of sea ice and snow cover. Retreat of snow cover and sea ice is accompanied by increased winter precipitation (NICHOLLS et al. 1996). Models predict that the enhanced temperature response of the Arctic to anthropogenic greenhouse forcing will be attended by increases in precipitation during winter, related to higher atmospheric water vapor content and poleward vapor transport (KATTENBERG et al. 1996). In the Arctic, it is predicted that as a climate warms, the active layer will deepen and permafrost will gradually disappear. The changes invoked by the degradation of permafrost will have impacts on the landscape, ecosystems, and the social and economic structure (ROMANOVSKY et al. 2002). Regarding the hydrology, water will be released from the permafrost when it is subjected to enhanced warming. This, in turn, increases the proportion of groundwater input to streams, increasing river and lake temperatures and altering chemical properties. In addition, taliks (a layer of unfrozen soil above the permafrost and below a pond) may form, creating a larger zone available for water storage (KANE et al. 1997). Likewise, thermokarsts may become more abundant, as their presence is an observed result of melting permafrost (HINZMAN et al. 2004). The degradation of permafrost in arctic systems may, as well, have negative impacts on existing infrastructure. Human disturbances to permafrost will be enhanced in a warming climate making it necessary to incorporate climate change in the design of future developments (ROMANOVSKY et al. 2002).

Altogether, it appears that first-order impacts to the Arctic, expected with a warming climate, result from a longer thawing / summer period combined with increased precipitation (IPCC 2001). The longer snow-free season and greater winter insulation produces secondary impacts that could cause deeper thaw of the active layer or greater melt of permanently frozen ice in glaciers and permafrost, increased biological activity

and changes in vegetative communities. Tertiary impacts arise as animals, people and industry respond to the changing ecosystem.

Not only might the climate warming impose major changes on the hydrology of arctic watersheds, but also hydrologic changes may have global implications (HINZMAN et al. 1992b). Those include impacts on the North Atlantic Deep Water (NADW) formation, and positive feedbacks in the carbon cycle and the energy budget that are suspected to further enhance global climate change (HINZMAN et al. 2004). Currently, the tundra acts as a major reservoir of carbon in peat. It is possible that climatic warming may stimulate growth of tundra plants, increasing the amount of carbon in storage. It is also possible that warmer soil temperatures will increase the rate of oxidation of organic compounds in the soil, resulting in a decrease in the amount of stored carbon. The response of the tundra biome will largely depend upon the amount of soil moisture: a wet tundra will continue to store carbon; a dry tundra will release substantial amounts of CO₂ to the atmosphere (HINZMAN et al. 1992b). Besides the uncertainty of the future development, there is evidence that the Arctic is recently experiencing a decline in water availability, providing the conditions for a shift to a net carbon source (HINZMAN et al. 2004). Secondly, earlier snowmelt and later snow accumulation in autumn facilitates an important positive feedback to climate warming: Solar radiation, previously reflected due to the high albedo of the snow, is mostly absorbed on the darker surface warming the ground and the surface boundary layer. Furthermore, an increasing freshwater flux into the Arctic Ocean could destabilize NADW formation and thereby cause a weakening or break-off of the thermohaline circulation (PETERSON et al. 2002; BROECKER 1997).

Quantifying the magnitude of hydrologic change due directly to climate change in the Arctic is seen to be difficult (KANE et al. 2003) because of the limited existing data base. From a quick examination of arctic hydrologic literature, one finds that most studies are of limited duration, many field studies start after snowmelt, most studies concentrate only on one or two hydrologic processes, and the quality of some of the data is compromised because of harsh environmental conditions. Due to the short duration of record, the stochastic variability of the hydrologic data is unknown. Studies report that there exist numerous gaps in the current understanding of basic scientific principles and processes

regarding the water cycle over the entire pan-arctic domain (VÖRÖSMARTY et al. 2001). Facing this challenge, scientists expect that computer models may improve our knowledge, accounting for the fact that observational data are sparse and future changes cannot be evaluated through field measurements. HINZMAN et al. (1992b) point out that the prediction of the eventual character of hydrology in a changed world is extremely difficult. The complex interactions of changing hydrologic and thermal processes would be difficult if not impossible to analyze without the use of detailed computer modeling.

1.2 Literature review: previous studies with models

The majority of land surface models used to study the impacts of climate change have been primarily designed for lower latitudes, and as such, are not capable of realistically simulating the physical processes operating in the extreme climate of the Arctic. However, increasing efforts have been made to adequately model arctic environments over the last two decades. Several modeling studies with varying focuses have been applied to the Alaskan Arctic, where field data from multiple-year-studies are available for some watersheds. In the following, three hydrological models are described that have been successfully applied to the Innavait watershed, the study area of this thesis.

HINZMAN et al. (1992b) studied the potential hydrological response during a period of global warming using the HBV model. The original version of this model was developed in 1975 by the Swedish Meteorological and Hydrological Institute as a conceptual runoff model and modified for cold regions use by BERGSTRÖM (1976). It can simply be described as a reservoir-type model with routines for snowmelt, soil moisture accounting, control of surface and subsurface hillslope runoff response, and a transformation function to handle stream routing (HINZMAN et al. 1992b). The model input data are observations of air temperature, precipitation, and estimates of evapotranspiration. Model output are snowmelt runoff and the entire summer runoff response. Despite of the good congruence of measured and simulated hydrographs, the authors report several shortcomings: First, the thermal model that calculates the soil thawing, and the hydrological model that simulates runoff are not coupled. Therefore, there are no

feedbacks from one to the other. Furthermore, the hydrological model is not mechanistic. And finally, the prediction capability could be improved by incorporating the redistribution of snow by winds and the retardation of runoff by snow damming.

Another model was applied to the Innavait watershed by STIEGLITZ et al. (1999). The simple land surface model TOPMODEL is used to explore the dynamics of the hydrologic cycle operating in arctic tundra regions. The model accounts for the topographic control of surface hydrology, ground thermal processes, and snow physics. This approach relies only on the statistics of the topography rather than the details of the topography and is therefore computationally inexpensive and compatible with the large spatial scales of today's climate models. As such, the model can easily be applied on an arctic-wide basis to explore issues ranging from the delivery of seasonal melt water to the Arctic Ocean to impacts of climate change on the hydrologic cycle. However, the authors report several deficiencies, such as the neglect of the snow heterogeneity and the non-representation of the beaded stream system.

A third modeling study with an application to Innavait Creek is presented by ZHANG et al. (2000). Here, a process-based, spatially distributed hydrological model is developed to quantitatively simulate the energy and mass transfer processes and their interactions within arctic regions (Arctic Hydrological And Thermal Model, ARHYTHM). The model is the first of this kind for areas of continuous permafrost, and consists of two parts: the delineation of the watershed drainage network and the simulation of hydrological processes. The last include energy-related processes such as snowmelt, ground thawing and evapotranspiration. The model simulates the dynamic interactions of each of these processes and can predict spatially distributed snowmelt, soil moisture and evapotranspiration over a watershed as well as discharge in any specified channels. Results from the application of this model demonstrate that spatially distributed models have the potential for improving our understanding of hydrology for certain settings. Nevertheless, the authors point out that an algorithm for snow damming, the usage of a higher resolution, and a better data collection network could improve the model results.

1.3 Objectives

The thesis presented here primarily aims to apply the spatially-distributed, physically based hydrological model **TopoFlow** to an arctic watershed. It first summarizes the hydrologically important processes of Imnavait Creek, a small Alaskan watershed that has been intensely studied. The study then focuses on comparing the physical hydrology, measured and observed in the field, with model results. The model is executed and evaluated for its capability to reproduce the different components of the hydrological cycle. Here, the objective is to provide the groundwork for further refinement of **TopoFlow**. The study aims to provide insight into the different processes and may help to predict what may happen in a climate change scenario. Thereby, it may take a step towards understanding the major changes of arctic hydrology if the climate changes due to global warming.

2. Study area

The Imnavait watershed is a small headwater basin of approx. 2 km², located in the northern foothills of the Brooks Range (68°30' N, 149°15' W), 250 km south of the Arctic Ocean (Figure 2.1). Imnavait Creek flows parallel to the Kuparuk River for 12 km before it joins the Kuparuk River that drains into the Arctic Ocean.

The elevation in this area ranges from 880 m at the outlet to 960 m at the southern headwaters. The area is underlain by continuous permafrost and the topography consists of low rolling piedmont hills. The landscape is characterized by east trending ridges and intervening rolling tundra plains (HINZMAN et al. 1991a; WALKER et al. 1989). Imnavait Creek has been intensively studied since 1985.

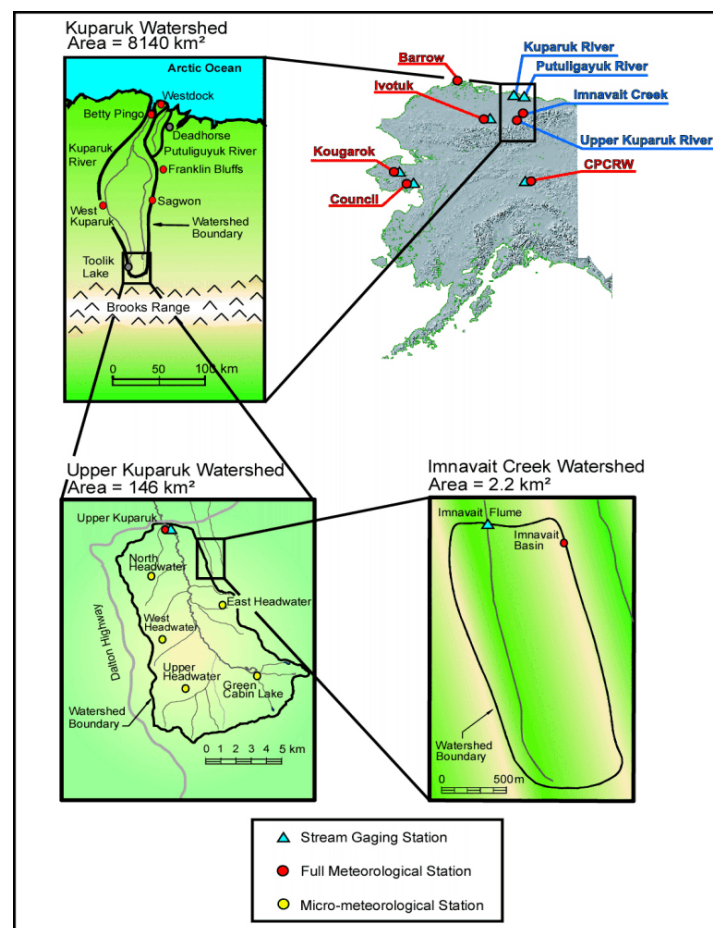


Figure 2.1: Map of Alaska with the location of the study area Imnavait Creek (image courtesy of the Water and Environmental Research Center, University of Alaska, Fairbanks)

2.1 Climate

The Imnavait Creek watershed belongs to the climate region of the polar tundra. According to the classification by Koeppen, polar climates are defined as regions where the mean temperature of the warmest month is below 10 °C, and only 2-4 months have average temperatures above freezing (HUPFER et al. 1996). The Arctic receives much less solar radiation than lower latitudes and also experiences higher annual variation, both of which affect all aspects of arctic hydrological and thermal regimes (HINZMAN et al. 1996).

In the Imnavait Creek watershed, the mean annual temperature averages $-7.4\text{ }^{\circ}\text{C}^1$ (HINZMAN et al. 1996). In January, the average air temperature yields $-17\text{ }^{\circ}\text{C}^2$, whereas it reaches $9.4\text{ }^{\circ}\text{C}^2$ in July (WERC Homepage). Here, the Brooks Range acts as a climatic divide between the colder north-facing, and the warmer south-facing slopes. Temperatures on the north-facing slopes (i.e. also in the Imnavait Creek watershed) are generally 10-15 °C colder throughout the year than those on the south side (NUTALL et al. 2005). The interannual variability in air temperature (expressed as standard deviation of mean monthly temperature) for the winter months is usually $> 3\text{ }^{\circ}\text{C}$, and for the summer months, usually $< 2\text{ }^{\circ}\text{C}$. This difference has been attributed to northward shifts in the arctic frontal zone during the summer (HINZMAN et al. 1996).

The annual precipitation averages 340 mm^1 . Two-thirds of which falls during the summer months of June, July and August (HINZMAN et al. 1996). Here, differences between the south- and the north-facing slopes of the Brooks Range are encountered, as well: The south-facing slopes achieve annual precipitation up to 460 mm, whereas it is generally lower on the north-facing slopes (NUTALL et al. 2005). Most rainfall is light ($82\% < 1\text{ mm h}^{-1}$) and appears evenly distributed over the catchment. Rainfalls are associated with the dissipating phase of convective storms generated over the Brooks Range or with air masses moving from the North Pacific Ocean. Maximum rainfall intensities generally occur in the first 4 to 5 hours of the event. High-intensity

¹ based on records from 1985-1993

² based on records from 1987-2000

(> 20 mm h⁻¹), short-duration rainfall is associated with convective storms which generally occur early in summer (HINZMAN et al. 1996).

Snow distribution and snow pack volumes in the Imnavait watershed are extremely variable both in time (year to year) and space (within the watershed). The spatial distribution is largely a function of wind and topography. At the end of the accumulation season, snow depths can range from a few centimeters on windswept ridgetops to more than 1 m in the bottom of the valley. Snow is redistributed by strong winds during winter time. It is normally deposited in the valley bottom, in small water tracks, and on the lee side of the slopes. The amount of redistribution varies from year to year depending upon the number and magnitude of the wind events. Winter snow accumulation generally starts around mid-September (HINZMAN et al. 1996). However, for comparison with other regions or water balance calculations, it is more common to give values of the water equivalent of the snow pack (SWE). A 20-year-record shows that the annual SWE in Imnavait Creek varies from 69 to 185 mm (BEREZOVSKAYA et al. 2005). Here, snowmelt is initiated between March 1st and March 27th, and is completed within 6-22 days. This reveals a considerable range in timing of snowmelt initiation, which is strongly dependent upon the presence of convective air masses transported to the north over the Brooks Range. The snowmelt is governed by different processes: Shortwave radiation is very near the annual maximum during spring melt. At night, longwave emittance from low clouds and fog can accelerate melt. Concurrently, energy is required to warm the snow pack and the surface organic layer to isothermal conditions prior to melt (HINZMAN et al. 1991b). By analyzing 5-year-subsets, BEREZOVSKAYA et al. (2005) find a trend in the total amount of SWE and the initiation date of snowmelt: In the last 5 years the average SWE increased by 27 mm, compared to the years 1985-1989. For the same time sequences, the snow pack ablated approx. 8-12 days later.

The Imnavait Creek watershed experiences primarily north-flowing katabatic winds that result from downslope drainage of denser air from the Brooks Range to the south. However, large wind events can originate from any direction, causing extensive drifts and wind slabs throughout the watershed. The consistency of predominantly southeast wind yields similar snow distribution each year, i.e., deposition in valley bottoms and on the lee side of slopes (HINZMAN et al. 1996).

About 77% of the annual sunlit hours in the watershed occur between March 21st and September 21st. Incident shortwave radiation is governed by sun angle, but is greatly reduced on cloudy days. Even on clear summer days the low solar angle (maximum at solar solstice is only 45°) means that incoming solar radiation is highly attenuated by the atmosphere. Net radiation becomes positive during daylight in March, and there are some days with a net positive energy balance; however, the magnitude of this gain is quite small. During snowmelt, an obvious increase in net energy is observed as surface albedo and reflected radiation sharply decrease. During midsummer, the net radiation varies around a value of approx. 10 MJ m⁻² day⁻¹ (HINZMAN et al. 1996). Most of this excess energy at the surface is utilized for sensible heat fluxes and evapotranspiration. About 5-20% of the energy is consumed for the thawing of the active layer (the shallow layer of soil above the permafrost that thaws – and then freezes – seasonally as a function of the net energy balance) (HINZMAN et al. 1996; BOIKE et al. 1998). During the summer, a gradual decrease in excess surface energy is seen as the amount of incoming solar energy diminishes. In early September, snow with its high albedo returns and the energy balance at the surface is again similar to late winter conditions (HINZMAN et al. 1991b). In October, the amount of incoming radiation is much less than during the spring thaw, but the net radiation balance is still positive. The primary reason that the heat transfer rate is low during the autumn is because of snowfall. Early-season snow will usually melt soon after touching the surface, which draws energy from the warmer soil surface to melt the snow. As the surface quickly cools to 0 °C and snow begins to accumulate, heat loss slows as the snow provides insulation (HINZMAN et al. 1996). During the winter, arctic tundra climate is affected primarily by radiative heat loss and atmospheric circulation (WELLER et al. 1974; OHMURA 1981). The Imnavait Creek watershed receives no direct solar radiation between December 5th and January 8th, and although several hours of diffuse radiation are incident on each day throughout the winter, the energy input is small. Low incoming radiation and high albedo determine that little energy is input to the active layer (HINZMAN et al. 1996).

Although air temperatures normally reach their annual minimum in January or February, the annual minimum in soil temperature occurs in late March or April. Surface soil warms rapidly by 6-7 °C within a few days in late May or June when solar radiation and

soil heat fluxes are near the annual maximum. The primary reason for the very rapid spring warming of the surficial soil layer is infiltration and freezing of snowmelt water in the still-cold soils and the release of substantial amounts of latent heat. The daily and hourly soil temperature variability is greatest in the summer. This variation decreases with depth. The thermal gradient reverses during freeze-up and spring melt, with the soil at 40 cm being warmer in winter and cooler in summer than the surface soil (HINZMAN et al. 1996).

As seen from the above mentioned relationships, the albedo of the surface is an important factor in determining the amount of energy available. From October to May and before the initiation of snowmelt – normally a few weeks before summer solstice – the tundra surface is characterized by a homogeneous high albedo near 0.8 (WELLER et al. 1974). Due to the uneven distribution of snow, the surface albedo varies greatly as the melt progresses (LISTON 1986). Between the period of spring snowmelt and fall snow accumulation, the tundra surface has its lowest albedo of ca. 0.2, which results in maximum energy exchange. Short-term increases in albedo may occur during midsummer, due to snowfall, which can occur on any day of the year. Initial snow accumulation in the autumn is usually near the equinox, and because solar radiation is considerably less at this time, arrival of new snow cover does not produce the dramatic changes in surface energy and water fluxes that occur during spring-snow ablation (HINZMAN et al. 1996).

Evapotranspiration is, besides runoff, the major process whereby water leaves the basin (HINZMAN et al. 1996). Its seasonal variation greatly depends upon the energy and water supply. Generally, with a relatively impervious barrier so close to the surface, wet conditions exist in the active layer near the surface which provides the conditions suitable for substantial evapotranspiration during the summer thawing months (KANE et al. 1989). Evapotranspiration is greatest after snowmelt and usually even exceeds precipitation, indicating a watershed drying. Evapotranspiration rates decrease throughout the summer, and the soil is recharged with water. Evapotranspiration rates also vary in the spatial dimension: On the hillslopes, the rate of evapotranspiration is limited due to the good drainage. Conversely, in the marshy areas of the valley bottom, the free water surface

frequently lies above the soil surface, so that evapotranspiration is only limited by the amount of energy available. KANE et al. (1989, 1990) found the pan evaporation during summer at Innavait Creek equal to 4 mm day^{-1} in average³. The total evapotranspiration amounts to 163 mm year^{-1} , based on measurements for three consecutive years.

2.2 Hydrology

Generally, hydrological processes in the Arctic are similar to hydrological processes in more temperate regions (KANE et al. 1989). However, the presence of permafrost results in marked differences (of discharge) in the response to rainfall or snowmelt (WOO et al. 1983c). As permafrost completely underlies the Innavait Creek watershed, it affects hydrological processes, microclimatology, and thermal regime: Ice-rich mineral soils at the permafrost table act as a barrier, preventing percolation from snowmelt or summer rains into deep groundwater; hence, the contribution to base flow from below the permafrost table is zero, effectively simplifying the hydrological dynamics. Because water is not lost to deep groundwater recharge, all water leaves the basin either through near-surface runoff or evapotranspiration (HINZMAN et al. 1996)⁴.

Innavait creek is a north draining, first order stream on the 1:63,360 USGS topographic map (WERC Homepage). The stream is beaded, meaning that the channel connects numerous interspersed small ponds. These ponds are on the order of 2 m deep and a few meters in length and width (KANE et al. 2000), see Figure 2.2.

³ based on measurements in 1986

⁴ In some places on the North Slope of Alaska (e.g. the adjacent Kuparuk River Basin), deep springs provide water for base flow throughout the year. The Innavait Creek watershed, however, is isolated from this subpermafrost groundwater source.

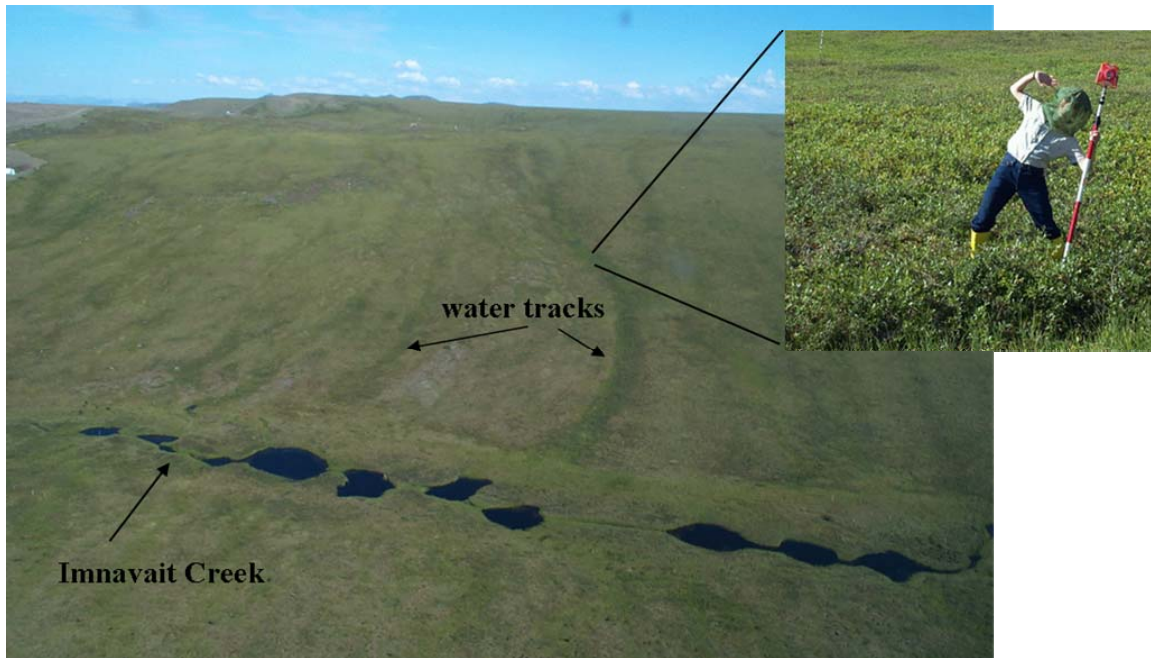


Figure 2.2: Beaded stream system of the Imnavait Creek watershed, July 2004

The headwaters of the creek are found in a nearly level string bog, or strangmoor, with many poorly defined and interconnecting waterways (OSWOOD et al. 1989). Along the hillslopes, small drainage channels, or water tracks, carry water off of the slopes down to the valley bottom (Figure 2.2).

They can be described as shrubby corridors with a width of ~2 m and spaced at ~10-20 m along the hillslope. The water tracks contain a system of interconnected deepenings, or small channels of ~5-10 cm width, that are partly directed parallel to the hillslope. Here, the water flow follows microtopographic features, such as tussocks and hummocks (P. OVERDUIN, personal communication). Although quite obvious in aerial photographs, most of these water tracks are difficult to detect on the ground, except when flowing during snowmelt and major storms because they are not incised (HASTINGS et al. 1989; MCNAMARA 1997). The water tracks generally take the most direct route down the slope but do not connect directly with the stream in the valley bottom. As the slope flattens out in the valley bottom, water moving down the water tracks disperses into numerous poorly defined channels and slowly makes its way over to the creek. Water moves downslope in these water tracks more rapidly than by subsurface means (KANE et al. 1989).

Runoff leaving the basin is usually confined to a period of four months, beginning during the snowmelt period in late May until freeze-up in September. Spring runoff is usually the dominant hydrological event of the year (KANE et al. 1988), producing the annual peak flow, and about 50% of the total annual runoff volume. Streamflow almost ceases after extended periods of low precipitation, whereas intense summer rainfall events produce substantial stream flow (HINZMAN et al. 1996). Whether runoff is produced from rainfall events during the summer depends upon intensity, duration and antecedent soil moisture conditions (KANE et al. 1989). Furthermore, the shape of the hydrograph depends on several factors, such as the state of the active layer, and mechanisms related to the channel network and the snow cover:

First, the role of the snow pack in retarding snowmelt generated runoff is obvious. Snow, redistributed by wind, accumulates in both, water tracks and valley bottoms, where melt water collects. At first, water seeps through the snow as in any porous medium. However, it reaches a degree of saturation when both snow and melt water start to move, cutting a channel through the snow pack. The importance of snow in hindering runoff can be evaluated by measuring the reduction of the snow pack when stream runoff begins. KANE and HINZMAN (unpubl. data) studied this relationship for three consecutive years on the west-facing slopes of the Innvait watershed. They found that the reduction of the water content of the snow pack reached 80% before stream runoff started. This is significant, because this slope represents 78% of the total basin area (KANE et al. 1989).

Another important mechanism is related to the beaded stream system. Here, small ponds that act as small reservoirs can store water intermediately. These ponds receive stream water, retain it, and release it only when full. These are abundant in the beaded stream of Innvait Creek (KANE et al. 1991b; MCNAMARA et al. 1998). Depending on the soil moisture condition this mechanism will result in a delayed hydrograph signal.

Finally, several stream processes are affected by the presence of permafrost, which has a large impact on the runoff response time. This is because the shallow active layer is confined on the bottom by permafrost, which limits the amount of soil water percolation and subsurface storage of water (VÖRÖSMARTY et al. 2001). Thereby, it accelerates the initiation of runoff (MCNAMARA et al. 1998). In addition, response times are shortened because vegetation in these areas tends to be sparse (CHURCH 1974).

Although the response times are much quicker in permafrost basins, the recession time of the stream has been shown to be longer than in basins without permafrost (DINGMAN 1973; MCNAMARA et al. 1998). This circumstance is explained later in this section.

While the soils are described in the next section, the role of the subsurface system and its impact on the runoff signal is explained as follows: DREW (1957) noticed that much of the horizontal flow occurs at the interface of the organic and the mineral soil. This fact refers to the different hydraulic conductivities of the soils: The unfrozen hydraulic conductivities of the organic layer ranges from 3 to 20 times greater than that for the mineral soil (HINZMAN et al. 1991a). Studies have shown that even frozen soils are not impermeable (KANE et al. 1983) and thus frozen ground should be thought of as a soil of low hydraulic conductivity.

The maximum depth of thaw ranges from 25 to 100 cm (HINZMAN et al. 1996), and thus, the ability of the active layer to store large quantities of groundwater is severely limited. In the flat areas, the mineral soil remains nearly saturated the entire year, and thus, changes in soil storage take place in the near-surface organic soils. The amount of water that goes into storage before runoff is produced, only depends upon the moisture levels within the active layer (KANE et al. 1989). The surficial organic layer is quite porous and drains when saturated. In contrast, the underlying mineral soil is usually saturated with water. Thus, the organic soils are immediately responsive to rain events, saturating and draining quickly, whereas the mineral soils have relatively stable moisture contents throughout the summer (HINZMAN et al. 1991a). Summarizing, the antecedent soil water content highly influences the runoff response, and seasonal characteristics of the soil storage capacity are evident in Imnavait Creek:

When snow ablation is occurring, the active layer is completely frozen, and surface runoff is the dominant discharge mechanism. The thawing of the active layer begins when the snow and ice cover are ablated. The initial thaw is rapid, but slows down as the depth of thaw increases (WOO et al. 1983c). Then, the near-surface organic soils with high porosity and low moisture contents readily accept melt water. From laboratory measurements of soil properties and field measurements of soil moisture content, on average about 15 mm of snowmelt water goes into storage in the active layer

(KANE et al. 1989). Due to the excessive water supply from snowmelt, the water table in the flatter areas rises above the ground surface to generate surface flow. Spring is therefore the time when the extent of surface flow is at a maximum. Generally, surface runoff exceeds subsurface flow by 2.5 times⁵ (WOO et al. 1983a). As summer progresses, the soil moisture content is reduced by an increasing depth of thaw and a continued evapotranspiration. This leads to a rapid depletion of the overall soil moisture content, and a non-saturated zone develops in most arctic basins. Occasional heavy rainstorms, however, can revive surface flow (WOO et al. 1983c). KANE et al. (1989) found that during summer, runoff is produced for all storms in excess of 15 mm of precipitation. Late summer and early fall rainstorms provide a recharge of soil moisture. During the winter, some desiccation of the organic soils takes place as an upward flux of water vapor from the soil increases the ice-free void space. However, it can be assumed that the net change from year to year in water storage in the active is not significant (LILLY et al. 1998; WOO et al. 1983b). Soil moisture values are similar from year to year just before freeze-up due to consistent and persistent autumn rainfall saturating the active layer (LILLY et al. 1998).

Recession constants are key characteristics when describing the hydrology of a basin, as it reflects physical features of the watershed (KANE et al. 2003). HOLTAN et al. (1963) found that in temperate regions the recession constant tends to increase with basin size. For regions underlain by permafrost, MCNAMARA et al. (1998) stated that permafrost accelerates the initiation of runoff and reduces the baseflow contribution. The authors studied recession times in Innavait Creek and found that the basin had an average recession time of 30.2 hours. An explanation was given by KANE et al. (2003), who stated that permafrost limits subsurface storage and water is retained in a shallow active layer where pathways are limited to evapotranspiration and runoff. An analysis of streamflow hydrographs (HINZMAN et al. 1993) reveals that, as summer progresses, the recession curves of stream discharge in Innavait Creek following a rain event increase slightly. This observation indicates that more of the soil profile is contributing to runoff in late summer, causing longer recession periods after a storm.

⁵ based on measurements on an arctic hillslope in Canada during spring and summer

2.3 Geology and soils

Innavait Creek is situated in an area of continuous permafrost. Its maximum thickness is estimated between 250 and 300 m (OSTERKAMP et al. 1985). The bedrock is composed of shale, sandstone, conglomerate, limestone and chert of Cretaceous, Triassic and Mississippian ages. The area was glaciated during the Pleistocene. The topography consists of low rolling piedmont hills with a wavelength of 1-2 km and amplitudes of 25-75 m (HINZMAN et al. 1991a). 78% of the basin is west-facing slope, 17% east-facing slope and 5% valley riparian area. Slopes vary from 1% to greater than 13% (KANE et al. 1989).

WALKER et al. (1989) give a detailed description of the terrain, vegetation and landscape evolution of the Innavait watershed. The creek originates in a gently sloping basin which collects water from weakly defined water tracks in the headwaters of the basin. The basin colluvium is generally fine-grained. Organic-rich deposits with variable amounts of granular material present in basins occur between smoothly rounded slopes on the Arctic Slope. The material appears to have moved into small basins from surrounding slopes by solifluction, creep and/or slopewash (WALKER et al. 1989).

The local hills are covered by glacial till of the Sagavanirktok River Glaciation (Middle Pleistocene). Most hill crests have till at the surface, providing rocky mineral substrate for plant communities, whereas hill slopes and valley bottoms are generally smoothly eroded and covered by colluvium and shallow peat deposits. Several bedrock knolls of the Fortress Mountain formation occur in 1% of the area and add considerably to the floristic diversity. The Fortress Mountain formation is Lower Cretaceous in age and composed dominantly of thick units of dirty gray-wacke-type gray to green sandstone. Thick units of clay shale and siltstone are interbedded with the sandstone and conglomerate. On the ridge crests and at scattered sites on the hill slopes, till is exposed at the surface. About 4% of the watershed has exposed till deposits. Flat exposed till deposits generally are rocky with gently undulating surface relief that includes blockfields and sorted frost scars. Most hill slopes in the region are defined as “retransported deposits”, which are relatively fine-grained organic-rich materials moved downslope by slopewash and solifluction. The till is covered by clay loam that has been

redistributed downslope and vegetated with tussock tundra. About 76% of the watershed is mapped as retransported deposits. Surface forms associated with retransported deposits include water tracks, frost scars and non-sorted stone stripes. The lower portions of stone-stripe complexes often grade into and may be the foundation for water track complexes.

Many of the landscape features often associated with permafrost (such as ice mounds, polygons or ice wedges) are not conspicuous in the watershed. However, the effects of frost action are evident in the presence of frost boils and translocated organics on the surface of the permafrost table. The soil profile experiences frost churning which in effect mixes pieces of the organic mat downward, so a layer of organics can be found on the surface of the permafrost table (HINZMAN et al. 1991a).

The shallow soils are defined as Histic Pergelic Cryaquepts and are quite variable consisting of about 10 cm of live and dead organic material over 5-10 cm of partially decomposed organic matter mixed with silt which overlays the glacial till. Through Carbon-14 dating, the age of these soils has been established to be at least $11,500 \pm 140$ years. The soils are mostly silty colluvium and residual material of glacial origin. The organic matter at the surface consists of partially decomposed mosses, sedges and other associated plants. Furthermore, the soil system shows a spatial heterogeneity, described by HINZMAN et al. (1991a). Generally, there is a thicker organic layer in the valley bottom (~50 cm) than on the ridges (~10 cm).

2.4 Vegetation

The north side of the Brooks Range is clothed in vegetation characteristics of Arctic and Alpine tundra (NUTALL 2005). The vegetation is mostly water-tolerant plants such as tussock sedges and mosses, but there are also lichens and shrubs such as willows, alder and dwarf birch. Although the Arctic Foothills are largely dominated by tussock-tundra vegetation, there are local areas of high vegetation diversity due to bedrock outcrops, riparian systems and regional variation due to influences such as loess, glacial history, elevation, and snow gradients (WALKER et al. 1989).

3. Data collection

Various research projects on the North Slope of Alaska have, since the mid 1980's, resulted in the establishment of several unmanned meteorological and research sites on a north-south transect. For logistical reasons, all of the present sites are located along the Dalton Highway or accessible from roads on the Prudhoe Bay oil field. The catalyst for this data collection program was the Department of Energy's R4D project at Imnavait Creek where the first meteorological data sites were established in 1985 (NSIDC Homepage). The measurement program is organized by the Water and Environmental Research Center at the University of Alaska, Fairbanks (WERC Homepage). In the Imnavait Creek basin there are four main sites where data collection has taken place:

- **Imnavait Basin (B-Site)**

68° 36' 58.6" N, 149° 18' 13.0" W; (937 m)

- **Imnavait Ridge (R-Site)**

68° 37' 27.9" N, 149° 19' 22.3" W ; (880 m)

- **Imnavait Valley (V-Site)**

68° 37' 02.7" N, 149° 19' 02.3" W, (876 m)

- **Imnavait Flume Station**

68° 37' 02.1" N, 149° 19' 08.1" W; (881 m)

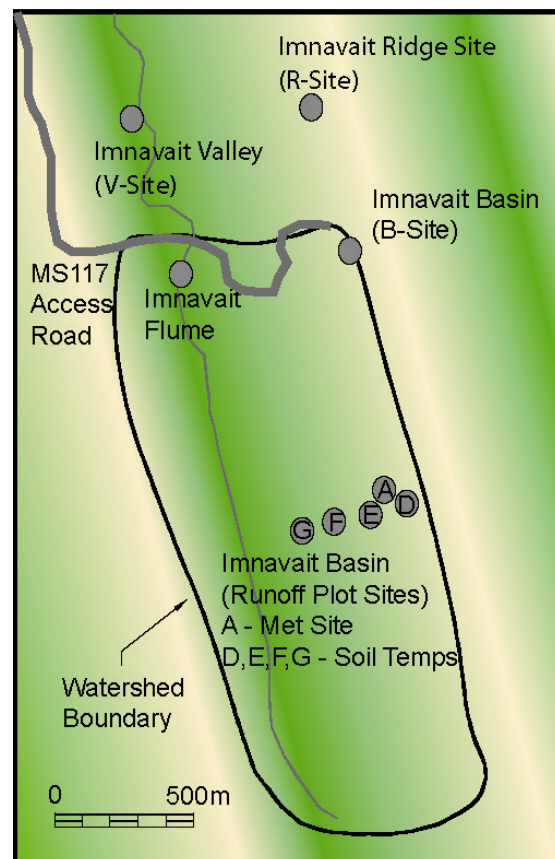


Figure 3.1: Map of the Imnavait Creek watershed and data collection sites (image courtesy of WERC)

Compared to other arctic study sites an immense amount of various data has been carried out in Innavait Creek. Comprehensive hydrologic studies have been ongoing since 1985 with all the major processes being monitored throughout the year (KANE et al. 1989).

In this study, measurements collected from 2001 to 2003 are used. Soil data from former studies complete the data collection presented in the following sections. The data can be broken down into four main categories: meteorological, hydrological, soil and snow pack data.

3.1 Meteorological data

A typical meteorological station is shown in figure 3.2. Sensors for air temperature, air pressure, wind speed, wind direction, relative humidity, radiation, soil temperature and precipitation measure automatically. Except for the radiation measurements, the recording takes place throughout the year. All meteorological data used in this study are conducted at the Innavait Basin site (B-Site).

Temperature

Air temperature is measured at 1 m, 3 m and 10 m height using a Campbell Scientific Model 207 Temperature Probe. The data are recorded and stored in hourly intervals.

Precipitation

Precipitation is measured with a tipping bucket rain gage with a windshield. Here, the rain volume is recorded in intervals of 0.3 mm.

Wind speed

Wind speed is measured at 1 m, 3 m and 10 m heights using a Met One Model 014A Anemometer.

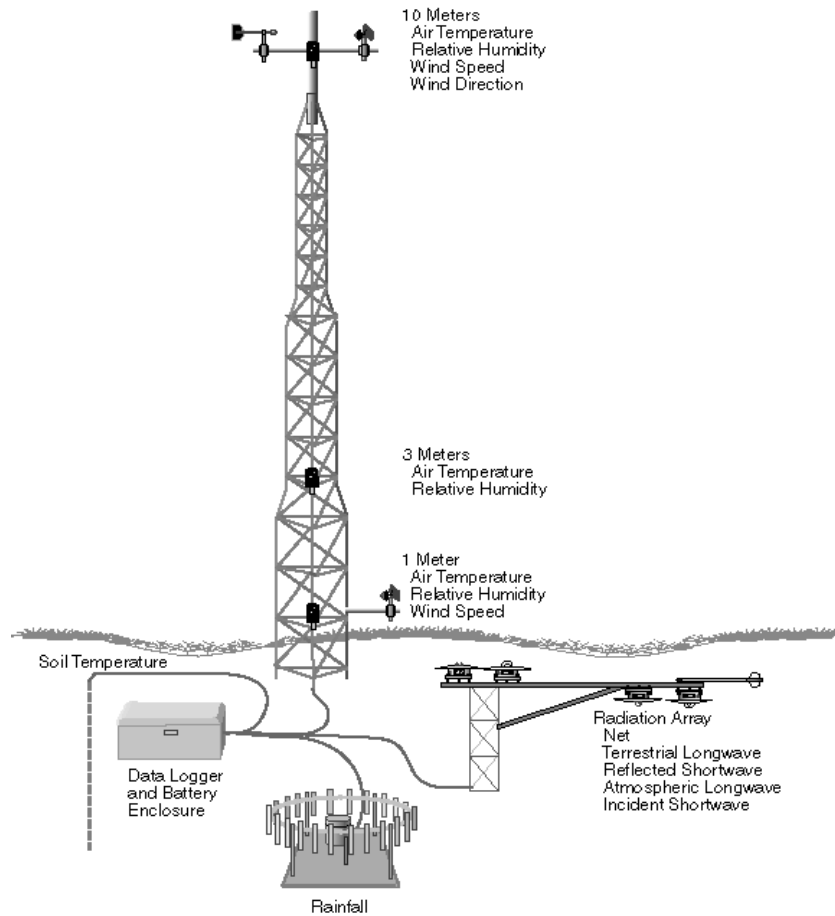


Figure 3.2: A scene of the meteorological station Innavait Creek Basin (image courtesy of Robert Gieck)

Radiation

Radiation instruments are installed in the spring usually during March or April and are taken down in the fall (late August or September). Since rime ice, snowfall and freezing precipitation can obscure the sensors in these instruments, values reported during periods of below freezing air temperature should be considered qualitative and not quantitative (KANE and GIECK 2001a). The following radiation components are measured: incoming and reflected short wave radiation, atmospheric and terrestrial long wave radiation, photosynthetically active radiation and net radiation.

In this study, only net radiation data are used. Net absorbed radiation is measured with a Swissteco model S-1 Net Radiometer; the accuracy is reported as $\pm 2.5\%$. Missing data occurred for 46 hours in early August 2003. For further use as model input, the time series is completed by averaging hourly values from the adjacent days.

Humidity

Relative humidity is measured with a Campbell Scientific Model 207 Humidity Probe at 1 m and 3 m height. In order to calculate the vapor pressure that is needed as an input into the model, Magnus' equation is used (FOKEN 2003):

$$E = 6.112 \exp\left(\frac{17.62T_a}{243.12 + T_a}\right) \quad (3.1)$$

where E is saturation vapor pressure at a certain temperature [mbar], and T_a is the air temperature [°C]. The actual vapor pressure e_a [mbar] is obtained by the multiplication of saturation vapor pressure and relative humidity [%].

3.2 Hydrological data

Stream flow

Figure 3.3 shows the H-flume at Imnavait Creek, which has been in operation since 1985. Stream discharge is estimated from stage data recorded by Leupold Steven's F1 water level recorders. A stage / discharge relationship is developed from discharge measurements made with Price AA (Gurley) and Pygmy cup type current meters. For the estimation of stream discharge from the recorded stage data a Montedoro Whitney electromagnetic current meter, using standard USGS stream cross section techniques, is used. Discharge is measured from the beginning of the snowmelt until freeze-up.

Channel properties

In July 2004, measurements were carried out at Imnavait Creek to obtain values for Manning's roughness parameter used in the modeling. These measurements were taken at two locations close to the flume station. Both sections were of several meters in length.

To determine the roughness parameter, Manning's Equation can be used (HERRMANN 1977; MAIDMENT 1992):

$$v = \frac{1}{n} R_H^{2/3} \sqrt{S_0} \quad (3.2)$$

where v is the velocity [m s^{-1}], n is the roughness parameter [$\text{s m}^{-1/3}$], R_H is the hydraulic radius [m], and S_0 is the slope. The hydraulic radius can be determined from $R_H = A/P_W$, where A is the cross-sectional area [m^2], and P_W is the wetted perimeter [m]. Values for S_0 , A , and P_W were derived from theodolite measurements, and the flow velocity was measured by using a current meter¹.



Figure 3.3: Innavait Creek H type flume station, July 2004

Several factors restricted the adequate determination of Manning's roughness parameter:

1) Due to the low flow velocities and the dense vegetation on the channel bed, the current

¹ The meter consists of a propeller that is rotated by the action of flowing water. Given the number of revolutions in a given time interval, velocity can be determined for the location of the current meter.

meter did not function properly. Instead, the flow velocity was determined by using the flow rate measured at the flume station. 2) The wetted parameter and the cross-sectional area are highly variable within a short distance. Values measured for P_w and A varied considerably even within the short sections chosen for the survey. 3) Considering the low topographic gradient and the short distance of the measurement, the determination of the slope is subject to major uncertainties. 4) The values obtained at the sections are not representative for the entire length of the Innavait Creek, as the channel properties vary considerably due to the beaded stream system shown in Figure 2.2.

Solving Equation (3.2) for the roughness parameter n , an average value of $0.01 \text{ s m}^{-1/3}$ is determined for Innavait Creek. However, considering the above mentioned restrictions, the roughness parameter is more likely to be underestimated. Its determination for modeling purposes is discussed in chapter 4.3 and 5.5.

3.3 Soil data

Soil profile

Soil profiles vary over the watershed depending on elevation. HINZMAN et al. (1991a) give values for a representative profile, shown in Table 3.1. These values are based on measurement at four sites that were constructed on the west-facing slope and evenly spaced from near top of the ridge to near valley bottom. The top organic layer is generally deeper in the valley bottom than on hillslopes and on the ridge. Here, the material contains less organic matter and the mineral layer is closer to the surface.

Soil temperature

Soil temperatures are measured at the Innavait Basin / Valley and Ridge site using YSI model 44007 Thermistors and 100 K ohm precision resistors. Measurements are collected at a daily interval. The instrument chains reach a depth of 115 cm, 50 cm and 250 cm at the three sites, respectively. For modeling purposes, however, hourly input data is required and therefore, the time series are interpolated using linear Kriging.

Depth [cm]	Description of a representative soil profile
0-3	Living <i>Polytricum sp.</i> (moss); vertical orientation; boundary clear, smooth
3-8 (Oi)	Loose spongy mat of partially decomposed moss and roots of <i>Vaccinium vitis-idaea</i> , <i>Ledum palustre</i> , <i>Cassiope tetragona</i> , <i>Eriophorum vaginatum</i> ; boundary abrupt, smooth principal avenue of water movement into pit
8-16 (A)	Very dark grayish-brown (10 YR 2/1) decomposed <i>Carex</i> roots and stems; boundary abrupt, smooth
16-20 (B)	dark brown (10YR 3/4) clay loam; prominent, fine, dark reddish-brown (10 YR 5/4-5/6) mottles; 2% pebbles<1cm diameter; few fine roots; weakly thixotropic; boundary abrupt, smooth
20-40 (C)	Very dark, grayish-brown (10 YR 3/2) fine, sandy loam; few weak dark reddish-brown mottles (10YR 5/4); few pebbles; ice lens partings are common; moderately tixotropic; boundary: permafrost

Table 3.1: Description of a representative soil profile at the Imnavait watershed (HINZMAN et al. 1991b)

The physical properties, such as the hydraulic conductivity, density and porosity, are related to the type of soil (HINZMAN et al. 1991a) and summarized in Table 3.2.

Horizon type	Depth [cm]	Hydraulic conductivity [$10^{-3} \text{ cm s}^{-1}$]	Bulk density [g m^{-3}]	Porosity
Organic	0 – 5	19.4	0.15	0.90
Organic	5 – 10	10.4	0.18	0.86
Organic/Mineral	10 – 15	3.76	1.39	0.70
Mineral	15 – 20	0.87	1.53	0.55
Mineral	20 – 25	1.42	1.33	0.54
Mineral	25 - 40	0.94	1.40	0.46

Table 3.2: Summary of the physical properties of soil samples taken at the Imnavait watershed (HINZMAN et al. 1991b)

Soil moisture

Soil moisture measurements are carried out with TDR (Time Domain Reflectometry) sensor profiles at three sites located on the west-facing slope. Data were recorded since July 2001 at hourly intervals down to a max. depth of 98 cm. The instrument measures the volumetric water content at three sites within and beside a water track on the hill slope. The location is illustrated in Figure 3.1 (locations D-F). Data are collected and analyzed by P. P. OVERDUIN (personal communication). To obtain information about the state of saturation of a soil layer, the volumetric water content must be related to the porosity at the corresponding depth. Mean effective porosities were estimated for each soil layer based on TDR water contents at saturation. They were used to calculate the water table height from the integrated active layer water content.

The active layer depth is calculated as a function of time by fitting the thaw dates at each TDR probe to the square root of time. Thaw depth is assumed to reach a constant value at the lowest TDR sensor; this assumption has little effect on the calculated water table heights, since the lower soil layers are saturated throughout the thawed period.

Maximum depth of thaw (MDT)

Values for the annual active layer depth are based on Circumpolar Active Layer Monitoring (CALM) measurements. This program is designed to monitor changes in the thickness of the active layer above permafrost (CALM Homepage). Currently 69 sites in the Arctic are evaluated each summer at the latest possible date prior to the annual freeze-up. The instrument used is a metal rod that is pushed vertically into the soil to the depth at which ice-bonded soil provides firm resistance. This determines the maximum depth of thaw (MDT). Measurements are done on a 1 km X 1 km grid with grid lines at 100 m intervals. For Imnavait Creek approx. 120 measurements are taken and averaged each year. Table 3.3 shows the annual average values for the years 1992 to 2004.

Year	1992	1993	1994	1995	1996	1997	1998	1999	2001	2002	2003	2004
Depth in cm	60	60	49	46	50	57	48	45	48	37	52	50

Table 3.3: Annual values for the maximum depth of thaw at the Imnavait watershed obtained from CALM grid measurements

Uncertainties related to the measurement method can originate from the following facts: 1) The soil contains considerable amounts of pebbles which can make it difficult to determine the actual boundary of permafrost. 2) The determination of MDT depends on the person who executes the measurement. 3) MDT is extremely variable within short distances (e.g. within and besides a water track). 4) The grid does not cover the entire watershed, but leaves out the southern part which is located at a higher elevation. Here, MDT is usually deeper than at lower elevations. Considering these uncertainties, MDT is more likely to be underestimated.

Another method to derive MDT is by analyzing soil temperature profiles. For this purpose, the soil temperature records described above are examined for the first positive temperatures occurring at each depth. Here, a temperature > 0.1 °C was defined as the

threshold temperature to account for the fact that the soil remains at 0 °C until the ice is melted completely. The accuracy of this method is restricted by the limited amount of data: Only three profiles account for the entire watershed. Several sensors malfunctioned, and no data are available at the Valley and Ridge site for 2003.

3.4 Snow pack data

Snow surveys were conducted at Innavait Creek since 1985. The water equivalent of the snow pack (SWE) is measured late each spring just prior to snowmelt. To provide SWE-data, snow depths are combined with pit studies to measure snow density, temperature and hardness profile (REYNOLDS et al. 1996). Snow pack depth and water equivalent are measured using an Adirondack snow sampler. The measurements are conducted along a valley transect, approximately in the middle of the basin. Each reported value is an average of at least 10 measurements (KANE et al. 2001b). Figure 3.4 shows the ablation curves for 2001 to 2003.

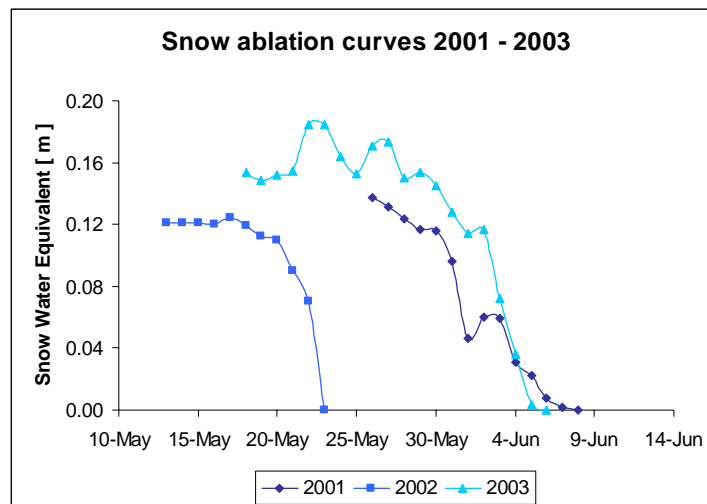


Figure 3.4: Snow ablation curves for the Innavait watershed 2001 to 2003. Measurements are based on snow surveys along a valley transect.

4. Modeling

This chapter contains the methods that are used to simulate the hydrology of an Alaskan Arctic watershed and analyze the simulation results. The newly developed, spatially distributed hydrological model `TopoFlow` is applied to the Imnavait Creek watershed described in chapter 2. It is based on the former hydrological model `ARHYTHM`, a brainchild of HINZMAN et al. (1995).

The main purpose of `TopoFlow` is to model many different physical processes in a watershed with the goal of accurately predicting how various hydrologic variables will evolve in response to climatic forcing (`TopoFlow` Homepage). Here, the detailed spatial simulation discerns `TopoFlow` from other models (see chapter 1.2) and, therefore, requires a Digital Elevation Model (DEM) and grids for the spatial distribution of input parameters. This groundwork is done with `RiverTools`, a hydrological software for GIS analysis of digital terrain, watersheds and river networks (`RiverTools` User's Guide).

The work related to the DEM is described in section 4.1. The structure of the model `TopoFlow` is elucidated in section 4.2, and in the last section its calibration and parameterization is documented.

4.1 The Digital Elevation Model

The hydrological response of a watershed is influenced by many interacting factors, primary among which is topography. The watershed topography serves as an important factor in determining the streamflow response of a basin to precipitation because it controls the movement of water within the basin. It also affects the spatial distribution of fluxes within the watershed such as surface and subsurface flow. It is essential to correctly depict slope, aspect and drainage characteristics of a watershed for use in spatially distributed models (ZHANG et al. 2000).

The Digital Elevation Model (DEM)

The original DEM was produced in 2001 by Intermap Technologies, using an airborne Star3i X-Band radar system (Intermap Technologies Homepage). This technology features postings of 2.5 m. The vertical resolution is 1 cm with 2.5 m accuracy. For modeling purposes, the pixel size is crucial for both the reproduction of small scale processes in the model, and to minimize computation time; a resolution must be found that satisfies both conditions. For the purpose of this study, the original elevation data are aggregated to a pixel size of 25 m x 25 m which is found to be a good compromise. Like this, the computation time could be reduced to approx. 1 hour per simulated day on a 1.8-GHz Pentium PC, respectively 10 minutes per simulated day on a UltraSPARC IIIi-processor.

The watershed area

RiverTools defines computationally the watershed area that contributes to a manually specified outlet. The first computation resulted in a drainage area of 1.45 km² which is considerably less than the value of 1.9 km² used in previous model studies (ZHANG et al. 2000), and the value of 2.2 km² obtained by manual delineation of topographic maps (e.g. KANE et al. 1989). It should be noted that the headwaters of the Imnavait watershed are complex topographically, i.e. a very flat area, and therefore, the southern watershed boundary is difficult to determine visually and/or by way of calculation. Initially, RiverTools produced a channel at the southwest border of the watershed that diminished its size. This channel could neither be found in aerial pictures nor through field investigation. The production of this channel by RiverTools was due to the fact that 3 pixels were significantly lower than the surrounding elevation¹. After they were adjusted to the height of the adjacent pixels no further outflow emerged and the resulting watershed area is 1.9 km². Simulated watershed shapes are very close to actual shapes.

¹ The deviation from the surrounding elevation was within the measurement accuracy of 2.5 m for the vertical resolution. NOLAN et al. (2002) report a misrouting of stream channels, using the same technology and hydrological software. They identify two sources of errors within the Star3i DEM: at seam boundaries due to the side-looking radar system, and ripples due to aberrations and multi-path error within the radome.

Figure 4.1 depicts the DEM of the Innavait Creek watershed, its channel network and watershed boundaries. For comparison with the natural appearance see Figure 2.2.

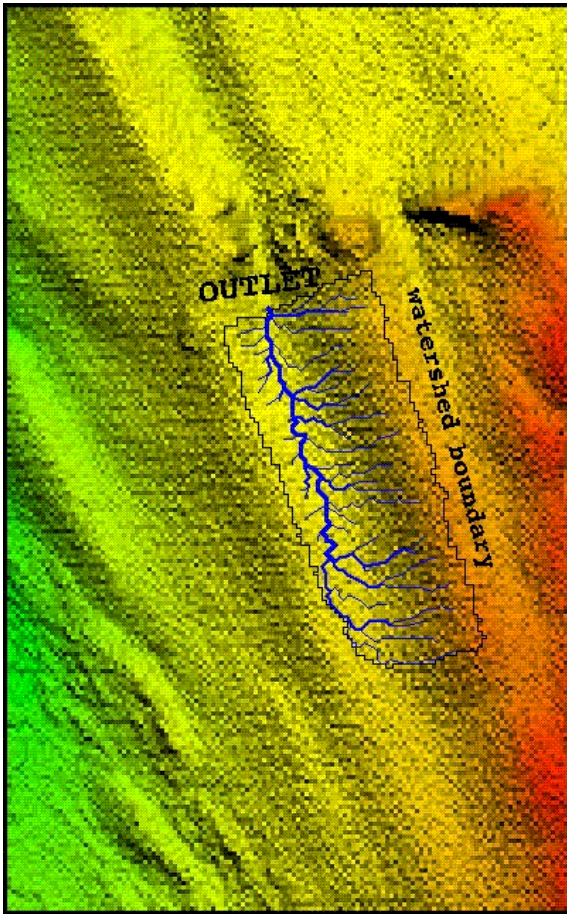


Figure 4.1: Digital Elevation Model of the Innavait watershed, its channel network and watershed boundaries as produced in RiverTools

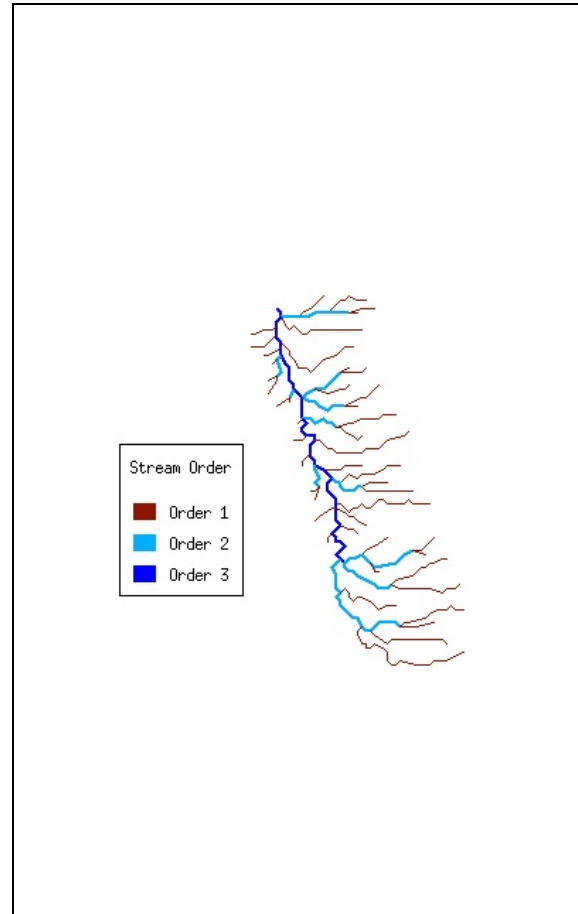


Figure 4.2: Channel network of the Innavait watershed with the Stream Orders produced in RiverTools

Flow direction and channel network

The DEM that is modified as mentioned above is used in RiverTools to generate several additional files that are needed to extract information for a river network. First, a depressionless DEM is created in order to extract the flow direction of each pixel². The flow grid indicates the direction in which water would flow away from the corresponding

² This is necessary due to the fact that the flow direction is ambiguous when none of a pixel's eight neighbor pixels has a lower elevation than it does (considering measurement accuracy). These pixels are referred to as artificial flats. Since this is common, RiverTools uses sophisticated algorithms to assign flow directions within flats in a self-consistent, iterative way (RiverTools User's Guide).

pixel in the DEM. To determine the flow direction, the algorithm “Imposed gradients plus” is used to center flow within flat valleys and reduce parallel flow³.

Furthermore, a `RiverTools` treefile is derived from the flow grid. This vector-formatted file stores data for the basin such as contributing area and relief. These attributes are stored for every Pixel in a given basin. The basin itself is derived by the specification of the Pixel that represents the outlet.

The next and most important step in `RiverTools` is the creation of the river network. There is no universal agreement as to how the heads of first-order channels (known as sources) can best be identified from a DEM and/or flow grid (`RiverTools` User’s Guide). Thus, different pruning methods are offered to the user who can choose the one that produces a river network that agrees best with the real conditions. In this study, a source identification method is chosen where streams that belong to a stream order of less than 3 are pruned. Thereby, the computed number of the Horton-Strahler stream order⁴ is reduced from 5 to 3. Considering the water tracks (described in chapter 2.2) to be channels, the simulated river network is comparable to the channel structure that is visible in aerial pictures. In their modeling study, ZHANG et al. (2000), also use a third order channel network for the Imnavait watershed.

Finally, grids of upstream areas, downstream slopes and Horton-Strahler order are produced with `RiverTools` for further use with `TopoFlow`.

³ `RiverTools` provides three different options for resolving flow direction in flats. “Imposed gradients” is the method proposed by GARBRECHT and MARTZ (1997) which attempts to center flow within flat valleys and reduces parallel flow. “Imposed gradients plus” is a new method which further refines flow within flats to eliminate virtually all parallel flow (`RiverTools` User’s Guide). This was necessary for the Imnavait watershed because otherwise no channel flow would emerge.

⁴ HORTON (1932, 1945) introduced a stream ordering concept that allows the channels in a river network to be assigned an integer value that determines their relative importance in a hierarchy of major and minor tributaries. Here, the first order refers to the main channel of a watershed. Correspondingly, the importance of a tributary decreases with an increasing number.

4.2 Model description of TopoFlow

This section elucidates the structure of the model TopoFlow, and how each process is incorporated via physical formulations. Although many processes are similar to other climatic regions, arctic hydrologic systems have unique characteristics, such as the existence of permafrost and a dynamic active layer. Figure 4.3 shows the components that are considered in the model structure. However, some processes have not yet been fully incorporated as physically based, because the model programming was still in progress during the time of this study.

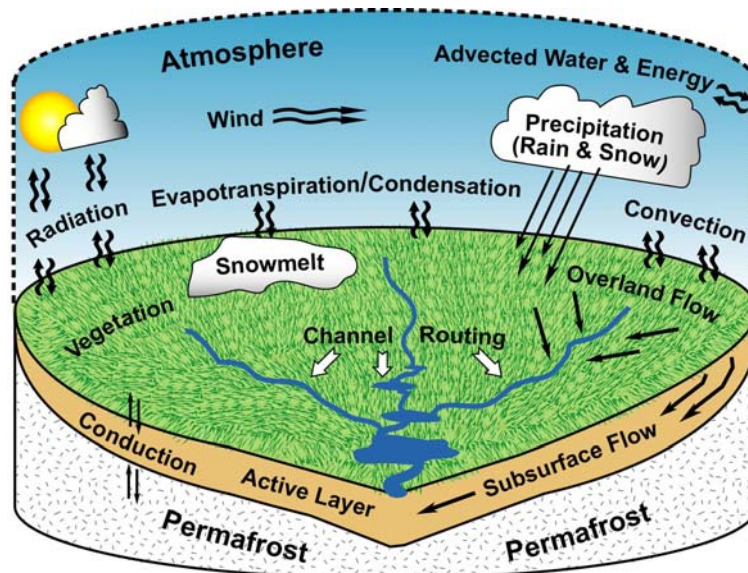


Figure 4.3: Hydrological and thermal processes simulated for every element within an arctic watershed (image courtesy of Scott Peckham)

Snowmelt

Snowmelt is a major component of the hydrological cycle in the Arctic. Thus, correctly simulating snowmelt and predicting subsequent runoff from the watershed are important components of arctic hydrological modeling. The annual snow cycle is characterized by a relatively long accumulation period of eight to nine months, followed by a short melt season (ZHANG et al. 2000). The hydrological simulation is initiated some hours prior to snowmelt, so it is not necessary to model accumulation or redistribution of snow. Thus, only the end of winter snow pack distribution is considered in the model.

Currently, TopoFlow provides the empirical degree-day method (SM-DD) to simulate the snow pack ablation. The implementation of the energy balance method (SM-EB) is planned. The latter is a physically based approach that requires a large set of input variables that is not available for many regions of the Arctic. In this study, both approaches are used for further comparison of their capability to reproduce the snow pack ablation. While the SM-DD ablation is determined by the model, SM-EB is calculated separately.

The degree day method (SM-DD)

The degree day method is based on the following equation (HINZMAN et al. 1991b; KANE et al. 1993 and 1997):

$$M_{SM} = C_0(T_a - T_0)/t \quad (4.1)$$

where M_{SM} is the water equivalent of snowmelt [mm per time step], C_0 is the degree day melt factor [mm day⁻¹ °C⁻¹], T_a is the air temperature [°C], T_0 is the temperature of snow when it reaches isothermal conditions of melting [°C], and t is the time steps per day. The approach adopted here does not consider cooling of the snow pack. Equation (4.1) is valid only when $T_a > T_0$. If $T_a < T_0$, then $M_{SM} = 0$.

The energy balance (SM-EB)

The energy balance of the snow pack is a physically based approach that considers the important heat transfer processes occurring on the surface of the snow pack, including heat storage within the snow pack. It can be expressed as:

$$Q_m = Q_{net} + Q_h + Q_e + Q_a + Q_c + Q_{cc} \quad (4.2)$$

where Q_m [W m⁻²] is the energy utilized for melting the snow pack when it is positive, Q_{net} [W m⁻²] is the net radiation energy, either measured by a net radiometer or calculated as the sum of individual incoming and outgoing long and short wave fluxes, Q_h [W m⁻²] is the sensible heat flux resulting from turbulent convection between the snow surface

and the air, Q_e [W m^{-2}] is the latent heat flux associated with evaporation/sublimation and condensation, Q_a [W m^{-2}] is the energy advected by moving water (i.e. rainfall), Q_c [W m^{-2}] is the energy flux via conduction from the snow to the soil, Q_{cc} [W m^{-2}] is the cold content of the snow pack, which is defined as the amount of heat needed to bring the snow pack to ripe condition prior to melt or the amount of energy that may be released in cooling or refreezing of liquid water in the snow during extended cold periods (BENGTSSON 1984). This energy deficit or cold content that accumulates when the melt is interrupted by cold weather must be satisfied prior to resumption of snowmelt. If Q_m in Equation (4.2) is negative, it means that the combined energy of $Q_{net}+Q_h+Q_e+Q_a+Q_c$ is not enough to overcome the cold content (Q_{cc}). This indicates that if there is liquid water within the snow pack, it will freeze or if no liquid water is present, the snow pack will cool further. This is typical on nights when the air temperature drops below freezing or when snowmelt is interrupted for days by a cold period.

In this study, two components of Equation (4.2) have been neglected: The advective heat transfer by moving water (Q_a) and the energy flux via conduction from the snow to the soil (Q_c). The temperatures and volumes of rainfall in the study area are typically low, so energy added to the snow through this mechanism is not very important during most of the year and particularly during snowmelt. Q_c is neglected because the vertical temperature gradient during melting is relatively small (ZHANG et al. 2000).

Sensible and latent heat fluxes to and from the surface of the snow pack are calculated using an aerodynamic approach. This approach takes into account turbulent transfer mechanisms and vertical gradients of temperature and vapor pressure in order to obtain sensible and latent heat fluxes (PRICE and DUNNE 1976; MOORE 1983):

$$Q_h = \rho_a C_a D_h (T_a - T_s) \quad (4.3)$$

$$Q_e = \rho_a L_v D_e (0.662/p)(e_a - e_s) \quad (4.4)$$

where ρ_a is the density of air [kg m^{-3}], C_a is the specific heat of air [$\text{J kg}^{-1} \text{ }^\circ\text{C}^{-1}$], T_a is the air temperature at height z [$^\circ\text{C}$], T_s is the surface temperature [$^\circ\text{C}$], L_v is the latent heat of vaporization [J kg^{-1}], p is the atmospheric pressure [mbar], e_a is the air vapor pressure at

height z [mbar], e_s is the surface vapor pressure [mbar], and D_h and D_e are heat and vapor transfer coefficients for neutral stability, respectively. The bulk exchange coefficient D_n [m s^{-1}] for neutral atmospheric stability can be obtained as a function of wind speed and roughness lengths using:

$$D_n = \kappa^2 (u_z) / (\ln((z - h) / z_0))^2 \quad (4.5)$$

where κ is von Karman's constant [0.41], u_z is the wind speed at height z [m s^{-1}], z_0 is the roughness length [m], and h is the snow depth [m]. For the determination of z_0 see section 4.3.

For non-neutral conditions, a correlation must be applied to account for the stability of the air just above the ground surface (PRICE and DUNNE 1976). To compensate for air stability, daily heat exchange coefficients are adjusted based on the air temperature profile between the surface and the reference height z , using D_s for stable and D_u for unstable conditions (BRAUN 1985). This is accomplished by comparing the air temperature T_a with T_s . If $T_a < T_s$, then the stable heat transfer coefficient is used:

$$D_s = D_n / (1 + 10R_i) \quad (4.6)$$

where R_i is the Richardson number, defined as:

$$R_i = \frac{gz(T_a - T_s)}{u_z^2(T_a + 273.15)} \quad (4.7)$$

where g is the gravitational constant [9.81 m s^{-2}], and z is the distance between instrument height and snow surface.

When the air density at the surface is less than the air density above the surface, an unstable situation occurs (i.e. $R_i < 0$) and the heat transfer coefficient is calculated:

$$D_u = D_n(1 - 10R_i) \quad (4.8)$$

Once the energy available for snowmelt (Q_m) is determined, the water equivalent of snowmelt equals:

$$M_{SM} = (1000Q_m)/(\rho_w L_f) \quad (4.9)$$

where M_{SM} is the water equivalent of snowmelt [mm of water per time step], ρ_w is the density of water [kg m^{-3}], L_f is the latent heat of fusion [J kg^{-1}], and Q_m is the summation of energy available for melt per unit area for time increment of calculation [J m^{-2}].

This calculation can be started at any time. No melting of the snow pack is allowed until the net energy overcomes the cold content of the snow pack. The energy input into the snow pack will be used to warm the snow until the cold content becomes zero when the snow is isothermal at 0°C . After that, additional energy will be used to melt snow. If the energy obtained by adding Q_{net} , Q_h , Q_e and Q_c is negative during calculation for each step, then the cold content increases by that amount. The initial cold content of the snow pack, when starting the calculation, can be evaluated by:

$$Q_{cc} = h\rho_s C_p (T_0 - T_{snow}) \quad (4.10)$$

where h , ρ_s and C_p are the depth [m], density [kg m^{-3}] and heat capacity of snow [$\text{J kg}^{-1} \text{ }^\circ\text{C}^{-1}$], respectively, T_{snow} is the average snow temperature [$^\circ\text{C}$], T_0 is the temperature of snow when it reaches isothermal condition of melting, usually 0°C .

Evapotranspiration

In the summer, with nearly 24 hours of sunshine daily, the Arctic receives large amounts of radiation relative to other seasons. Here, 40% to 65% of the radiation energy is consumed by the evapotranspiration process.

Currently, TopoFlow provides the Priestley-Taylor approach (ET-PT) to simulate evapotranspiration. The implementation of the energy balance method (ET-EB) is planned. The latter is a physically based approach that requires a large set of input variables that is not available for many regions of the Arctic. In this study, both approaches are used for further comparison. While ET-PT is used in the model simulation, ET-EB is calculated separately using the formulas described below.

The Priestley-Taylor method (ET-PT)

The Priestley-Taylor equation (PRIESTLEY and TAYLOR 1972) is:

$$Q_{et} = \alpha_{PT} (0.406 + 0.011T_a)(Q_{net} - Q_c) \quad (4.11)$$

where Q_{et} is the energy utilized for evapotranspiration of water moisture from the surface [$W m^{-2}$], α_{PT} is the parameter relating actual to equilibrium evaporation, T_a is the air temperature [$^{\circ}C$], Q_{net} is the net radiation energy [$W m^{-2}$], and Q_c is the conductive energy between the surface and subsurface [$W m^{-2}$]. Q_c can be obtained from Fourier's Law:

$$Q_c = K_s \frac{T_z - T_s}{z} \quad (4.12)$$

where K_s is the thermal conductivity of the soil [$W m^{-1} ^{\circ}C^{-1}$], T_z is the soil temperature [$^{\circ}C$] at depth z below the surface [m], and T_s is the soil surface temperature [$^{\circ}C$].

ROUSE et al. (1977) found that the parameter α_{PT} varies with vegetation type and soil moisture content. Its determination is discussed in the next section.

The amount of water that is lost through evapotranspiration can be evaluated as:

$$M_{et} = \frac{1000Q_{et}}{\rho_w L_v} \quad (4.13)$$

where M_{et} is the water loss [mm per time step], ρ_w is the density of water [kg m^{-3}], and L_v is the latent heat of vaporization [J kg^{-1}].

The energy balance method (ET-EB)

The energy balance technique is a widely used method for determining evaporation and/or transpiration. It can be expressed as:

$$Q_{et} = Q_{net} + Q_h + Q_c \quad (4.14)$$

where Q_{et} is the energy utilized for evapotranspiration of water moisture from the surface [W m^{-2}], Q_{net} and Q_h can be obtained in the same way as in the process of snowmelt described previously. Q_c is the conductive energy between the surface and subsurface [W m^{-2}], and can be obtained from Equation (4.12). The amount of water that is lost through evapotranspiration can be calculated by Equation (4.13).

Flow routing

There are three different flow processes that must be included to describe the hydrology in the Arctic: channel flow, overland flow and subsurface flow in the shallow active layer, (HINZMAN et al. 1993). These processes operate over similar spatial scales but markedly different temporal scales. Subsurface water flows through soil pores and therefore, at low velocities in the laminar regime. Overland flow occurs when saturation of the active layer forces flow through tussocks or over very porous living plants or mosses (ZHANG et al. 2000). Both overland flow and channel flow occur in the turbulent flow regime. To maximize model efficiency, different time increments are used in the flow routing within the channels (Δt_{CF}), over the soil surface (Δt_{OF}), and through the subsurface (Δt_{SF}). The size of each time step is based upon the element size, slope and

hydraulic properties. The critical consideration in determining time-step size is that a parcel of water must not completely cross one element or channel segment in less than one time step. For all three flow types, the maximum time-step increment is limited by the Courant condition. To satisfy this condition, the time step is $\leq \Delta x / c$ (BEDIENT and HUBER 2002; CIRIANI et al. 1977), where $c = v \pm \sqrt{gy}$, Δx is the smallest grid scale of an element or channel [m], v is the flow velocity [m s^{-1}], and y is the water depth [m], and g is the gravitational constant [m s^{-2}].

The flow routing is based on the finite element (control-volume based) method vs. finite difference (S. PECKHAM, personal communication). The flow direction for each pixel is given by the flow grid derived by `RiverTools` and described previously. Using the divergence theorem, the flow can be calculated by integrals around the pixel boundary instead of over the interior.

Subsurface Flow

In the Arctic, subsurface hydrological processes are limited to the shallow active layer because continuous ice-rich permafrost is essentially an impermeable boundary to water flow (ZHANG et al. 2000). In `TopoFlow`, the active layer can be divided into up to 10 horizontal layers. The layered system of soil horizons regulates moisture movement into and through the active layer. Each layer has its own characteristics such as thickness, hydraulic conductivity and porosity.

For each layer i at any element j , the flow rate q [$\text{m}^3 \text{s}^{-1}$] is calculated by Darcy's Law:

$$q = K_i S_j A_i \quad (4.15)$$

where K_i is the hydraulic conductivity of layer i [m s^{-1}], A_i is the cross-sectional area of flow for each layer [m^2], and S_j is the slope of element j . The latter becomes the hydraulic gradient by considering the water table around this element. The total amount of subsurface flow Q [m^3] within a time step Δt_{SF} from an element j is given by:

$$Q_j = \sum_i K_i S_j A_i \Delta t_{SF} \quad (4.16)$$

After each time-step calculation, the volume of water stored in each element is compared with its level of saturation to determine if there is subsurface flow downslope. The time step Δt_{SF} for the subsurface flow should be such that water will not flow past the whole element within one time increment.

The active layer starts thawing after snowmelt, continues to thaw during the summer, and reaches its maximum thickness in autumn. Therefore, the soil depth in Darcy's equation potentially changes with each time step. Soil moisture capacities for each soil layer also change, because they are related to the soil depth. As the hydraulic conductivity is different for the frozen and the unfrozen soil, flow rates in the frozen layers differ significantly from those in the unfrozen soil. When this study was conducted, a physically based representation of the above-mentioned process was not yet available. Instead, input files with changing hydraulic conductivities are used to account for the thawing of the soil. Figure 4.4 depicts the process of thawing given as an input to the model. Here, K_T and K_F are the hydraulic conductivities for the thawed and the frozen soil, respectively. The gradient controlling how the thaw depth evolves with time is determined by the α_{TD} value described in the next section.

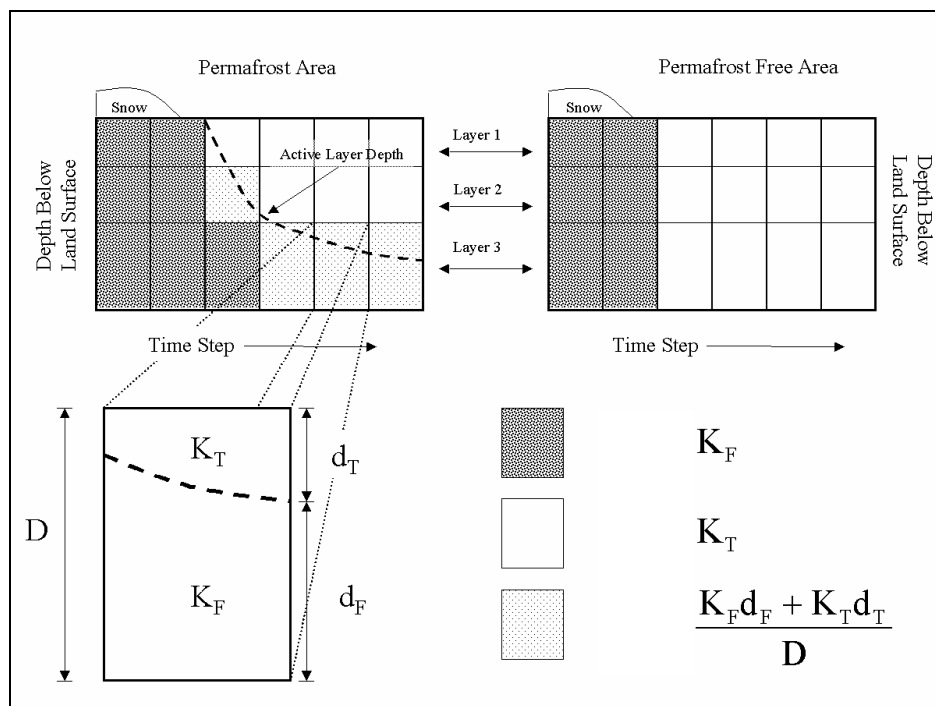


Figure 4.4: Processing of the thawing active layer in TopoFlow. K_T and K_F are the hydraulic conductivities for the thawed and the frozen soil, respectively (image courtesy of Robert Bolton).

Overland Flow

In this model, overland flow occurs when the water table rises above the surface. It is assumed that all of the water from precipitation or snowmelt is instantaneously infiltrated, meaning that the percolation time from the surface to the water level is neglected. The water content in each element may change with each time step, and the total storage capacity of each element may also increase or decrease as the active layer thaws. The kinematic wave solution has been shown to be an excellent tool for most cases of overland flow calculation (EAGLESON 1970; CIRIANI et al. 1977; ANDERSON et al. 1990). Under the kinematic wave assumption, the friction slope (S_f) and the bed slope (S_0) are equal, and Manning's equation can be used to express the relationship between flow rate and depth (MAIDMENT 1992):

$$q = vA = \frac{C}{N} AR_H^{2/3} \sqrt{S_f} \quad (4.17)$$

where q is the rate of lateral flow per unit length [$\text{m}^3 \text{s}^{-1} \text{m}^{-1}$], v is the fluid velocity [m s^{-1}], A is the cross-sectional area [m^2], $R_H = A/P_W$ is the hydraulic radius [m], P_W is the wetted perimeter [m], N is the roughness coefficient for overland flow, and C is a unit factor. For a sheet flow, as assumed in this model, $R_H \approx y$, where y is the uniform water depth over each element [m]. Thus, Equation (4.17) now becomes:

$$q = \frac{C}{N} B \sqrt{S_0} y^{5/3} \quad (4.18)$$

where B is the projected length on the plane perpendicular to flow direction [m] and equals A/y . The overland flow balance for each element within the time step Δt_{OF} can be written explicitly as:

$$\Delta S = (\sum q_{in} - \sum q_{out}) \Delta t_{OF} \quad (4.19)$$

where ΔS is the change of storage in each element within Δt_{OF} .

After each time step, a new total water content for each element is obtained and then y is determined by subtracting the storage capacity of the soil from the total water content. This new y is used to calculate the flow rate leaving/entering each element based on Equation (4.18). It should be noted that when calculating the mass balance for each element using Equation (4.19), precipitation input, evapotranspiration and contribution from subsurface flow is included. The contribution of subsurface flow to Equation (4.15) has been equally partitioned over Δt_{SF} . This is because the simulations of subsurface flow are calculated on a larger time increment than overland flow.

Channel Flow

The method used for overland flow is similarly used for channel flow routing. Within the reach of every channel, Manning's formula shown in Equation (4.17) can be applied. Here, the roughness parameter for the stream channel is denoted by n . The shape of the cross-section and the channel width can be specified by the user for each stream order. From these values, R_H can be calculated taking into account the water depth y at each pixel. The mass balance after each time step Δt_{CF} can be written as:

$$\Delta S = (\sum q_{in} - \sum q_{out}) \Delta t_{CF} \quad (4.20)$$

The mass balance is conducted by considering the amount of flow entering each channel reach from the upstream reach, the overland flow, the subsurface flow from the adjacent elements, and the flow exiting each channel reach. This model does not take into consideration any loss from the stream channel reverting back to subsurface flow or to evaporation. A new water depth y is then used to determine the quantity of flow exiting during the subsequent time step based on Equation (4.17). The choice of time step Δt_{CF} follows the same condition as described above. Again, because channel flow is simulated on a much smaller time increment than overland flow or subsurface flow, the contributions from overland and subsurface flow to the channel segment are equally partitioned over Δt_{CF} .

4.3 Calibration / Parameterization

The main subject of the following section is to describe the determination of the calibration parameters found in the model equations. For an appropriate calibration it is important to consider their different characteristics: Some have an equivalent in nature that can, at least theoretically, be determined through field observation, whereas others are purely related to the model algorithm. Some parameters are subjected to calibration, whereas others are based on measured values. And finally, the parameters differ in their impact on simulation results. This is important to consider in the calibration sequence (DINGMAN 2002).

Snowmelt

Both methods, SM-DD (model-generated) and SM-EB (calculated separately), are used in this study to compare their ability to reproduce the snow pack ablation. Figures 5.15 to 5.17 show basin-averaged snowmelt simulation results for the Imnavait watershed in 2001 to 2003.

Degree-day method (SM-DD)

Based on the degree day method two parameters mainly determine the simulated snowmelt: the melt factor C_0 and the threshold value of the air temperature T_0 . In this study, values of 2.3 to 3.5 mm day⁻¹ °C⁻¹ for C_0 , are found to produce the best results. T_0 , is set between 0 and -1.2 °C. The values of threshold temperature are usually less than 0 °C because some ablation can occur through radiative melt when the air temperature is below freezing. In comparison, ZHANG et al. (2000) use optimized values obtained from an analysis of several years of $C_0=2.7$ mm day⁻¹ °C⁻¹ and $T_0=-0.2$ °C for simulating the snow ablation in the Imnavait Creek watershed. Figures 4.5 and 4.6 give evidence of the influence of both parameters on the evolution of snow pack ablation.

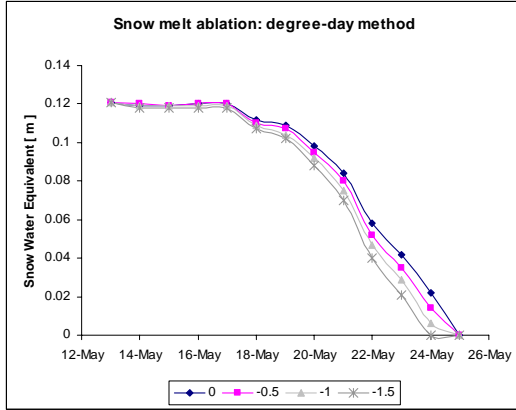


Figure 4.5: Simulated snow ablation with the degree-day-method using different T_0 -values (shown in the legend)

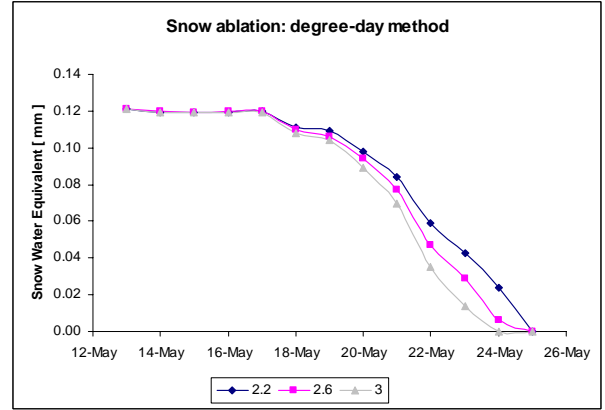


Figure 4.6: Simulated snow ablation with the degree-day-method using different C_0 -values (shown in the legend)

The energy balance (SM-ET)

When using the energy balance method for snowmelt (and later evapotranspiration), the average surface roughness length z_0 in equation 4.5 needs to be evaluated, using:

$$z_0 = \exp\left[\frac{u_2 \ln(z_1) - u_1 \ln(z_2)}{u_2 - u_1}\right] \quad (4.21)$$

where z_1 and z_2 are the two heights at which wind-speed measurements are made [m], and u_1 and u_2 are the wind speeds at the two heights z_1 and z_2 [m s⁻¹].

The value for z_0 over snow found in literature ranges from 0.00015 m (BRAUN 1985) and 0.0005 m (ANDERSON 1976) to 0.005 m (PRICE et al. 1976). In this study, a constant value of 0.0013 m for surface roughness length is used for the simulation of the melt period. This value is based on calculations from HINZMAN et al. (1993), who determined this constant in the Innavaik watershed from several hundred wind speed profiles between 1.5 and 10 m, using Equation (4.21). ZHANG et al. (2000) obtained good results in their model application to the Innavaik watershed, using the same value. Standard values are used for latent heat of fusion ($3.34 \cdot 10^6$ J kg⁻¹), latent heat of vaporization ($2.48 \cdot 10^6$ J kg⁻¹), water density (1000 kg m⁻³), specific heat of air (1005.7 J kg⁻¹ °C⁻¹), density of air (1.2614 kg m⁻³) and heat capacity of snow (2090 J kg⁻¹ °C⁻¹).

Evapotranspiration

Both methods, ET-PT (model-generated) and ET-EB (calculated separately), are used in this study to calculate the amounts of water lost by evapotranspiration. Figures 5.3 to 5.8 show basin-averaged hourly evapotranspiration for the Imnavait watershed in 2001 to 2003.

The Priestley-Taylor method (ET-PT)

The parameter α_{PT} is an empirical parameter that relates actual to equilibrium evaporation. ROUSE et al. (1977) found that the parameter α_{PT} varies with vegetation type and soil moisture content. Thus, for optimum results it should be calibrated to a particular surface type. For a soil moisture deficit of zero (saturation) JACKSON et al. (1996) use an α_{PT} of 1.26. In comparison to that, MENDEZ et al. (1998) give a range for α_{PT} from 0.91 to 1.15 for an Arctic watershed at the Coastal Plain of Alaska. Here, the first value applies to the uplands that are drier and have less vegetation.

In this study, values of 0.9 (in 2003) and 0.95 (in 2001 and 2002) give good results, see chapter 5.1 and 5.4. These values are used for the entire watershed, as the model does not provide a spatial distribution of the α_{PT} value. The calibration is based on the best alignment of the results obtained from ET-EB, as this approach is physically based. The second parameter in the ET-PT equations is the thermal heat conductivity, which is not subjected to calibration, as there is field data available. HINZMAN et al. (1991a) found the effective thermal heat conductivity K_s equal to $0.45 \text{ W m}^{-1} \text{ }^\circ\text{C}^{-1}$ when the organic soil is thawed with a moisture content near field capacity.

Figure 4.7 illustrates the influence of the α_{PT} parameter on the amount of evapotranspiration.

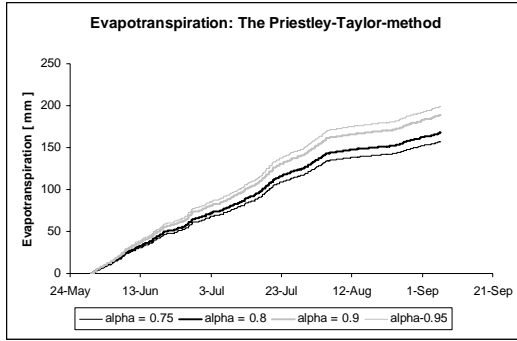


Figure 4.7: Simulated evapotranspiration for 2002, using the Priestley-Taylor method and different values for α_{PT} .

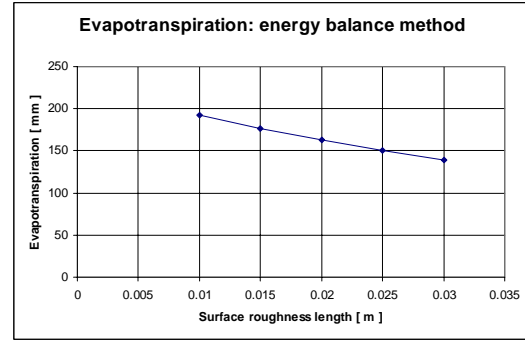


Figure 4.8: Calculated total evapotranspiration for 2001, using the energy balance method and different surface roughness parameters.

The energy balance method (ET-EB)

The determination of the surface roughness length is similar to the one used in SM-EB, see Equation (4.21). During snowmelt, the surface roughness increases as the vegetation protrudes through the snow pack. PRICE (1976) concludes, from fieldwork in Schefferville, Quebec, that protruding small vegetation will increase the z_0 from 0.005 to 0.015 m as the melt progresses. BRAUN (1985) uses optimized values between 0.00015 m and 0.007 m for the Alpine region in Switzerland. The above-mentioned study of HINZMAN et al. (1993) yields an average value of 0.02 m for the Innavait watershed after snowmelt, and no clear seasonal trends are determined. The application of a constant value refers to the small stature of the vegetation that remains at the same height throughout the summer. Because of this profound analysis, a roughness length of 0.02 m is used in this study. Even though z_0 is not subjected to calibration, it is, in fact, crucial for the total amount of water lost by evapotranspiration. Figure 4.8 illustrates this influence.

Flow routing

The computation time is an important factor for spatially distributed models. Thus, the calculated time steps should be adjusted to the necessary minimum. A 1-h time step (Δt_{SF}) is used in the calculation of subsurface flow through the soils. Based on the hydraulic conductivity of surface organic soils and the maximum slope of the watershed, the distance of subsurface water movement in 1 h is < 2 m, which is less than the grid scale for each element. The overland and channel flow velocities are higher than those for subsurface flow. Thus, a smaller time step (Δt_{OF} , Δt_{CF}) of 5 s is implemented in 2001 and 2003. In 2002, however, a time step of 1 s is used to handle the exceptionally high flow velocity due to a rain event in late autumn.

Subsurface Flow

Detailed data of soil properties are obtained from field investigation in the Imnavait Creek watershed (HINZMAN et al. 1991a) and shown in detail in chapter 3.3. In this study the combination of horizontal soil layers and the assignment of parameters that determine the subsurface flow (see Table 4.1) are based on studies by HINZMAN et al. (1991a) and the application of ARHYTHM to the same study site by ZHANG et al. (2000).

Soil layer depth [cm]	Porosity [%]	Hydraulic conductivity [10^4 m s^{-1}]
0 – 10	0.88	1.50
10 – 20	0.63	0.35
20 – 30	0.50	0.35
30 – 40	0.48	0.10
40 – permafrost table	0.40	0.10

Table 4.1: Soil parameters of Imnavait Creek used as model input.

Concerning the impact of soil parameters on subsurface flow, model studies reveal that the maximum depth of thaw (MDT) has the highest influence, followed by the porosity and the hydraulic conductivity. Therefore, only the first parameter is elucidated in more detail.

The α_{TD} value is the parameter that determines MDT, used in the model representation of the thawing active layer. Different values with their corresponding thaw depths are given in Figure 4.9.

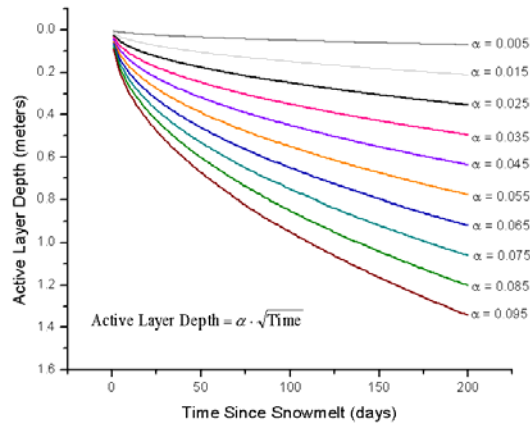


Figure 4.9: Evolution of the active layer depth for different α_{TD} values (image courtesy of Robert Bolton)

Figure 4.10 shows the evolution of a gradually thawing active layer when used as a model input for 2001, and corresponding values obtained from soil temperature measurements. Here, the α_{TD} value is calibrated such, that MDT matches the CALM grid measurements, whereas the thaw gradient during snow melt is calibrated to agree with soil temperature data. Therefore, α_{TD} is set to 0.068 during the snow melt period and 0.032 during the summer period. The input files for 2002 and 2003 are done correspondingly. For the interpretation of the measured data see chapter 3.3.

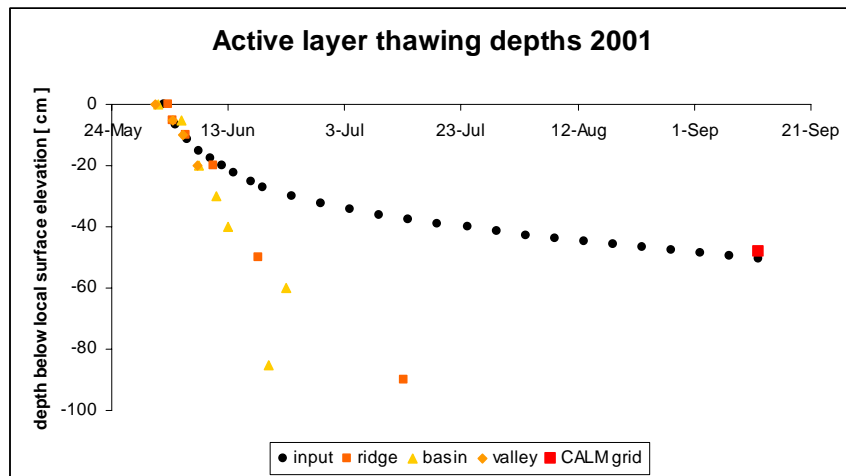


Figure 4.10: Thaw depth of the active layer 2001 as a model input ($\alpha_{TD} = 0.068$ during snow melt period 25/5-14/6; $\alpha_{TD} = 0.032$ during summer period 15/6-13/9), determined from soil temperature measurements at the Ridge, Basin, and Valley site, and from CALM grid measurements (average value)

Generally, TopoFlow is able to handle spatially distributed hydraulic conductivities that represent the spatial variation in soil profiles within the watershed. The recent model performance does not allow the use of spatially distributed hydraulic conductivities and the thawing of the soil representing conductivities at the same time. In the case of a whole summer runoff simulation, the thawing of the soil is an important factor and cannot be neglected. Thus, the simulations are done on spatially homogeneous soil parameters (Table 4.1). Spatially distributed soil parameters are only used for the simulation of single rain events where the evolution of the thaw depth can be neglected (e.g. Figures 5.22 to 5.24).

Overland flow and channel flow

The crucial factor in determining overland and channel flow is the roughness parameter in Manning’s Equation (4.17). Generally, the roughness of the surface retards the flow and, according to ZHANG et al. (2000), the roughness coefficient values for overland flows are typically greater than that for channel flow. In this study, the coefficient is subjected to calibration within the range of values obtained from field measurements and literature. For channel flow, the channel bed width must be specified, as well. Table 4.2 contains the corresponding values for each stream channel order.

	Manning’s roughness parameter [s m^{-1/3}]	Channel bed width [cm]
Overland flow	0.30	-
Water tracks	0.15	5
Stream order 2	0.10	15
Stream order 1	0.07	40

Table 4.2: Overland and channel flow parameters used as model input.

From field measurements (see section 3.3), a roughness coefficient of 0.01 is obtained for the main channel. Compared to that, MAIDMENT (1992) gives a value of 0.02 to 0.1 for natural stream channels with irregular sections and a slight channel meandering. Concerning the roughness parameter for overland flow, studies have shown that it can reach values of up to 1.0 (EMMETT 1970). In the application of ARHYTHM to the Innavait watershed, the authors use a roughness parameter of 0.3 and 0.03 for overland and channel flow, respectively (ZHANG et al. 2000). The value used in this study has

been increased during calibration, taking into account the measurement restrictions (described in section 3.3) and the deficiencies in the model representation of the channel network (see section 5.5). The general influence of the roughness parameter on the simulated hydrograph is discussed in chapter 5.5.

5. Results

The results of a hydrological model application to Innavait Creek, an Alaskan watershed, are presented in this chapter. The objective is to elucidate the processes that occur, interact and influence the hydrology in the special environment of the Arctic. These processes are highly complex and are further complicated by the limited amount of data that are available for such remote regions. However, the interactions taking place in Arctic environments garnered increased attention in recent decades because impacts of a changing climate are suspected to become apparent there first (e.g. IPCC 2001). In this context, models that reproduce processes on a regional scale can help to reveal the response to assumed changes in the climatic conditions.

This study focuses on the evaluation of the recently developed hydrological model, TopoFlow. The study examines a period of three years, 2001-2003. The model is used to simulate discharge from the beginning of the snowmelt until freeze-up. Field data of meteorological variables, as described in chapter 3, are used as an input to drive the model. The outputs of discharge, snow ablation curve, evapotranspiration, and water level in the active layer are compared to measured data in the following chapter.

	2001	Days	2002	Days	2003	Days
Snowmelt period	25/05 – 14/06	20	13/05 – 29/05	17	26/05 – 15/06	20
Summer period	15/06 – 13/09	90	30/05 – 06/09	99	16/06 – 16/09	92

Table 5.1: Time intervals of snowmelt period and summer period 2001-2003.

In the first section, the observed meteorological components and hydrological processes are described to give an overview of the annual and monthly variability. As well, the seasonal variation of the conditions that determine the hydrology, such as soil moisture, the thawing of the active layer and changes in storage capacity, is discussed here. In section 5.2 measured and simulated hydrographs of snowmelt runoff and summer runoff caused by storm events are discussed. Different methods to simulate snow pack ablation are compared in section 5.3. Annual water balances are calculated for each year using different methods. These results are presented in section 5.4. The year 2001 is used furthermore to reveal model sensitivities that are shown in section 5.5, and the reproduction of hydrological processes is discussed in more

detail. In the last section, simulation results of discharge are presented for different climate change scenarios.

For simulation purposes, the time series are divided into the period of snowmelt runoff and summer runoff as shown in Table 5.1. The snowmelt simulation is started 10 hours before the first positive air temperatures were recorded. The end of snowmelt or the beginning of summer period is defined as the lowest record of discharge after the snow pack has ablated completely. The end of the summer period is marked by the end of the measured discharge when the instruments were taken out of the flume station before freeze-up.

It should be noted that every term discussed in this study is subject to uncertainties and should be interpreted carefully. As described in previous sections, observational data underlie instrument restrictions; simulated data, first of all, give evidence of the quality of model simulations rather than reveal the truth; and calculated values, as well, can only be as reliable as their sources and the assumptions should be included in the interpretation. However, these uncertainties are of a different order of magnitude and are the subject of this study as well.

5.1 Observed meteorological variables and hydrological processes

The years 2001 to 2003 differ considerably in terms of hydrological and meteorological components. This is especially interesting for a model application because it reveals the model's capacity to deal with changing conditions and still reproduce the hydrological processes correctly.

First of all, the water balances, as depicted in Figure 5.1, show the differences in the yearly amount of water that enters and leaves the watershed. For this diagram, measured data are used for the rain, snow, and discharge components. Evapotranspiration is calculated with the energy balance approach as described in chapter 4.2. The storage equals the residual term of the input (rain and snow) minus the output (discharge and evapotranspiration). Thus, the storage term also includes the sum of errors caused by measurement uncertainties.

It should be noted that in 2003, all values are calculated until the cumulative evapotranspiration achieves negative values. This is done because the ceasing of the discharge occurs 6 days after freeze-up started. This unusual occurrence is discussed later in this section.

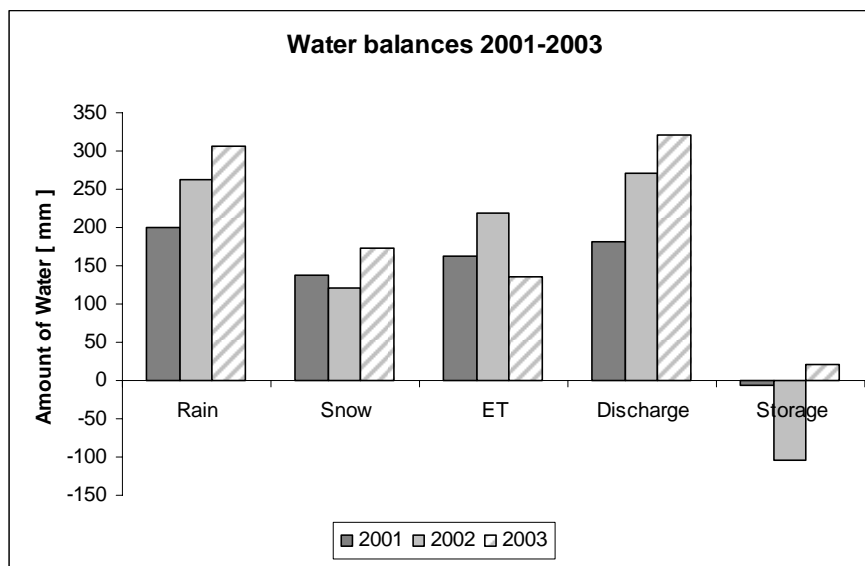


Figure 5.1: Water balance components 2001-2003. Rain, snow, and discharge are based on measured data. Evapotranspiration is calculated using the energy balance method.

In 2001 to 2003, the mean annual precipitation amounts to 337 mm, 384 mm, and 479 mm, respectively. Runoff accounts for 54%, 71% and 67% of the water budget. The rate of evapotranspiration of the water budget is 48%, 57% and 28%. In each year, the snow pack is a

major source that adds water to the system. For the years of this study it accounts to 33-41% of the total amount of water added.

The storage term, calculated as the residual term, shows large differences from year to year. Whereas in 2001 and 2003 the change in storage is small and ranges within the expected spread, the 2002 loss in storage amounts to 105 mm, which demands further clarification. This is discussed in more detail in section 5.4.

In Arctic regions, where runoff formation is highly influenced by the underlying permafrost, several factors determine the seasonal characteristics of runoff formation. This applies in particular to the evolution of the water table, the advancing depth of the active layer and the fluctuating conditions for evapotranspiration. This, in turn, determines the soil moisture content, and respectively the storage capacity of the soil.

WOO et al. (1983a and 1990) describe a typical seasonal cycle of the above-mentioned components in arctic environments: When snowmelt starts, the soil is completely frozen and thawing of the upper layer does not start before the snow cover has ablated completely. Due to the high amount of water released from melt, there is a moisture gain during the snowmelt period followed by a decline during the dry post-melt days. The initial thaw of soil is rapid, but slows down as the depth of thaw increases. Ground thaw seldom begins simultaneously on all parts of a slope because the snow cover disappears unevenly. Areas with a thin snow pack become bare first and therefore have earlier soil thawing. Consequently, there are considerable spatial variations in thaw depth during the melt period. This is further complicated by uneven thaw rates of different soil materials.

Evapotranspiration rates are highest directly after snowmelt, but can achieve considerable amounts during snow ablation, as well. BOIKE et al (2003) show that evapotranspiration consumes about 30% of the net energy in Ivotuk, Alaska, during snow ablation. In early summer, evapotranspiration is favored by a high soil moisture content. From then on, evapotranspiration leads to a depletion in the overall soil moisture content (WOO et al. 1983c). The suprapermfrost water table declines and a non-saturated zone develops extensively in most basins. In addition, continued thawing of the active layer increases its storage capacity, which allows it to absorb most of the low rainfall without yielding immediate runoff. However, rainfall events are often able to increase the soil moisture storage. The authors point out that moisture in the active layer is subject to perennial redistribution. During rain fall and surface flow events, moisture content at the near-surface level rises quickly but afterwards, good drainage and evaporation reduce the moisture equally

as fast. The surface layer therefore experiences moisture fluctuations during the thaw period. As the frost table descends, the ground ice melts and becomes a source of water to the saturated zone. Freeze-up terminates the hydrologically active season, with the first negative temperatures usually occurring in early September. As snowfall commences and the active layer freezes, streamflow and evapotranspiration cease or become practically insignificant. Other than snow accumulation and redistribution by drifting, the only hydrologic activities are the migration of water vapor in the active layer and snow pack.

In the Imnavait watershed, 2001 represents an average year in most hydrologic components, whereas 2002 and 2003 show special characteristics that differ from mean values. 2003 is the wettest of the years with the highest amount of rain and snow, the smallest amount of evapotranspiration and the highest discharge. Conversely, 2002 is characterized by a high amount of evapotranspiration and even a decrease of water stored in the soil as ground ice.

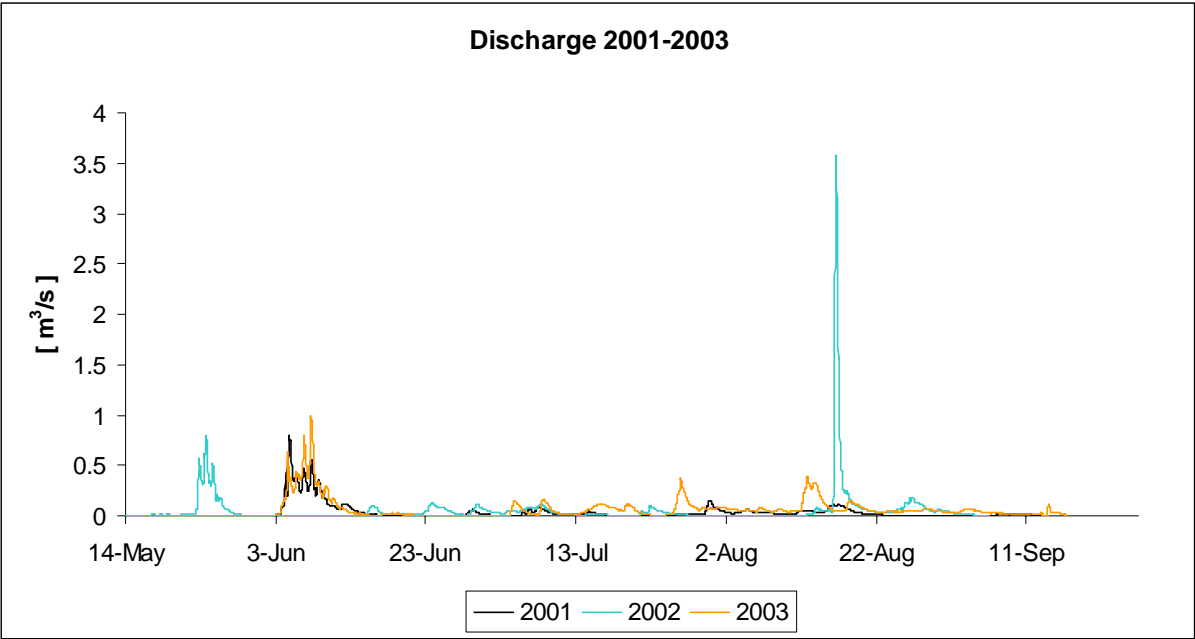


Figure 5.2: Measured discharges at Imnavait Flume station 2001-2003

Figure 5.2 shows the measured discharges of all years from the beginning of snowmelt until freeze-up. While a more detailed analysis, including the comparison to the simulation is given in the following section, it should be stated here that the hydrographs reveal distinct differences each year. The early onset of snowmelt in 2002 causes a considerably earlier start of discharge. And, whereas in 2001 and 2003 the melt discharge is the highest discharge of the year, the peak discharge in 2002 originates from a rain event in late summer.

It has been well documented, that spring runoff as a result of snowmelt is usually the most important annual hydrologic event in arctic watersheds. In small watersheds however, the largest floods on record can, as well, be due to rainfall or a combination of rainfall and snowmelt (WOO 1983a; KANE et al. 1990).

While in temperate regions, baseflow tends to dominate the total discharge, in arctic watersheds that are highly influenced by the underlying permafrost, surface runoff is an important discharge mechanism. This characteristic is evident in Imnavait Creek, where the suprapermafrost groundwater flow ceases rapidly after storm events.

Rain rates are usually small and most of the summer precipitation occurs in the form of drizzle (WOO 1990). Thus, combined with a high infiltration capacity of the porous organic soils at the surface, most of the rain infiltrates and continues as subsurface flow. Nevertheless, surface runoff can occur when excessive water supply raises the water table above the ground surface and prevents further infiltration (WOO 1983a and 1990). In addition, refreezing of melt water seals the soil pores and generates surface runoff. Spring is therefore the time when surface flow is at a maximum. For the time period of this study, maximum rain rates in summer reach values of 9 mm hour⁻¹ in 2001, 9.3 mm hour⁻¹ and 8.7 mm hour⁻¹ in 2002 and 2003 respectively. Still, the connection between the magnitude of rain events and the following runoff is complex and strongly related to the storage capacity of the soil preceding the precipitation. Thus, even major rain events can be infiltrated completely if the antecedent soil moisture conditions are dry. On the other hand, minor rain events can result in a pronounced runoff signal if the storage capacity is limited due to saturated conditions.

This circumstance is evident in each year of this study. For example in 2002 the highest storm event of 9.3 mm hour⁻¹ recorded at the 21st of July results in a barely noticeable rise in runoff, after a 7 hour delay. Instead, a following rain event of 7 mm hour⁻¹ the next day generates a rise in discharge that exceeds the previous one by three times in peak and total amount. Also, the highest discharge on record with about 3.7 m³ s⁻¹ is generated by a precipitation of 6 mm hour⁻¹ about 5 hours earlier. In the first case, a dry period of 7 days preceded the heavy rain event, whereas in the last two cases, precipitation was recorded previously.

2003 has the longest record of discharge, lasting until mid September and exceeding the other years by 3 to 10 days. What makes this fact interesting for hydrological studies are the meteorological circumstances: At the time where the last peak occurs, freeze-up has already started and surface temperatures show negative values for approx. 6 days. Also the energy

balance calculation gives negative values and latent heat flux is directed downward - indicating condensation on the surface - since the freeze-up began. In addition, the last rain event that could have generated the runoff, is recorded 7 days prior to the peak in discharge. Under these circumstances, discharge is unusual, and it should be noted that in the other years, discharge records end before freeze-up begins. An explanation (R. GIECK, personal communication) for this could be, that frazil ice and snow in the channel had blocked the outflow of one of the ponds upstream. When the dam broke, a small flood surge passed through the flume. What confirms this presumption of a transient spike is the fact that a distinct drop in the flow rate to a very low level is recorded 24 hours prior to the spike. This drop could be representative of storage occurring. Short term, transient spikes are recorded regularly during snowmelt when slush flows occur.

So far, several facts are examined that complicate the relationship between rain and a resulting hydrograph signal. Another important mechanism is related to the beaded stream system (see Figure 2.2). Here, the water can be stored intermediately in small ponds that act as small reservoirs. The ponds receive stream water, retain it, and release it only when full. Depending on the soil moisture condition, this may result in a delayed hydrograph signal.

WOO et al. (1983c) refer to another mechanism found in a continuous permafrost region on Cornwallis Island, Canada. Here, subsurface ponding occurs and causes delayed hydrograph signals. The authors elucidate that a frost table with local depressions can pond groundwater, which may be rapidly released when part of the frozen sill is breached by continual thawing. There is evidence in the hydrographs of arctic watersheds that suggest such subsurface ponding, when abrupt hydrograph rises occur in a snow-free non-rainy period. The authors report multiple peaks in the rising hydrograph that are attributed to successive pulses of water from a considerable subsurface pond or from a series of smaller ponds draining during the course of a warm, rainless spell.

The occurrence of delayed hydrograph signals, as well as rising runoff curves where the previous rain event dates back a couple of days, is found in the hydrographs of Imnavait Creek during the course of this study. This gives evidence to the assumption that the above-mentioned mechanisms also occur in this site. Which of the mechanisms plays the major role cannot be concluded from the existing data used in this study.

As seen in Figure 5.1, different amounts of water leave the basin by evapotranspiration every year. Cumulative evapotranspiration, and daily evapotranspiration rates are shown in Figures 5.3 to 5.8. Priestley-Taylor (ET-PT) values are calculated by the model, whereas energy balance (ET-EB) calculations are done externally because at the time of this study, ET-EB was not yet available in the model.

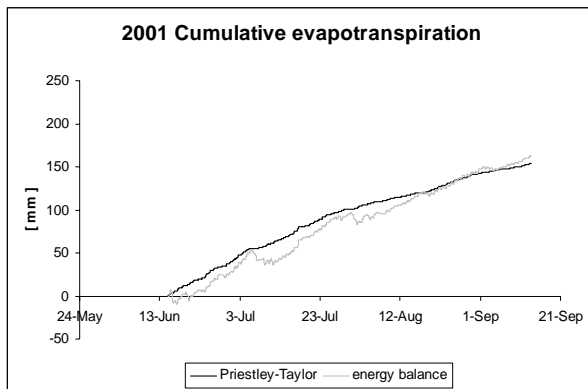


Figure 5.3: Cumulative hourly evapotranspiration 2001. $\alpha_{PT}=0.95$ in the Priestley-Taylor calculation.

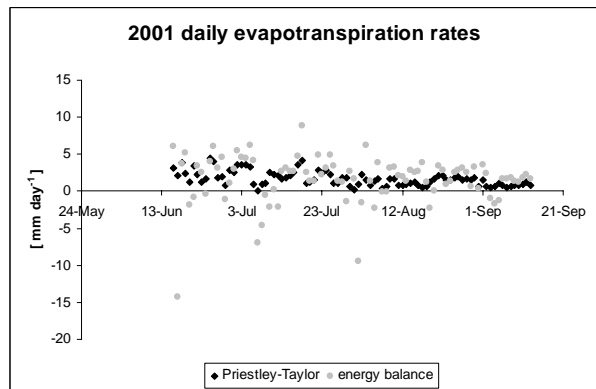


Figure 5.6: Daily evapotranspiration rates 2001.

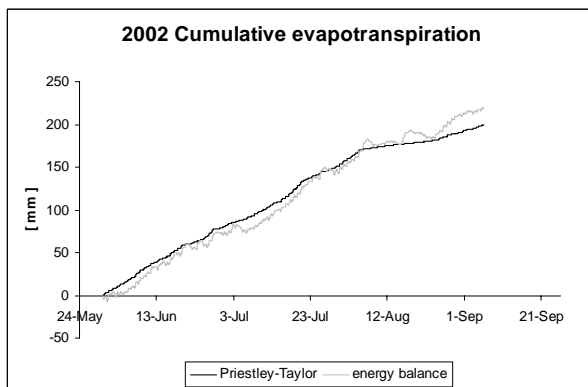


Figure 5.4: Cumulative hourly evapotranspiration 2002. $\alpha_{PT}=0.95$ in the Priestley-Taylor calculation.

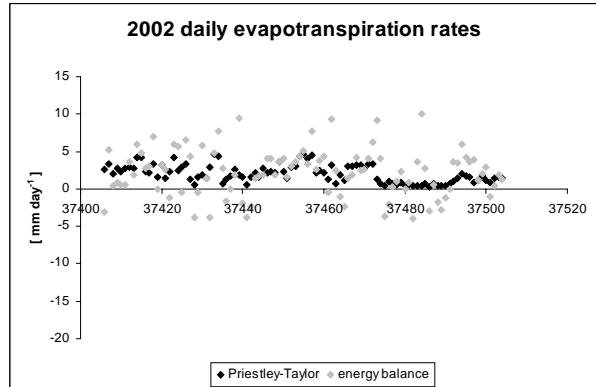


Figure 5.7: Daily evapotranspiration rates 2002.

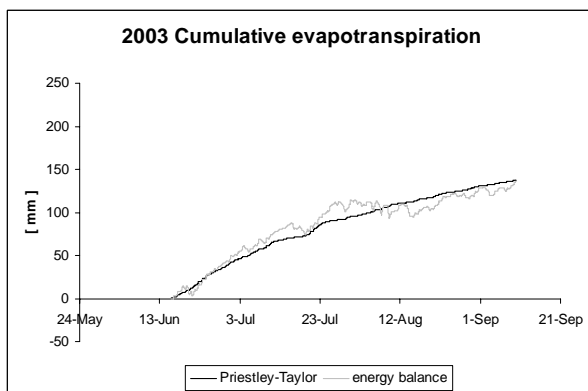


Figure 5.5: Cumulative hourly evapotranspiration 2003. $\alpha_{PT}=0.9$ in the Priestley-Taylor calculation.

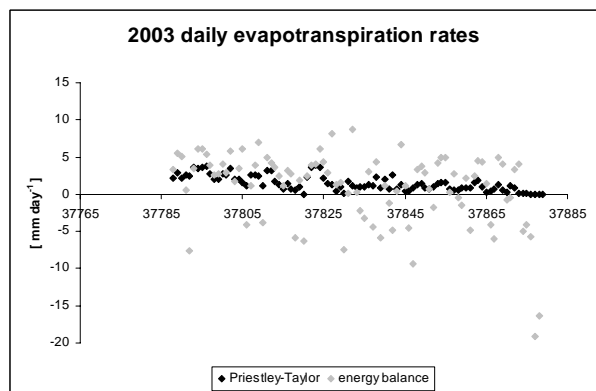


Figure 5.8: Daily evapotranspiration rates 2003.

In the total amount, ET-PT agrees well with the results of ET-EB. For the latter, a constant value of 0.02 m for surface roughness length is used. HINZMAN et al. (1992a) obtained this value by averaging several hundred wind profile measurements. The influence of this parameter on the amount of evapotranspiration is pronounced and illustrated exemplarily in Figure 4.8. The parameter α_{PT} in ET-PT is reported to be, on average, 1.26 for open water and saturated surfaces (PRIESTLEY and TAYLOR 1972), but it can vary considerably from site to site, depending on soil moisture, atmospheric conditions, vegetation and other factors (ROVANSEK et al. 1996). Thus, for best results it should be calibrated to a particular surface type (MENDEZ et al. 1998). In this study, α_{PT} was found to give the best results when set to 0.95 (in 2001 and 2002) and 0.9 (in 2003). KANE et al. (1990) used a value of 0.95 for the Innavaik Creek watershed.

Figures 5.3 to 5.8 illustrate the differences between ET-PT and ET-EB. Whereas fluctuations are pronounced in ET-EB, and fluxes are occasionally directed downward, ET-PT shows a steady rise without major fluctuations. This is due to the fact that both methods differ in the representation of the ventilation term, including the deficit in saturation and the wind component. ET-EB obtains this term from measurements, whereas in ET-PT this term is replaced by a constant. In all years, the ET-EB calculation shows the highest flux rates in early summer when both energy and water are relatively abundant. However, the summer season in 2002 is characterized by unusually high evapotranspiration. The climatic conditions leading to this observation are discussed below.

Table 5.2 shows monthly mean values for different meteorological variables during the simulation periods. Here it becomes evident, that the meteorological conditions were conducive to evapotranspiration in 2002. Considerably higher air temperatures and net radiation caused an early onset of snowmelt and a delay in freeze-up. Therefore, the summer season is prolonged. In June and July, higher net radiation, wind speed and lower humidity sustained high evapotranspiration rates, whereas the air temperature remained below the average. In section 5.4 cumulative evapotranspiration calculations are compared in more detail.

	May	June	July	August	September	Average May-September
Air temperature (2m) in [°C]						
2001	-7.5	7.6	8.9	6.7	2.0	3.5
2002	0.2	5.6	8.6	3.8	3.1	4.3
2003	-3.8	8.7	7.3	4.9	-3.7	2.7
Net radiation (2m) in [W/m²]						
2001	-11.8	122.9	102.1	70.3	43.4*	65.4
2002	74.3	136.3	123.4	58.3	59.8*	90.4
2003	-10.7	132.4	92.5	68.0	42.9*	65.0
Wind speed (3m) in [m/s]						
2001	1.2	1.5	1.6	2.0	1.3	1.5
2002	3.2	3.1	2.9	3.3	2.9	3.1
2003	4.1	2.1	3.4	2.7	3.6	3.2
Humidity (1m) in [%]						
2001	74	80	85	85	86	82
2002	74	77	76	82	79	78
2003	82	70	79	83	84	80
Cumulative liquid precipitation in [mm]						Sum May-September
2001	0 ¹	49.5	96.3	44.7	13.5 ²	204.0 ^{1,2}
2002	11.4	59.4	61.2	139.8	39.6	271.8
2003	0.3 ³	25.2	158.7	110.4	11.4 ⁴	306.0 ^{3,4}

Table 5.2: Monthly averaged meteorological components. Because of missing data: *until 5/9 ¹from 27/4 ²until 24/9 ³from 19/5 ⁴until 16/9

Depending on the energy available, the active layer depth varies each year and can achieve different values depending on the location within the watershed. In addition, the soil water content of the previous year is of importance for the maximum depth of thaw (MDT): If the soil was relatively dry when freeze-up started, less energy is consumed by melting of the ground ice in the following spring, and is therefore available for deepening the active layer. Hence, the specific MDT in each year is not simply correlated to the average air temperature, but also depends on the antecedent soil water content, the extent of snow cover and its course of ablation. From this consideration, the highest MDT would be expected for 2002, where: 1) the average temperature exceeds the records of 2001 and 2003, 2) the summer season is prolonged by an early onset of snowmelt and 3) the storage term in the water budget calculation indicates a considerable loss, itself indicating an enhanced melting of ground ice. An opposing mechanism is related to the exceptionally high evapotranspiration: As the energy is primarily consumed by evapotranspiration, less energy is available for the thawing of the soil. However, CALM grid measurements as described in chapter 3.3 state a minimum MDT of 37 cm for 2002 compared to the other years of this study (2001: 48 cm, 2003: 52 cm). This contradiction is further examined in the following sections.

5.2 Hydrograph Analysis

The classic verification of model performance is to compare measured and predicted hydrograph data. The model performance of discharge calculation generally relies upon three criteria: visual inspection of simulated and measured hydrographs, visual inspection of cumulative discharge between simulated and measured hydrograph, and the Nash-Sutcliffe coefficient (ZHANG et al. 2000). The latter is given by (NASH and SUTCLIFFE 1970):

$$r^2 = 1 - \frac{\sum_{t=1}^n [Q_{sim}(t) - Q_{obs}(t)]^2}{\sum_{t=1}^n [Q_{obs}(t) - \bar{Q}_{obs}]^2} \quad (5.1)$$

where r^2 is the correlation coefficient indicating the quality of simulated discharge ($0 < r^2 < 1$), Q_{sim} is the simulated discharge [$\text{m}^3 \text{s}^{-1}$], Q_{obs} is the measured discharge [$\text{m}^3 \text{s}^{-1}$], and \bar{Q}_{obs} is the average of Q_{obs} .

Measured versus simulated hydrographs for the years 2001 to 2003 are depicted in Figures 5.9 to 5.11. The corresponding cumulative discharges are shown in Figures 5.12 to 5.14. It should be noted that, due to the model configuration, the simulation is split into snowmelt and summer period. Evapotranspiration is only calculated during summer runoff because the energy balance approach was not yet available when this study was conducted. Thus, the Priestley-Taylor method is used during summer, but cannot be used during snowmelt, see chapter 4.2. The initial water table at the beginning of the summer simulation is set to the simulated height of the water table at the end of the snowmelt period. The pronounced step in discharge between both periods is caused by this split.

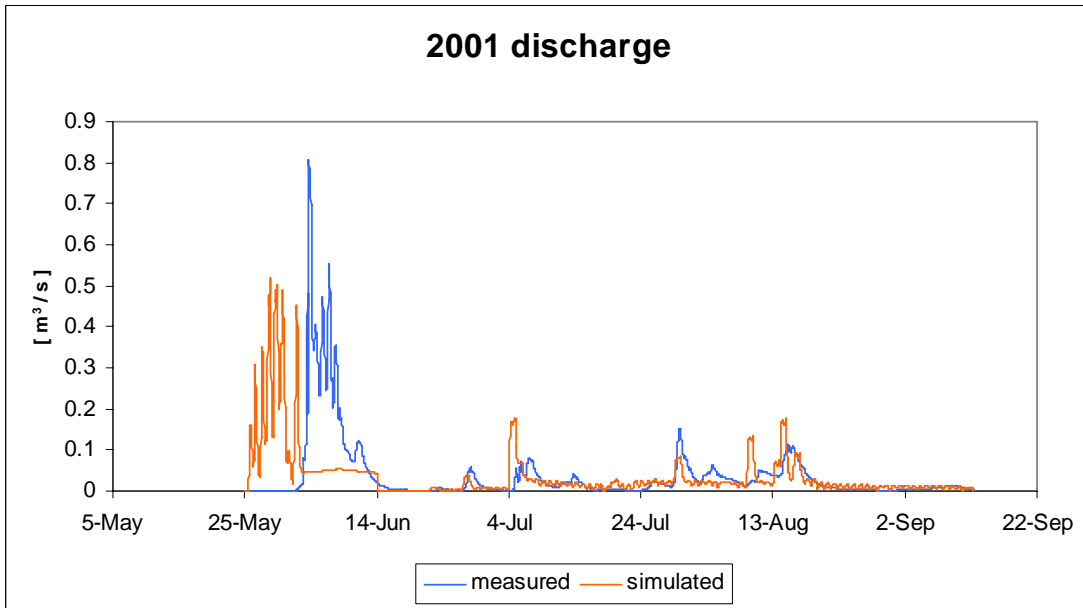


Figure 5.9: Measured and simulated discharge 2001

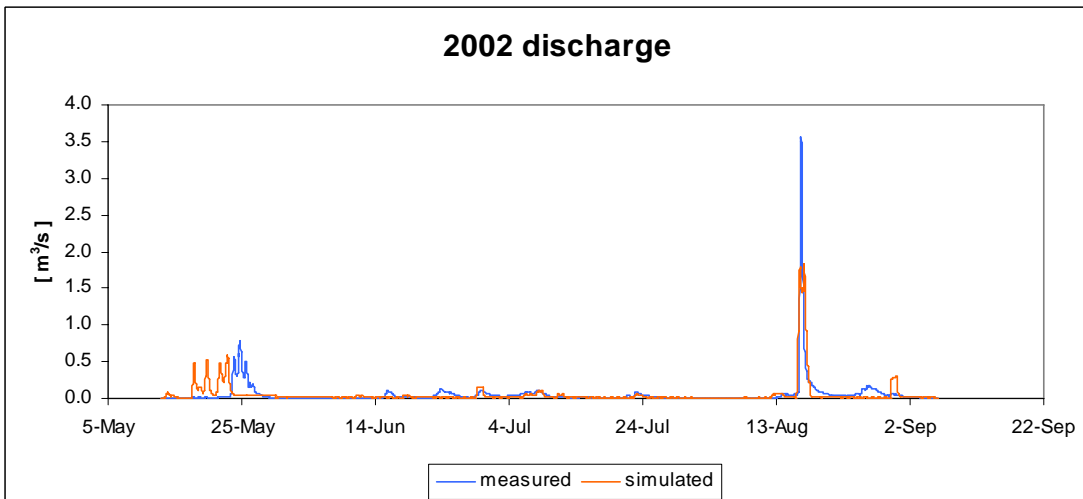


Figure 5.10: Measured and simulated discharge 2002

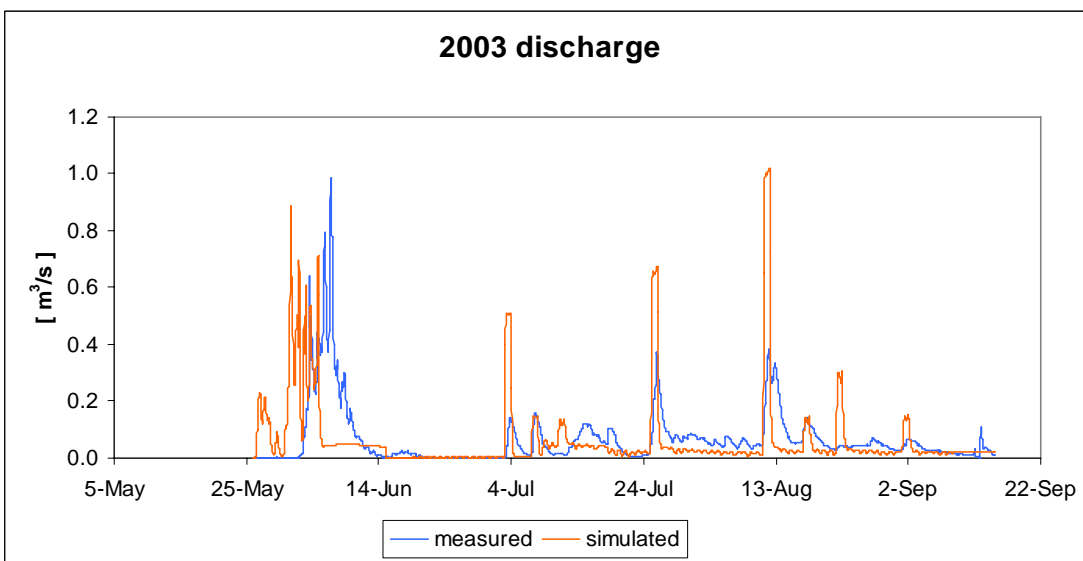


Figure 5.11: Measured and simulated discharge 2003

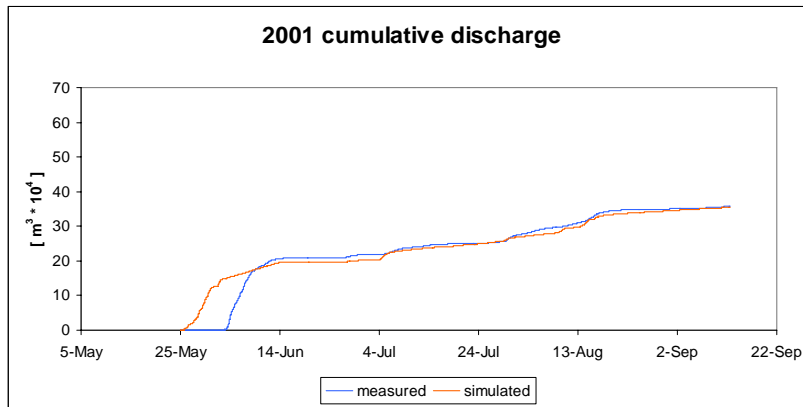


Figure 5.12: Measured and simulated cumulative discharge 2001

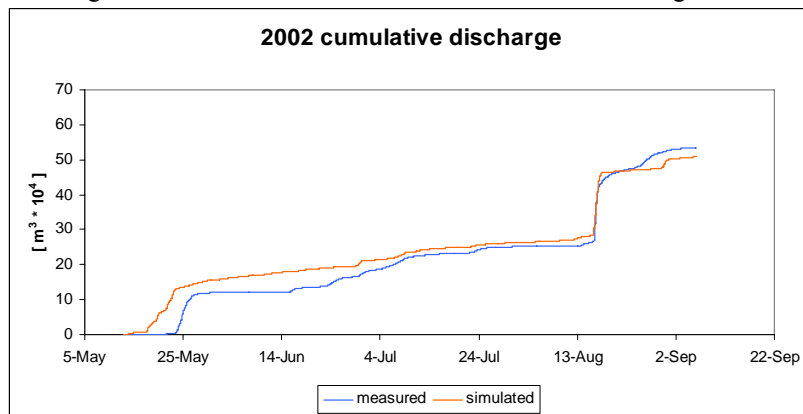


Figure 5.13: Measured and simulated cumulative discharge 2002

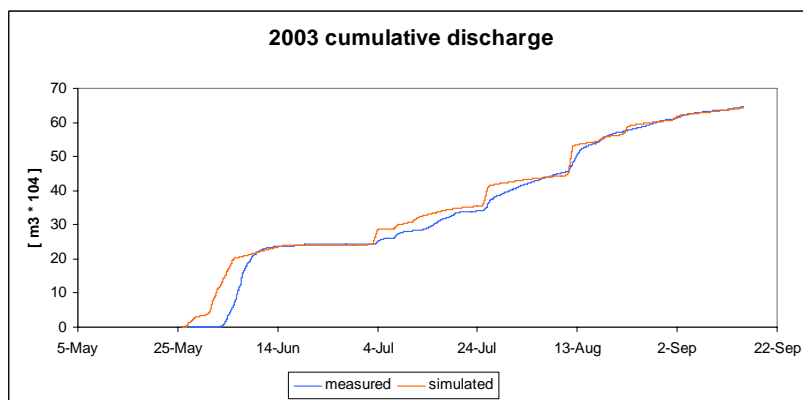


Figure 5.14: Measured and simulated cumulative discharge 2003

Snowmelt discharge

In all simulations, the onset of discharge occurs distinctly earlier than the measured one. The deviation accounts for 7 days in 2001, 4 and 3 days in 2002 and 2003. Whereas this difference to the measured hydrograph is obvious, the total volume of melt discharge is very close to reality. The model predicts that snowmelt runoff is initiated a few days before it actually occurs because an algorithm for snow damming (explained below) has not been incorporated into the model. In addition, the degree-day approach for snow ablation does not consider the increase of the snow density during the course of ablation. Thus, all meltwater contributes directly to simulated runoff, whereas in reality, meltwater percolates through the snow pack

and increases its density. However, KANE et al. (1989) find from measurements in the Imnavait watershed that the reduction of the snow water equivalent reaches up to 80% before stream runoff starts. This reveals that the retarding effect of the snow damming is more important than the intermediate storage of meltwater. Due to the pronounced offset of simulated discharge, the Nash-Sutcliffe coefficient is not calculated for the snowmelt period. Another pronounced difference between measured and simulated snowmelt hydrograph is the decline of base flow after the snow pack has ablated completely. In reality, the base flow ceases completely, whereas in the simulation it remains at a constant value until the snowmelt simulation is terminated. Furthermore, the total amount of snowmelt discharge is overestimated by 30% in 2002. Both deviations can be caused by two different sources of uncertainty: 1) The uncertainties related to the measurements used as an input and 2) errors caused by shortcomings in the model performance. The second source is discussed in section 5.5. An uncertainty of snow water equivalent (SWE) measurements arises from the fact that one snow course is done in the cross-section of the watershed that does not account for the spatial variability of the snow cover. However, HINZMAN et al. (1996) show that, based on a 20-year-record, the transect gives a reliable estimate of the total snow pack.

In this study, an average value for initial SWE is used as an input, whereas in reality the variability of snow distribution with topography is pronounced (KANE et al. 1991b). Accumulation on leeward slopes is about 65% more than on windward slopes, although slope angles differ only by 2-3 degrees (HINZMAN et al. 1996). Snow pack distribution and density affect runoff processes in several ways: because of snowdrifts, snow pack water content can vary by a factor of 2-3 over a distance of a few meters. The result is a fast melt where snow pack is thin, and a development of bare patches, with considerable edge effect around the drifts during melt.

With high winds and low vegetation height, snow in this region of the Arctic tends to blow into valleys and accumulate. As such, it takes considerably longer to melt a snow pack where the depth is substantially increased over a reduced area compared to a pack that is uniformly distributed over the landscape (KANE et al. 1991b). Furthermore, on the valley floor, where snow pack is thick and dense, it functions as a dam, holding until the force of the water overcomes the bonding strength of the snow (HINZMAN et al. 1996). In addition, snow accumulation near stream channels and water tracks yields a higher proportion of runoff and less evaporation than if the snow was uniformly distributed throughout the watershed. From field observations in the Imnavait watershed, snow damming retards snowmelt runoff for

several days and results in higher peak flows than would occur without that process (ZHANG et al. 2000).

WOO (1983a) report that a typical runoff hydrograph for an arctic hillslope shows diurnal fluctuations during this period, reflecting the influence of daily snowmelt cycles. This feature can be found in all snowmelt hydrographs that are presented in this study. However, the signal is more pronounced in the simulated hydrograph where it prevails throughout the melt discharge. This, again, indicates that other processes that would tend to attenuate diurnal fluctuations are not adequately incorporated in the modeling.

Summer discharge

The predicted cumulative discharge agrees well with the measured discharge volume, whereas the simulated hydrograph caused by summer storm events shows perceptible deviation from the recordings: simulated discharge consistently leads site data. Measured peak discharges are usually lower and have a longer recession time. Peak discharges are consistently overestimated in 2003, but show no consistent trend in 2001 and 2002. The Nash-Sutcliffe coefficients, calculated using Equation (5.1), are 0.64, 0.9, and 0.33 for 2001 to 2003, respectively. Here, a weekly average is taken for the simulated and measured discharges. The results are discussed later in this section.

In their model application to Imnavait Creek, STIEGLITZ et al. (1999) also report the fact that modeled summer storm discharge consistently leads site data. Here the lead-time is relatively small and the cause of the problem is the beaded stream system, explained in the previous section.

A constant feature that can be found throughout the entire simulated hydrograph is a wave signal with amplitudes of about 0.004 to 0.01 m³ s⁻¹ and a wavelength of one day. A comparison with the simulated evapotranspiration reveals that the fluctuations in runoff are caused by the diurnal cycle of evapotranspiration. At noon, when evapotranspiration is at a maximum, discharge traverses the minimum of the wave. The signal is more pronounced when evapotranspiration yields higher amounts and vice versa. In reality, this feature cannot be found and, thus, adverts a model sensitivity that is not favorable. For further details see section 5.5.

As mentioned in the previous section, according to the CALM grid data the maximum depth of thaw (MDT) is considerably shallower in 2002 (CALM Homepage). The soil input for the simulation is based on these measurements and an error in this source could have contributed

to the differences between the measured and simulated hydrograph in 2002. Several considerations give evidence of an error in this source: 1) The CALM grid value averages measurements taken primarily in the lower regions of the watershed. As MDT is usually deeper near the ridges (HINZMAN et al 1991a), the CALM value more likely underestimates MDT of the entire watershed. 2) The loss in storage obtained by the water balance calculation indicates a deeper thaw depth. 3) Measurements of the soil water content show that 2001 was a relatively dry year and consequently, in 2002 less energy was consumed to melt near-surface ground ice, but was available for a deeper thaw. 4) The base flow in the 2002 simulated hydrograph is consistently lower than the measured one, which supports the assumption that MDT was deeper than the CALM grid average value.

The general influence of MDT on the simulated hydrograph is discussed in section 5.5.

The base flow of the simulated hydrograph in 2003 shows an overestimation at the beginning, and an underestimation at the end of the summer season. This leads to the assumption that the real storage capacity was higher in the first and lower in the second time period. Hence, a difference between simulated and real storage capacities indicate an insufficiency in the model reproduction of subsurface processes, such as subsurface flow determined by soil properties as well as the evolution of water table height. This supposition is further examined in section 5.5.

The Nash-Sutcliffe coefficients reveal that the model performance differs significantly from year to year. The congruence of measured and simulated discharge is relatively high in 2002, where significant runoff is produced by a single, and exceptionally high rain event. Conversely, r^2 is less impressive in 2003, where precipitation occurs evenly distributed over the summer. This indicates that the model performs well in the quantitative reproduction of storage-related processes, whereas it requires further refinement in the timing of small-scale, short-term processes. These are related to the ponds of the beaded stream system, and the water storage in the active layer. For an exceptionally high rain event as in 2002, the reservoirs of these systems are completely filled and runoff is released immediately. Thus, the adequate reproduction in the model only depends upon the magnitude of the reservoirs. On the other hand, light and continuous rain as in 2003 complicates the processes taking place in the reservoirs: the releasing and recharging processes overlap in time and the following runoff signal is distorted. These processes are more difficult to represent realistically in the model, and the following sections give further evidence of shortcomings in this component.

5.3 Snowmelt Analysis

Snowmelt in the Arctic and Subarctic generally occurs over a short time period, typically less than 10 days. During the course of this study, the snow pack ablates within 6 to 13 days. The 2002 melt concludes the earliest, followed by 2003 and 2001, in that order.

The initial snow water equivalent (SWE) for a given year is obtained from snow survey measurements done each year prior to ablation. An average value is used for the entire watershed. The sources of uncertainty related to SWE measurements were stated previously.

Two methods, the degree-day method (SM-DD) and the energy balance approach (SM-EB) are used to determine the snow pack ablation. The first method is used in the model simulation, whereas SM-EB is calculated separately, because this approach is not yet available. Both methods show a fairly close congruence with the measured snow ablation, but differences occur in the onset of melt as well as in the ablation gradient.

The degree-day method achieves a slightly better congruence than the energy balance method. This is mainly due to the fact that SM-DD is an empirical approach and the curve can be fitted to the measured one by calibration as described in chapter 4.3. Here, values of 2.3 to 3.5 mm day⁻¹ °C⁻¹ for the degree-day melt factor, C_0 , are found to give the best results. The threshold value of air temperature, T_0 , is set between 0 to -1.2°C.

For the energy balance approach, a constant value of 0.0013 m for surface roughness length is used. HINZMAN et al. (1992a) determined this value in the Imnavait watershed from numerous windspeed profiles, and ZHANG et al. (2000) obtained good results in their model application. In this study, the roughness length is not subjected to calibration. Standard values are used for latent heat of fusion and vaporization, water density and specific heat of air.

Figures 5.15 to 5.17 show the simulated and the measured ablation curve for 2001 to 2003.

Using the energy balance method, the onset of melt is delayed in all years, ranging from 2 to 5 days. The alignment of the modeled snowmelt completion with measured data shows no consistent trends. In 2001, the modeled snowmelt is completed earlier than the measured ablation, whereas it is delayed in 2002. In the degree-day method, the onset of snowmelt coincides exactly with the real onset, but the end of snowmelt is delayed in all years.

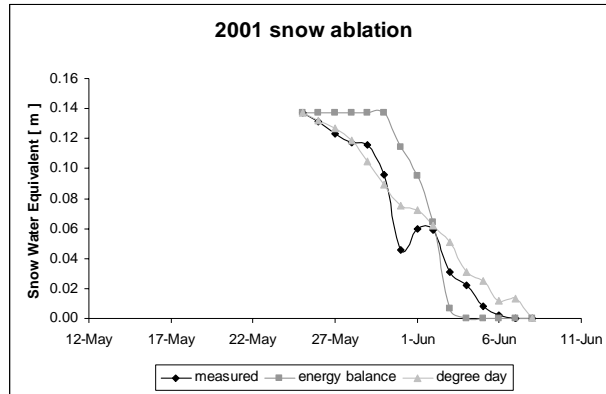


Figure 5.15: Measured and simulated snow ablation 2001

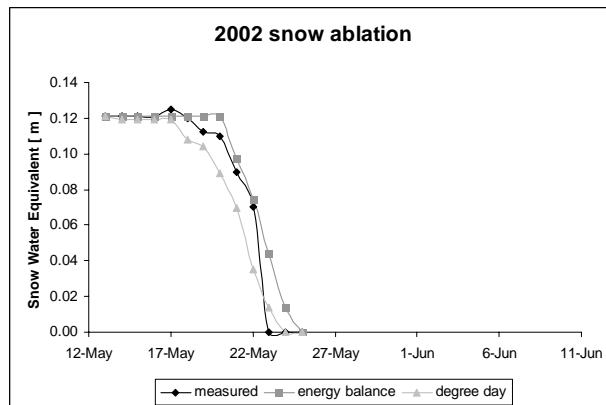


Figure 5.16: Measured and simulated snow ablation 2002

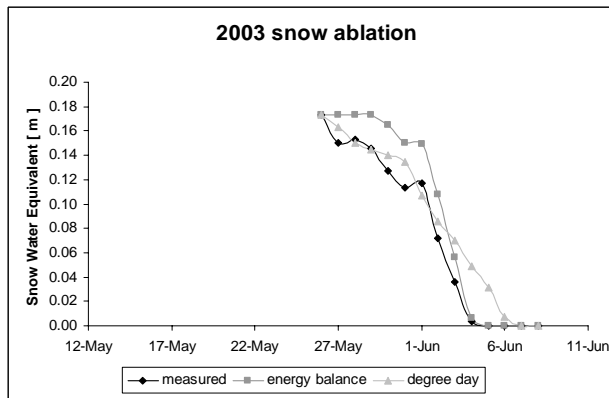


Figure 5.17: Measured and simulated snow ablation 2003

The discrepancy in congruence of the simulation and the recording could partly be due to the fact that field measurements are made daily in the morning, whereas both melt algorithms operate at hourly time steps. In addition, both methods neglect the change in the snow density during the course of ablation. However, the pronounced spatial variability of the snow pack was stated previously, and other studies emphasize that the consideration of snow-cover heterogeneity over complex Arctic terrain provides a better representation of the end-of-winter snow water equivalent, and an improved simulation of the timing and amount of water discharge due to snowmelt.

5.4 Water balance

Hydrologists agree that a water balance is an important part of characterizing the hydrology of a basin. The values of the different components and their ratio can lend insight into the relative amount of water that enters into the suprapermafrost groundwater system / active layer. The accurate reproduction of the amounts of water entering and leaving a basin is crucial to ensure the quality of a model simulation.

A water balance is calculated for each year of the study in order to determine the relative importance of various hydrologic quantities and to estimate the year-to-year changes in basin storage. A water balance equation that has been applied to arctic watersheds (WOO et al. 1983b) is:

$$\Delta S = P - ET - R \quad (5.2)$$

where ΔS is the change in basin storage, P is the precipitation, ET is the evapotranspiration and R is the runoff [mm].

The annual water balance considers the water year to extend between the first lasting September snowfall (when snow would stay for winter) and the arrival of snowfall in the following September.

Calculations are executed for measured and simulated discharge. Three different approaches to determine evapotranspiration are used: The Priestley-Taylor (ET-PT) method is used in the model simulation, energy balance calculations (ET-EB) are done separately by using observational data and finally, evapotranspiration is calculated as the residual term of the water balance (P minus R), neglecting the storage term ΔS .

Cumulative precipitation values are obtained from the meteorological station located in Imnavait Basin. Snow pack values are obtained from surveys done in the spring prior to ablation. Runoff, an integrated value for the basin, is obtained from streamflow measurements at the outlet of the basin for the measured component, and from modeled streamflow for the simulated component.

Tables 5.3 and 5.4. summarize the annual water balance components for 2001-2003.

	Precipitation [mm]		
	SWE	rain	total
2001	137	199.8	336.8
2002	121	263.1	384.1
2003	173	305.7	478.7

Table 5.3: Components of the annual water budget in Imnavait Creek watershed 2001-2003. The source term is precipitation [mm] based on observation for the maximum snow water equivalent (SWE) and rain.

		Runoff [mm]			Evapotranspiration [mm]			Δ Storage [mm]	
		snow-melt	summer	total	<i>P-R</i>	energy balance	Priestley-Taylor	ET=EB	ET=PT
2001	observed	104.8	76.3	181.1	155.7			-7.1	
	simulated	99.2	80.6	179.8	157.0	162.8	153.6	-5.8	3.4
2002	observed	60.5	210.3	270.8	113.3			-105.1	
	simulated	78.6	172.5	251.1	133.0	218.4	199.1	-92.1	-66.1
2003	observed	120	201.6	321.6	157.1			21.4	
	simulated	121	200.1	321.1	157.6	135.7	137	21.9	20.6

Table 5.4: Components of the annual water budget in the Imnavait Creek watershed 2001-2003 in [mm]. The sink terms are runoff, divided into snowmelt and summer runoff for observation and simulation resp., and evapotranspiration obtained from the water balance (precipitation minus runoff) / energy balance and Priestley-Taylor-method.

The source term, summarizing annual solid and liquid precipitation, accounts for 400 mm on average. Streamflow represents the dominant form of basin water loss, averaging 64% of the water budget. Here, snowmelt runoff accounts for 38% of the annual discharge. Water loss due to evapotranspiration achieves considerable amounts with an average of 162 mm per year, taking into account the different calculation methods. The storage term was found to be the most variable, and during the three-year-period of this study accounts for a net change of -91 mm. Here, a negative sign denotes a loss of water stored in the soil during the hydrological year.

Except for the last term, these values are comparable with previous studies in Imnavait Creek basin. KANE et al. (2000) report an annual precipitation value of 340 mm for an eight-year average. Whereas 2001 matches this value, the following two years exceed it considerably. From the same study, the authors determined a percentage of runoff for the water budget of 46%. Thus, the 2001-2003 period achieves higher percentages compared to the average.

The eight-year-record of snowmelt contribution to total runoff amounts to 47%, and evapotranspiration is 54% of the water budget. The latter, being 162 mm during the course of this study, is equivalent to 41% of the water budget. KANE et al. (1990) found evapotranspiration in Imnavait Creek to equal 163 mm on average, ranging from 30% to 60% of the water budget.

In 2001 and 2003, the deficit and excess in storage does not exceed 4% of the annual precipitation. But in 2002, an annual water balance deficit of about 100 mm is encountered. WOO et al. (1983b) report that, for an arctic watershed, the annual change in storage rarely exceeds 10% of precipitation. In another study, HOLECEK et al. (1975) explain an annual water-balance deficit of more than 100 mm as a result of underestimating snow accumulation. As stated previously, SWE measurements include some uncertainty, and are more unsteady than the runoff and precipitation components. Thus, an underestimation of the maximum snow depth in 2002 can have contributed to the unusually high storage term, that is, as the residual term, a sum of all errors. Still, it remains questionable why this should be the case for 2002, but not for the other years of this study. In addition, SWE measurements are reported to achieve high accuracy (L. HINZMAN and P. OVERDUIN, personal communication).

As the storage term is not subject to direct measurements, its magnitude can only be estimated from changes in the soil moisture content. Here, the spatial and temporal variance is large, and average statements contain major uncertainties. However, considering the soil properties in the study area, a loss of 100 mm as encountered in the 2002 calculation, would equal a drop of mean water table height of approximately 20 cm within the hydrological year. Generally, this is a realistic scenario (P. OVERDUIN, personal communication), but several facts indicate an alternate condition: 1) According to the soil temperature records and the CALM grid data, the active layer depth was at least not deeper in 2002 than in 2001, and 2) soil moisture data indicate that, considering the soil water content, 2001 was in fact a drier year than 2002 (P. OVERDUIN 2005, unpublished data).

Generally, simulated runoff agrees well with observations, but in 2002 the snowmelt discharge is overestimated by the model, whereas the adjacent summer runoff is underestimated. The factors that might have led to this discrepancy were already discussed in section 5.2.

Major deviations occur in the evaluation of total annual evapotranspiration between the different methods. Whereas the energy balance and Priestley-Taylor method calculate ET

based upon meteorological observations, ET equal to $P-R$ is obtained as the residual in the water budget, assuming no change in soil moisture. This leads to a considerable discrepancy between this approach and the other two methods. In 2001, however, the storage term is negligible and $P-R$ lies within the range of values obtained by $ET-EB$ and $ET-PT$.

	Seasonal characteristic of the climate state from the beginning of the snowmelt until freeze-up	R/P	ET/P	$\Delta S/P$
2001	average	0.54	0.48	-0.02
2002	warm / wet	0.71	0.57	-0.27
2003	cold / very wet	0.67	0.28	0.04

Table 5.5: Partitioning of annual precipitation (P) into runoff (R), evapotranspiration (ET) and change in soil moisture (ΔS). Precipitation and runoff are based on observations, evapotranspiration is calculated by the energy balance and ΔS is the residual term of the water balance.

The main interest in studying water balances is to explore relationships between the climatic state and the hydrologic response of the watershed. Consequently, an overall climate state for the years of interest is determined for further conclusions. Here, precipitation and temperature are related to mean values obtained from multiple-year-studies mentioned in section 5.1. Consequently, 2001 can be described as an average year, whereas 2002 exceeds the previous year in both variables. Summer 2003 was unusual with lower mean temperatures and exceptionally high precipitation records.

A measure of the significance of runoff relative to annual precipitation is given by the runoff ratio R/P . Corresponding ratios are calculated for evapotranspiration and the storage term. Table 5.5 contains the annual ratios between the source term P and the sink terms R , ET and ΔS , respectively. R/P is generally high in comparison with other climatic regions of the world, but it fits well with values reported for tundra areas (WOO 1983a). A high ratio of runoff to precipitation is typical of impermeable areas, which, in this case, is the frozen ground (WOO et al. 1983b).

The ET/P ratio shows a wider spectrum than R/P , reflecting that evapotranspiration is more closely related to climatic conditions and, thus, subject to their variability. Generally, ET/P is higher in more temperate climate zones.

Considering that the $\Delta S/P$ ratio in 2002 is probably overestimated, the tendency of these values indicate that cold and wet years favor an augmentation in storage, whereas warm conditions support a loss in storage.

DÉRY et al. (2003) present a water budget study for 10 consecutive years for the Kuparuk River Basin, where Imnavait Creek is one of its subbasins. The authors find the component ratios R/P , ET/P and $\Delta S/P$ to equal 0.64, 0.41 and 0.01, respectively. These values are in good agreement with the average values found here: 0.64 for R/P and 0.44 for ET/P . Excluding 2002, $\Delta S/P$ also compares well.

Relating these ratios to the overall climate state, the authors conclude that warm, dry years favor a relatively more intense response of river discharge and evapotranspiration to precipitation input, whereas cool, wet years tend to augment soil moisture. The last statement also applies to the years of this study, with 2003 indicating a net gain in storage, even though the runoff to precipitation ratio is quite high. There is no incidence of warm and dry conditions during the years of this study, but 2002, a relatively warm and wet year indicates that both components, runoff and evapotranspiration are intensified under these conditions. The interesting part for the gain or loss in storage is, however, if the intensified demand for moisture overwhelms any increase in precipitation. This is apparently not the case in 2002, where the increased temperatures seemed to have warmed the soil, inducing a higher contribution of melted ground ice¹ to runoff. Compared to 2001, this year yields a 32% increase in precipitation and a 0.8 °C higher mean summer temperature. From this, it could be concluded, that such a pronounced increase in precipitation still does not compensate for the effect of warming, thus, resulting in a drying of the soil. However, conclusions from a one-year-study should be treated carefully and cannot reveal general coherences. Therefore, model simulations can be helpful to get to more statistically substantiated conclusions.

¹ The correct amount of ground ice is difficult to estimate because the volumetric content does not only depend on the porosity of the soil, but also on water vapor fluxes within the soil. Generally, the ice content is highest at the permafrost / active layer interface and decreases towards the surface.

5.5 Reproduction of hydrological processes in the model

The quality of a hydrological model not only depends on the congruence of simulated and measured discharge, but also on a reliable reproduction of sub-processes within the hydrological cycle. WOO (1990) states that modeling of permafrost hydrological regimes requires good appreciation of the moisture distribution in the active layer. Therefore, sensitivity studies can reveal insufficiencies in the model performance and help to develop more robust routines that resemble the physical processes in nature. Several issues were already discussed in the previous sections, and are summarized in the following part.

Snowmelt

The processes influencing snow ablation and runoff are highly complex. DÉRY et al. (2003) and KANE et al. (2000) investigate the effects of topography and snow redistribution by wind on the evolution of snowmelt in the Upper Kuparuk River basin, to which the Imnavait Creek basin belongs. The authors point out that the consideration of snow-cover heterogeneity over complex arctic terrain provides a better representation of the end-of-winter snow water equivalent, and an improved simulation of the timing and amount of water discharge due to snowmelt. In addition, it leads to an alteration of the energy budget and water budget components. The alterations include a delay and a reduction in the amplitude of the spring melt peak in water discharge, changes in the intensity of evaporative fluxes, and an enhancement of surface sensible and ground heat fluxes that arise from a reduction in total surface albedo. By including various snow processes into a three-layer model, such as snow melting and refreezing, dynamic changes in snow density, and snow insulating properties, they yield a better result than with simpler snow models and a uniform snow cover.

Still, the interactions and physics of snow damming are difficult to model. However, other modeling studies (JORDAN 1991; LYNCH-STIEGLITZ 1994) account for this effect by transferring all meltwater from the shallow snow pack to the deep snow pack instead of delivering the water directly to the surface runoff and/or to ground infiltration.

Evapotranspiration

Evapotranspiration calculations with the Priestley-Taylor (ET-PT) method are in good agreement with the values obtained by the energy balance (ET-EB) approach. Nevertheless, ET-EB is based on physical processes whereas ET-PT includes empirical relationships. Thus, ET-EB is the preferable method and should be included in the model. Simulation results could be further improved by using spatially distributed input values for the α_{PT} coefficient in ET-PT and the roughness coefficient in ET-EB.

As mentioned in section 5.2 the current setting of ET-PT used in the model causes a wave signal in the hydrograph that does not comply with real conditions. The signal is transferred from evapotranspiration to runoff via subsurface flow. Therefore, it is assumed that the evolution of the water table in the model, as described below, causes this discrepancy.

Subsurface flow

The importance of a reliable reproduction of subsurface processes by the model was stated in section 5.2. There are several components that play a crucial role in simulating subsurface processes realistically. If these processes and their interactions are not reproduced by the model, this can lead to modified hydrograph signals.

First of all, the infiltration into the soil determines the way by which water is added to the antecedent soil water content. If rain rates exceed the infiltration capacity, water runs off as overland flow and leads to a faster runoff signal. Water that enters the soil continues its way horizontally and vertically. Its travel speed and direction are mainly determined by the soil properties and the soil water content. Both processes are not taken into account by the model routine, which adds all rain or water from snowmelt instantaneously to the antecedent water table height. As rain rates are usually low and the infiltration capacity of the organic layer is high, the first process is negligible. But neglecting the percolation time of infiltrated water to the water table leads to two distinct zones in the soil: A completely dry zone overlies the completely saturated zone, whereas in reality a transition zone divides the unsaturated zone from the saturated zone.

Second, an uneven and spatially variable thaw depth can cause alternating seepage and re-emergence of water down a slope. This is because areas with a shallower frost table favor surface runoff, but areas with a deeper frost table require a thick zone of saturation to generate surface flow. In addition, the configuration of the frost table is highly dynamic, causing day-to-day changes in water storage capacity in the active layer. Also, a frost table with local depressions can pond groundwater, which may be released when part of the frozen sill is

breached by continual thawing, as already explained in section 5.2. Figure 4.10 gives evidence of the spatial variability the of active layer depth in the Innavaik watershed.

These spatially distributed processes are not taken into account in the model structure, where the thawing of the soil is given by a uniform input. Thus, a physically based thawing routine that considers the spatial variability of soil properties would improve the representation of processes that determine the active layer depth.

Figure 5.18 gives evidence of the influence of the maximum depth of thaw (MDT) on total discharge. Here, an increased MDT of 20 cm is used in the summer simulation 2001. The increase in total runoff indicates that more ground ice melts due to a deeper MDT and leaves the watershed by subsurface flow.

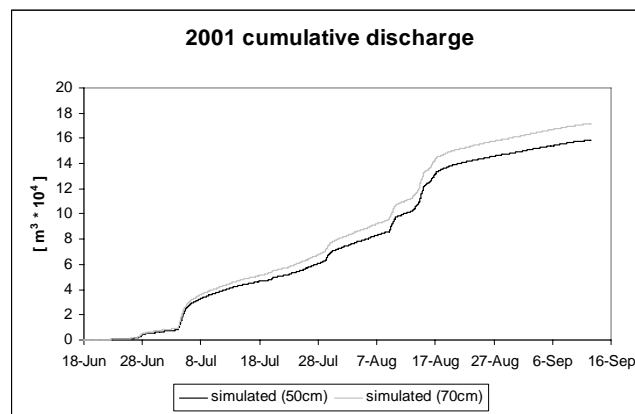


Figure 5.18: Simulated cumulative summer discharge 2001 shows the influence of the active layer depths. Maximum depth of thaw in brackets.

Finally, the above-mentioned processes determine the evolution of the local water table. Figure 5.19 depicts the simulated water table height during summer 2003 at different locations within the watershed.

The sudden rises are due to the instantaneous infiltration routine described above. Comparing the different locations within the watershed, the model reproduces the fact that the ridge sites are generally drier than the valley sites. Here, the water can even pond on flat hilltops due to the low gradient. Model results further suggest that water is dammed in the valley most of the summer; water tracks on the hill slope are generally wetter than adjacent sites; and the soil moisture has decreased at all sites at the end of the summer.

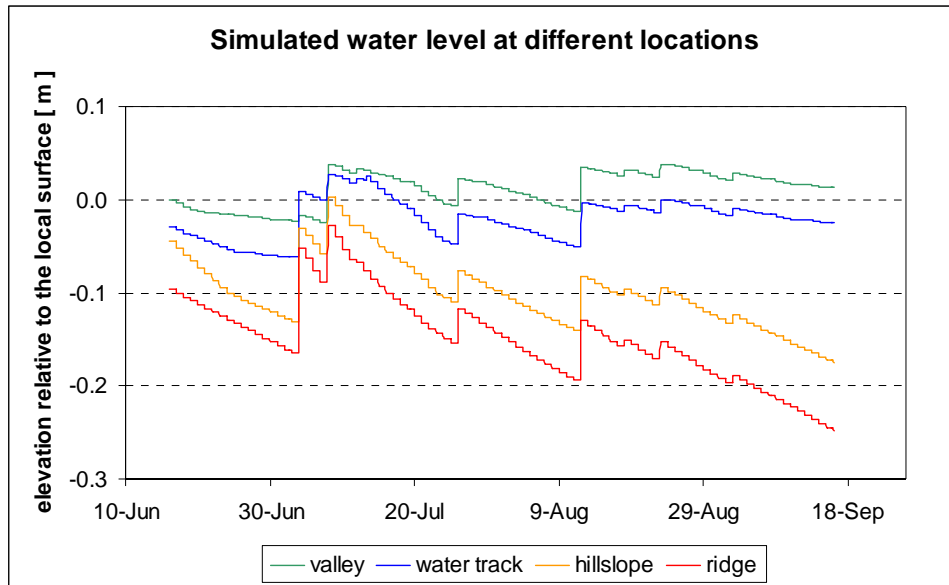


Figure 5.19: Evolution of the water level during the summer simulation 2003 at different locations within the watershed. The unit is distance [m] relative to the local surface elevation.

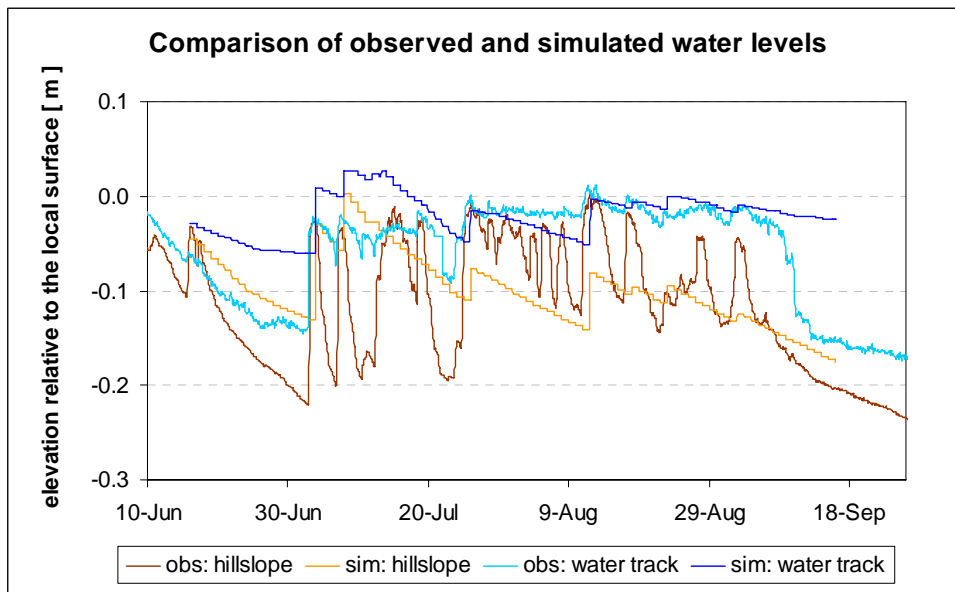


Figure 5.20: Comparison of simulated (sim) and measured (obs) water levels during the summer 2003 at the hillslope and water track. The unit is distance [m] relative to the local surface elevation.

A comparison with soil moisture measurements at qualitatively comparable locations is depicted in Figure 5.20. At the hillslope site, measured responses to precipitation events are larger in amplitude than modeled, but mean values and the rate of water level decrease are well-matched. As in the modeled conditions, the hillslope site is generally drier than the adjacent water track, and undergoes greater fluctuations in water table depth in response to rain events. The soil moisture depletion at the end of the summer is evident in both records.

Figure 5.21 gives evidence of the utmost importance of the initial water table height. Here, the initial water table height is set to the simulated water table height at the end of the snowmelt season.

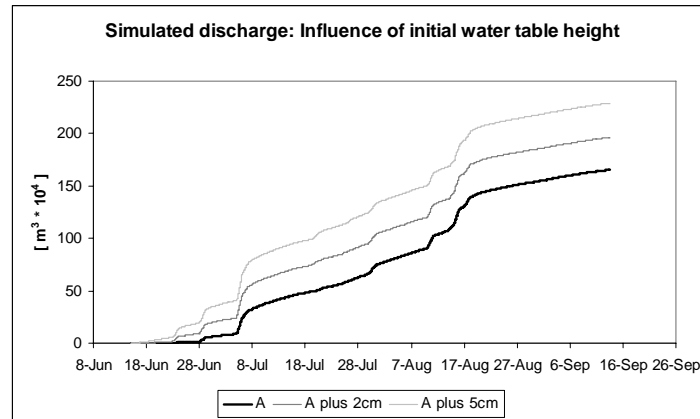


Figure 5.21: Simulated discharge 2001 using different initial water table heights. Case A represents the water table height as simulated at the end of snowmelt discharge.

It should be noted that only the initial state was given as an input, whereas the further evolution of the water table is calculated by the model. Here, a small increase of 2 cm (5 cm) causes an increase of 19% (38%) in the total amount of discharge. On the one hand, the influence of the antecedent soil water content on total discharge is characteristic for arctic watersheds where subsurface processes are limited to the shallow active layer². On the other hand, one should be aware of this sensitivity when calibrating the model.

The initial water table in the snowmelt simulation is set to the surface level, or several mm below, in order to resemble the frozen soil condition. At first sight, this is an unrealistic setting as the amount of water does not increase during winter and definitely does not reach surface elevation when freeze-up starts. However, surface runoff, as it is characteristic for melt runoff, can only be generated in the simulation with the following setting: Horizontal conductivities are set to near zero when the soil is assumed to be frozen. But, in contrast to real conditions, the infiltration capacity cannot be lowered due to the model performance described above. Thus, if the initial water table was set to a low elevation, all meltwater would be infiltrated instantaneously down to the height of the water level, remain here until horizontal conductivities change to unfrozen conditions and finally would be released in a delayed and smoothed hydrograph. Hence, frozen soil conditions can only be represented

² This accounts especially for the Imnavait Creek watershed. In some adjacent watersheds, however, subpermafrost groundwater processes can contribute to surface discharge.

within the current model structure if the initial water table is set close to surface elevation and surface runoff can arise.

Even though an adaptation of the initial water table to the simulated height prior to freeze-up the previous year would have been preferable, other factors limit the magnitude of this deviation from reality. WOO et al. (1983a) state that, throughout the winter, an upward flux of water vapor from the soil increases the ice-free void space in the active layer, so that in spring some meltwater can infiltrate the frozen soil. Yet, infiltration ceases rapidly when the soil pores are sealed by ice. If the ground temperature remains below zero at that time, any meltwater reaching the base of the snow pack would refreeze as basal ice. Even if the frozen materials are initially friable and highly porous, an addition of water quickly freezes in the soil to seal its pores, rendering the frozen zone impermeable to subsequent water percolation (WOO 1990). Hence, the above-mentioned setting of the snow runoff simulation gets closer to the conditions described here. Still, a physically based approach for the thawing of the soil would be preferable, as it could reproduce the fluctuating conditions internally.

Channel flow

A good reproduction of the channel network and its flow characteristics is important to simulate channel runoff realistically. In the Imnavait Creek watershed, the channel network shows distinct characteristics as mentioned in the previous chapters. The most important features are the water tracks along the hillslopes and the beaded stream system. The channel network used as an input for the simulation is described in chapter 4.1. There is a limited amount of parameters in the model that can be changed in order to represent the characteristics of each stream order. Therefore, the approximation to nature is mainly limited to the setting of the channel roughness, the channel width and the percentage of each stream order to the total network.

The small ponds constituting the beaded stream system are not realistically considered in the model because only a singular channel width can be applied to each channel order. The lack of a process that retards runoff by an intermediate storage was described in the previous section. Here, a more complex and spatially distributed representation of the channel network would help to account for the beaded stream system.

The roughness coefficient and channel width used for the water tracks in the model do not account for their complex nature. Figure 2.2 shows that the water tracks actually consist of shrubby corridors. Here, the water flow follows the microtopographic features, such as

tussocks and hummocks. Conversely, the model setting uses well-defined channels that follow the steepest gradient of the Digital Elevation Model.

Figures 5.22 and 5.23 show the influence of the channel roughness parameter on the succeeding runoff signal.

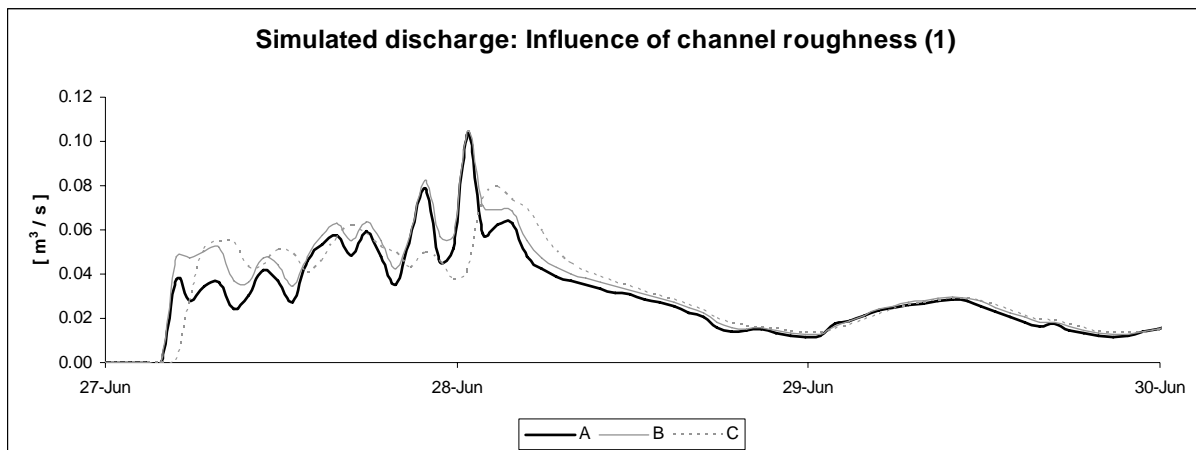


Figure 5.22: Simulated discharges 2001 using different channel roughness parameters. The values for each case are given in Table 5.6.

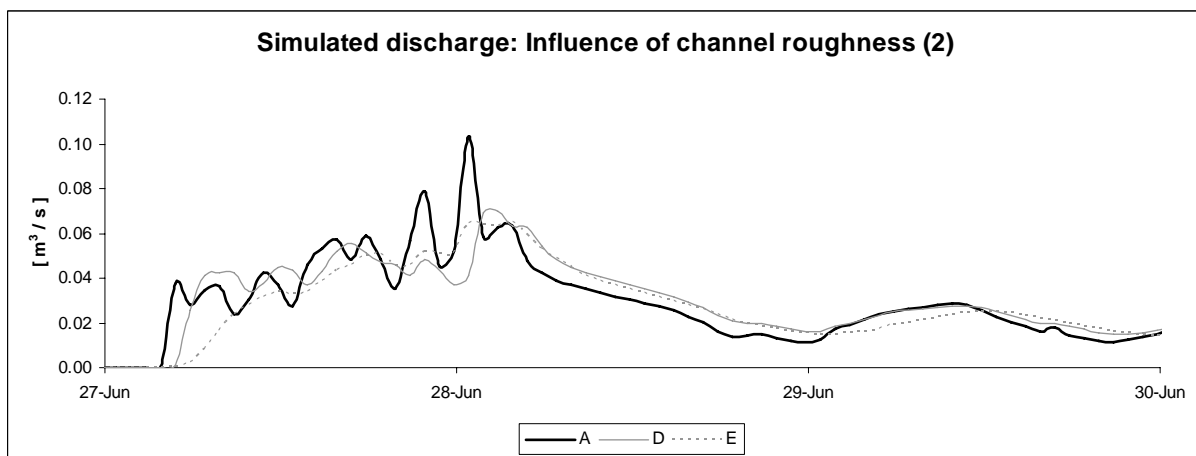


Figure 5.23: Simulated discharges 2001 using different channel roughness parameters. The values for each case are given in Table 5.6.

	A	B	C	D	E
Overland flow	0.3	0.3	0.3	0.9	0.3
Water tracts	0.025	0.05	0.1	0.1	0.45
Order 2	0.02	0.04	0.08	0.08	0.35
Order 1	0.015	0.03	0.06	0.06	0.25

Table 5.6: Channel roughness values for Cases A-E depicted in Figure 5.22 and 5.23.

An increase of Manning's roughness parameter significantly delays the runoff response, whereas the total amount of discharge remains constant. The simulation shows that peaks in the hydrograph are leveled for the high roughness values in case D and E. These values

exceed those found in the literature, see chapter 4.3, but show that a single value is insufficient and cannot account for the complexity of nature.

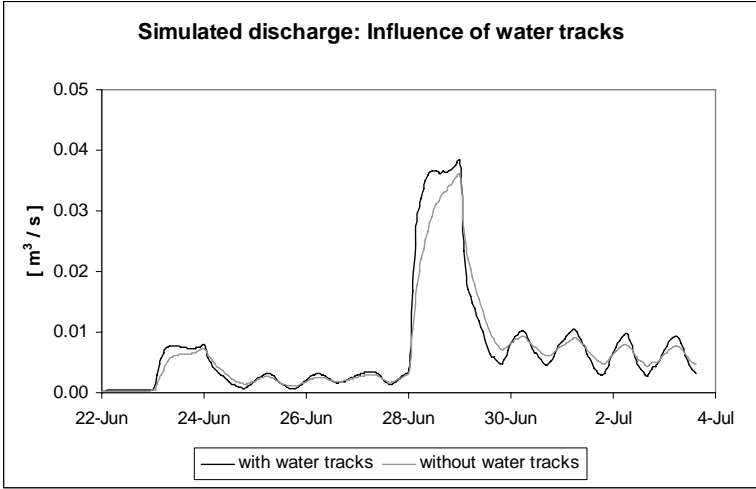


Figure 5.24: Simulated discharge 2001 illustrating the influence of water tracks.

Figure 5.24 shows simulated hydrographs where the effect of water tracks (described in chapter 2.2) on the hydrograph is tested. The first simulation is based on the channel network depicted in Figure 4.2, whereas in the second simulation the water tracks are leveled to the adjacent surface elevation. The simulation indicates that the existence of water tracks accelerates runoff and leads to higher amplitudes in the hydrograph than would be present without them. Still, the efficiency of the water tracks in carrying water down the hill slopes strongly depends on the model parameters mentioned above.

5.6 Simulation of future climate changes

Over the past century, the Arctic has undergone changes in the climatic conditions, as described in chapter 1. A regional warming at rates of 0.5°C or more per decade (DÉRY et al. 2003) has induced changes in other hydrometeorological conditions, including an increase in precipitation (SERREZE et al. 2000), an intensification of freshwater discharge from major rivers (PETERSON et al. 2002), and an enhancement of evaporative fluxes (SERREZE et al. 2000). As Arctic precipitation increases, there remains uncertainty on how the additional input of freshwater will be partitioned into streamflow and evapotranspiration. The interactions are further complicated by a contribution of melted ground ice to base flow when increasing temperatures deepen the active layer during summer. An open question is, whether a change in climate will lead to a drying of the soil, or to wetter conditions.

A modeling study of the carbon dynamics (STIEGLITZ et al. 2000b) suggests that precipitation rates in a warmer environment will be sufficient to counter any increase in evaporative fluxes, thereby leading to wetter soil conditions and enhanced river runoff. On the other hand, HINZMAN and KANE (1992b) conclude from a hydrological modeling study that the impacts of rising air temperatures on soil moisture conditions strongly depend on the amount of precipitation. Superimposing precipitation increases on the warming scenarios would increase soil moisture, evapotranspiration, and runoff. Decreasing precipitation would have the opposite effect.

Global and regional climate models predict different changes for the future climate state of the Arctic depending on the warming scenario as well as on model performance. Regardless the unanswered question, which scenario is the most likely one, changes on the hydrology can be investigated by presuming various conditions and using those as an input to model simulations.

This was done in this study for different climate change scenarios that include a change in three parameters: 1) the summer temperature, 2) the summer precipitation and 3) the maximum depth of thaw; see Table 5.7. It should be noted, that the last has to be given as an input, as the model does not include a physically based routine to calculate this parameter internally.

	A 10	A 20	C 10	C 20	E 10	E 20
Temperature	+ 2 °C					
Precipitation	-	-	+ 8 %	+ 8 %	- 10 %	- 10 %
Maximum depth of thaw	58 cm	68 cm	58 cm	68 cm	58 cm	68 cm

Table 5.7: Climate change scenarios A, C, and E, and their changes in mean summer temperature, precipitation and maximum depth of thaw, relative to the observed conditions in 2001.

2001 is taken as a reference year, i.e. all changes of the above-mentioned parameters are relative to the observed climate conditions in 2001. Thus, changes in the output, such as simulated runoff and evapotranspiration, can be compared to the 2001 simulation based on the real dataset. The year 2001 was chosen because this simulation yielded the best agreements with observational data, see section 5.2.

Simulations were executed only for the summer season, lasting from June 15th until September 13th. As described in the previous sections, model performance during snowmelt was found to have insufficiencies in reproducing important processes and was therefore excluded from this simulation of a changing climate. All scenarios include a constant increase of the temperature profile of 2 °C. Precipitation was increased by 8% in the C-scenarios and decreased by 10% in the E-scenarios. It was held constant in the A-scenarios. The change was distributed equally over the summer season, sustaining the range between minimum and maximum precipitation rates. Two different maximum depths of thaw (MDT) were used as an input. The scenario depths exceed the 2001-value of 48 cm by 10 cm and 20 cm (indicated by “10”, resp. “20” in the notation). In fact, MDT is a function of air temperature, time, soil properties, soil water content and the spatial and temporal extent of snow cover. For a reliable determination of how an increase in air temperature affects MDT, a physically based heat conduction model would be necessary. For simplification, the assumption of a 10 cm (20 cm) deepening of MDT by a 2 °C warming was based on a study by KANE et al. (1991a). The authors determine that a gradual but steady warming of 2 °C would lead to a deepening of 10 cm (20 cm) after 20 years (45 years).

Table 5.8 contains the components of the summer water budget for the different scenarios.

The source term precipitation (P) was given as an input. The sink terms runoff (R) and evapotranspiration (ET) were obtained from model simulation, using the Priestley-Taylor method with an α_{PT} of 0.95. The storage term was calculated as the residual of the water balance as in section 5.4. It should be noted that ΔS and the ratios R/P , ET/P and $\Delta S/P$ cannot be compared directly to the values in Table 5.4 and 5.5 because those include the snowmelt

period components. This is why the storage term in Table 5.8 is significantly greater, indicating that drying of the soil takes place during the summer season while a recharge of soil moisture is associated with the snowmelt period.

	<i>P</i> [mm]	<i>R</i> [mm]	<i>ET</i> [mm]	ΔS [mm]	<i>R/P</i>	<i>ET/P</i>	$\Delta S/P$
Simulated 2001	190.2	80.6	153.6	-44.0	0.42	0.81	-0.23
A10	190.2	82.0	160.0	-51.8	0.43	0.84	-0.27
A20	190.2	84.9	160.0	-54.7	0.45	0.84	-0.29
C10	205.2	92.7	160.0	-47.5	0.45	0.78	-0.23
C20	205.2	95.4	160.0	-50.2	0.46	0.78	-0.24
E10	172.2	64.1	160.0	-51.9	0.37	0.93	-0.30
E20	172.2	67.0	160.0	-54.8	0.39	0.93	-0.32

Table 5.8: Components of the summer water budget (15/06-13/09) in the Imnavait Creek watershed for the 2001 simulation and different climate change scenarios. The source term is precipitation (*P*) based on observation in 2001 and a 8% increase (10% decrease) in the C-scenarios (E-scenarios). The sink terms are runoff (*R*) and evapotranspiration (*ET*) obtained from the simulation. In all scenarios the temperature was increased by 2 °C based on the 2001 observation. The change in storage (ΔS) is calculated as the residual term for each case.

The A-scenarios show that a warming of 2 °C without additional precipitation results in a higher *R/P* and *ET/P* ratio. Here, the increase in runoff is generated by a contribution of ground ice melted due to a deeper MDT. Runoff is significantly higher in the C-scenarios, where an increase in precipitation is presumed as well. The opposite accounts for the E-scenarios, where runoff decreases due to less precipitation input. Here, the additional base flow generated by a deeper MDT cannot compensate for the lack of water supply from precipitation.

Except for the C10-scenario, all scenarios indicate an increased loss in storage compared to the reference amount in 2001. This indicates that an increased precipitation of 8% together with a 10 cm deeper thawing of the soil compensates for the water loss due to higher evapotranspiration. From this, it can be concluded that by keeping the other parameters constant, any further enhancement of precipitation would lead to wetter soil conditions, whereas any further warming would lead to a drying of the soil.

6. Summary and conclusions

This study presents the application of the hydrological model TopoFlow to the Imnavait Creek watershed, Alaska. It summarizes the hydrologically important processes in this arctic basin, and focuses on the modeling of three consecutive years. The model is evaluated for its capability to reproduce the different components of the hydrological cycle. Model simulations are done for different climate change scenarios to evaluate the impacts on the hydrology.

The years of this study, 2001-2003, differ considerably in terms of hydrological and meteorological components. While 2001 represents an average year, 2002 is relatively warm and wet. 2003 is characterized by relatively cold and wet conditions. Whereas in 2001 and 2003 the melt discharge is the largest runoff event of the year, the peak discharge in 2002 originates from an exceptionally high rain event in late summer. The annual water balances reveal that streamflow represents the dominant form of basin water loss (64% of the water budget). Snowmelt runoff accounts for 38% of the annual discharge. Water loss due to evapotranspiration achieves considerable amounts (28-57% of the water budget), with maximum values in 2002. In 2001 and 2003, the change in storage is small and does not exceed 4% of the annual precipitation. But in 2002, an unusually high deficit of about 20% of the water budget is encountered. Conversely, measurements of soil moisture and the maximum depth of thaw suggest that the net change in storage was in fact not exceptionally high in 2002. This implies that the storage calculation as the residual term of the water balance is relatively unsteady, as it includes the sum of all errors.

In all simulations, the total volumes of melt and summer discharges are very close to measured values. This reveals that the model is generally able to handle the different meteorological conditions and performs quantitatively well. The different components of the water cycle are represented in the model, but several refinements are necessary in the qualitative reproduction of some sub-processes: The onset of discharge from snowmelt occurs distinctly earlier than the measured discharge (3-7 days). This is due to the fact that an algorithm for snow damming has not been incorporated in the model. Furthermore, the simulated summer hydrograph shows perceptible deviation from the recordings: simulated discharge consistently leads site data; measured peak discharges are usually lower and have a longer recession time; peak discharges are consistently overestimated in 2003. These deficiencies are expressed via the Nash-Sutcliffe coefficients: they are 0.64, 0.9, and 0.33 for 2001 to 2003, respectively, for weekly averages of measured and simulated discharge. The good performance in 2002, and the less satisfying one in 2003 reveals that the model requires

further refinement in the small-scale, short-term reproduction of storage-related processes. The deviations can be attributed to the following facts: 1) the channel grid used in the simulation does not consider the ponds of the beaded stream system; 2) the spatial variability of the active layer depth, as well as of meteorological variables, is not represented in the simulation; 3) the instantaneous infiltration used in the modeling does not account for the complex soil moisture distribution in reality.

The snow ablation is simulated with the degree-day and the energy balance method. The degree-day method achieves a slightly better congruence with the measured ablation curve than the energy balance method. Differences occur in the onset of melt as well as in the ablation gradient. Evapotranspiration during summer is simulated using the Priestley-Taylor method. Here, α_{PT} of 0.95 (in 2001 and 2002) and 0.9 (in 2003) give a good agreement with the results obtained by the energy balance approach. Further comparison to the amount of evapotranspiration calculated as $P-R$ (precipitation minus runoff) indicates that this approach is less accurate, because the storage term is neglected.

The model is highly sensitive to the initial height of the water level that is given as an input to start the simulation. This implies that calibration is required and thus, simulations of future climate changes are seen to be difficult. In this study, 2001 is taken as a reference year to achieve comparable results with future climate change scenarios. These include a change in the summer temperature (+2 °C), the summer precipitation ($\pm 10\%$), and the maximum depth of thaw (+10/+20 cm). Results indicate that a warming of 2 °C without additional precipitation results in a higher R/P and ET/P ratio. Here, the increase in runoff is generated by a contribution of ground ice melted due to a deeper thaw depth. Runoff is significantly higher in the scenarios where an increase of precipitation is superimposed over the warming. The opposite accounts for the scenarios where precipitation input is decreased. All scenarios are characterized by an increased loss in storage. This indicates that the enhanced evapotranspiration overwhelms the increase in precipitation and results in a drying of the soil.

Future work

The quality of a hydrological model not only depends on the congruence of simulated and measured discharge, but also on a reliable reproduction of sub-processes within the hydrological cycle. Despite the generally good performance of TopoFlow, further refinement of the following processes could improve the model capabilities: 1) a snow ablation routine that accounts for the intermediate storage by snow damming, and melt water percolation and

refreezing in the snow pack; 2) the consideration of snow heterogeneity within the watershed; 3) the inclusion of an evapotranspiration-routine based on the energy balance approach; 4) a physically based thawing routine that considers the spatial variability of soil properties; 5) a more complex infiltration routine that accounts for vertical water movement through the soil; 6) a more robust subsurface flow routing that diminishes the high sensitivity towards the initial water table; 7) a more realistic reproduction of the channel network that considers intermediate storage by ponds.

Furthermore, an application of the model to larger areas, and areas underlain by discontinuous permafrost would provide more representative results for the entire Arctic.

Finally, the climate change scenarios used in this study are based on the assumption that recently observed changes in the Arctic will continue or increase in the future. Global and regional circulation models, however, suggest that global warming may be accompanied by regional cooling, and that impacts may vary greatly depending on the location (e.g. SAHA 2005). Thus, hydrological simulations based on the meteorological outputs of circulation or downscaling models would provide more reliable results.

References

- Anderson, E.A.** (1976): A Point Energy and Mass Balance Model of a Snow Cover. *NOAA Technical Report NWS 19. US Department of Commerce, National Weather Service: Silver Spring, MD.* 150 pp.
- Anderson, M.G. and Burt, T.P. (Eds.)** (1990): *Process Studies in Hillslope Hydrology.* Wiley: Chichester. 539 pp.
- Ashford, G. and Castledon, J.** (2001): Inuit observation on climate change. *Final report. Internat. Inst. for Sustainable Development.* <http://iisd1.iisd.ca/cas1/projects/inuitobs.htm>, 27 pp.
- Bedient, P.B. and Huber, W.C.** (2002): *Hydrology and Floodplain Analysis. 3rd Edition,* Prentice-Hall Publishing Co. 763 pp.
- Bengtsson, L.** (1984): Snowmelt Induced Urban Runoff in Northern Sweden. *Hydrol. Sci. Journal* 37:263-275.
- Berezovskaya, S., Kane, D.L. and Hinzman, L.D.** (2005): Snowmelt hydrology of a headwater Arctic Basin Revisited. *Eos Trans. AGU, 85(47), Fall Meet. Suppl., Abstract C41A-0195.*
- Bergström, S.** (1976): Development and application of a conceptual runoff model for Scandinavian catchments. *Ph.D. Thesis. SMHI Reports RHO No. 7, Norrköping.*
- Boike, J., Roth, K. and Overduin, P.P.** (1998): Thermal and hydrologic dynamics of the active layer at a continuous permafrost site. *Water Resources Research* 34(3):355-363.
- Boike, J., Hinzman, L.D., Overduin, P.P., Romanovsky, V., Ippisch, O. and Roth, K.** (2003): A comparison of snowmelt at three circumpolar sites: Spitsbergen, Siberia, Alaska. *Proceedings of 8th International Conference on Permafrost, Zurich, Switzerland, 21-25 July 2003:*79-84.
- Braun, L.N.** (1985): Simulation of Snowmelt and Runoff in Lowland and Lower Alpine Regions of Switzerland. *Züricher Geographische Schriften, Geographische Institut der Eidgenössischen Technischen Hochschule: Zürich; Heft 21,* 166 pp.
- Brown, J. and Hinkel, K.** (2000): Circumpolar Active Layer Monitoring (CALM) Network. <http://www.geography.uc.edu/~kenhinke/CALM/sites.html>.
- Broecker, W.S.** (1997): Thermohaline circulation, the Achilles Heel of our climate system: Will man-made CO₂ upset the current balance?. *Science* 278:1582-1588.
- Ciriani, T.A., Maione, U. and Wallis, J.R. (Eds.)** (1977). *Mathematical Methods for Surface Water Hydrology.* Wiley: Chichester. 181-194.
- Chapman, W.L. and Walsh, J.E.** (1993): Recent variations in sea ice and air temperature in high latitudes. *Bull. Amer. Meteor. Soc.* 74:33-47.
- Church, M.** (1974) Hydrology and Permafrost with Reference to Northern America. *Permafrost Hydrology.* 7-19.
- Déry, S., Crow, W.T., Stieglitz, M. and Wood, E.F.** (2003): Modeling snow-cover heterogeneity over complex arctic terrain for regional and global climate models. *Journal of Hydrometeorology*5:33-48.
- Déry, S., Stieglitz, M., Rennermalm, A.K., Wood, E.F.** (2005): The water budget of the Kuparuk River Basin, Alaska. *Journal of Hydrometeorology.* In press.
- Dingman, L.S.** (1973). Effects of Permafrost on Stream Characteristics in the Discontinuous Permafrost Zone of Central Alaska. In: *Permafrost, North American Contribution to the Second International Conference, Washington D.C. National Academy of Sciences.* 447-453.
- Dingman, L.S.** (2002): *Physical hydrology. Prentice Hall 2nd Edition.* 646 pp.

- Drew, M.C.** (1975): Comparison of the effects of a localized supply of phosphate, nitrate, ammonium and potassium on the growth of the seminal root system, and the shoot, in Barley. *New Phytol* 75:479-490.
- Eagleson, P.S.** (1970): *Dynamic Hydrology*. McGraw-Hill. New York. 462 pp.
- Emmett, W.W.** (1970): The hydraulics of overland flow on hillslopes. *Geological Survey Professional Paper* 662-A.
- Foken, T.** (2003): *Angewandte Meteorologie. Mikrometeorologische Methoden*. Springer. 290 pp.
- Garbrecht, J. and Martz, L.W.** (1997): The Assignment of Drainage Direction over Flat Surfaces in Raster Digital Elevation Models. *Journal of Hydrology* 193:204-213
- Groisman, P.Y. and Easterling, D.R.** (1994a): Variability and Trends of Precipitation and snowfall over the Eastern United States and Canada. *J. Climate* 7:184-205.
- Groisman, P.Y. Karl, T.R. and Knight, R.W.** (1994b): Observed Impact of snow cover on the heat balance and the the rise of continental spring temperatures. *Science* 263:198-200.
- Hastings, S.J., Luchessa, S.A., Oechel, W.C. and Tenhunen, J.D.** (1989): Standing biomass and production in water drainages of the foothills of the Philip Smith Mountains, Alaska. *Holarctic Ecology* 12:304-311.
- Hengeveld, H. and Kertland, P.** (1998): An Assessment of New Research Developments Relevant to the Science of Climate Change. *CO2/Climate Report 98-1, Environment Canada, and Climate Change Newsletter* 10(3):3-36. Bureau of Resource Sciences, Australia.
- Herrmann, R.** (1977): Einführung in die Hydrologie. B.G. Teubner Stuttgart. 151 pp.
- Hillel, D.** (1980): *Fundamentals of Soil Physics*. Academic Press. New York. 283 pp.
- Hinzman, L.D., Kane, D., Gieck, R., Everett, K.R.** (1991a): Hydrologic and thermal properties of the active layer in the Alaskan arctic. *Cold Regions Science and Technology* 19:95-110.
- Hinzman, L.D. and Kane, D.L.** (1991b): Snow hydrology of a Headwater Arctic Basin 2. Conceptual Analysis and Computer Modeling. *Water Resources Research* 27(6).
- Hinzman, L.D., Wendler, D., Gieck, R.E. and Kane, D.L.** (1992a) Snowmelt at a small Alaskan arctic watershed 1. Energy Related Processes. *Northern Research Basins Conference, Whitehorse, YT Canada*. 171-197.
- Hinzman, L.D. and Kane, D.L.** (1992b): Potential Response of an Arctic Watershed During a Period of Global Warming. *Journal of geophysical Research* 97:2811-2820.
- Hinzman, L.D., Wendler, D., Gieck, R.E. and Kane, D.L.** (1993). Snowmelt at a small Alaskan arctic watershed: 1. Energy related processes. In: *Proceedings of the 9th International Northern Research Basins Symposium/Workshop, Canada, 1992, Prowse TD, Ommanney CSL, Ulmer K (Eds); (Vol. 1), NHRI Symposium, No. 10. National Hydrology Research Institute: Saskatoon, Saskatchewan*. 171-226.
- Hinzman, L.D., Kane, D.L. and Zhang, Z.** (1995): A spatially distributed hydrologic model for arctic regions. *International GEWEX Workshop on Cold-Season/Region Hydrometeorology. Summary Report and Proceedings. 22-26 May 1995, Banff, Alberta, Canada. Int. GEWEX Project Office Publication. Series, No. 15, Washington, D.C.* 236-239.
- Hinzman, L.D., Kane, D.L., Benson, C.S. and Everett, K.R.** (1996): Energy Balance and Hydrological Processes in an Arctic Watershed. In: *Reynolds, J.F. and Tenhunen, J.D. (Eds.) (1996): Landscape Function and Disturbance in Arctic Tundra. Ecological Studies* 120. Springer. 437 pp.
- Hinzman, L.D. et al.** (2004): Evidence and Implications of recent climate change in northern Alaska and other Arctic regions. *Climate Change XXX*, 48 pp. In press.
- Holtan, K.N. and Overton, D.E.** (1963): Analyses and Application of Simple Hydrographs. *Journal of Hydrology* 2:309-323.

- Holecek, G. R. and Vosahlo, V. M.** (1975): Water balance of three High Arctic nival regimes. *Proceedings Canadian Hydrology Symposium, Winnipeg* 75:448-461.
- Horton, R.E.** (1932): Drainage basin characteristics. *Eos Trans Am Geophys Union* 13:350-361.
- Horton, R.E.** (1945): Erosional development of streams and their drainage basin; hydrophysical approach to quantitative morphology. *Geological Society of America Bulletin* 56:275-370.
- Hupfer, P.** (1996): Unsere Umwelt: Das Klima. Globale und lokale Aspekte. *B.G. Teubner Leipzig*. 296 pp.
- IPCC / McCarthy, J.J. et al. (Eds.)** (2001): Climate Change 2001: Impacts, Adaptation, and Vulnerability. *Cambridge University Press. New York 2001*. 1032 pp.
- Jackson, T.H., Tarboton, D.G. and Cooley, K.R.** (1996): A Spatially-distributed Hydrologic Model for a Small Arid Mountain Watershed. *Working Paper WP-96-HWR-DGT/002, Utah Water Research Laboratory: Logan, UT*.
- Jordan, R.** (1991): A one-dimensional temperature model for a snow cover. *U.S. Army Corps of Engineers, Cold Regions Research and Engineering Laboratory, Special Report 91:16-49*.
- Kane, D.L. and Stein, J.** (1983): Water Movement Into Seasonally Frozen Soils. *Water Resources Research* 19(6):1547-1557.
- Kane, D.L. and Hinzman, L.D.** (1988): Permafrost hydrology of a small arctic watershed. In: *Senneset, K. (Eds) Proc 5th Int Conf Permafrost, Tapir, Trondheim, Norway:590-595*.
- Kane, D.L., Hinzman, L.D. Benson, C.S. and Everett, K. R.** (1989): Hydrology of Imnavait Creek, an arctic watershed. *Holarctic Ecology* 12:262-269.
- Kane, D.L., Gieck, R.E. and Hinzman, L.D.** (1990): Evapotranspiration From a Small Alaskan Arctic Watershed. *Nordic Hydrology* 21:253-272.
- Kane, D.L., Hinzman, L., Zarling, J.** (1991a): Thermal response of the active layer in a permafrost environment to climatic warming. *Cold Regions Science and Techn.* 19(2):111-122.
- Kane, D.L., Hinzman, L.D., Benson, C.S. and Liston, G.E.** (1991b): Snow Hydrology of a Headwater Arctic Basin 1. Physical Measurements and Process Studies. *Water Resources Research* 27(6):1099-1109.
- Kane, D.L., Gieck, R.E., Wendler, G. and Hinzman, L.D.** (1993): Snowmelt at a small Alaskan arctic watershed: 2 Energy related modeling results. In: *Proceedings of the 9th International Northern Research Basins Symposium/Workshop, Canada, 1992, Prowse TD, Ommanney CSL, Ulmer K (Eds); (Vol. 1), NIHRI Symposium, No. 10. National Hydrology Research Institute: Saskatoon, Saskatchewan.* 227-247.
- Kane, D.L., Gieck, R.E., and Hinzman, L.D.** (1997): Snowmelt modeling at a small Alaskan arctic watershed. *Journal of Hydrologic Engineering, ASCE* 2(4):204-210.
- Kane, D.L., Hinzman, L.D., McNamara, J.P., Zhang, Z., and Benson, C.S.** (2000): An Overview of a Nested Watershed Study in Arctic Alaska. *Nordic Hydrology* 31(4/5):245-266.
- Kane, D.L. and Gieck, R.E.** (2001a): Meteorologic and Hydrologic Data Sets for the North Slope of Alaska along the Kuparuk River Watershed 1985-2001. *WERC Homepage*.
- Kane, D.L., Hinkel, K.M., Goering, D.J., Hinzman, L.D. and Outcalt, S.I.** (2001b): Non-conductive heat transfer associated with frozen soils. *Global Planet. Change* 29(3-4):275-292.
- Kane, D.L., Gieck, R.E. and Bowling, L.C.** (2003): Impacts of Surficial Permafrost landforms on Surface Hydrology. In: *Proceedings of the Eighth International Conference on Permafrost, Zurich, Switzerland. July 21-25, 2003.* 507-511.
- Kattenberg, A., Giorgi, F., Grassl, H., Meehl, G. A., Mitchell, J. F., Stouffer, B. R., Tokioka, T., Weaver, A. J. and Wigley, T. M.** (1996): Climate models-projections of future climate. In: *Houghton, J.T et al (Eds.): Climate Change 1995. The Science of Climate Change, Contribution of working group 1 to the second assessment of the Intergovernmental Panel on Climate Change, Chapter 3, Cambridge University Press.* 289-357.

- Krupnik, I.** (2002): Watching ice and weather our way: Some lessons from Yupik observations of sea ice and weather on St. Lawrence Island, Alaska. *In: Krupnik, I. and Jolly, D. (Eds): The Earth is faster now: Indigenous Observations of Arctic Environmental Change. Arctic Research Consortium of the United States, Fairbanks, USA. 156-197.*
- Lilly, E.K., Kane, D.L., Hinzman, L.D. and Gieck, R.E.** (1998): Annual water balance for three nested watersheds on the North Slope of Alaska. *In: Proceedings, 7th International Permafrost Conference, Yellowknife NWT, Canada. 669-674.*
- Liston, G.E.** (1986): Seasonal snow cover of the foothills region of Alaska's arctic slope: a survey of properties and processes. *MS Thesis, University of Alaska, Fairbanks.*
- Lynch-Stieglitz, M.** (1994): The development and validation of a simple snow model for the GISS GCM. *J. Climate 7(12):1842-1855.*
- Maidment, D.R. (Ed.)** (1992): Handbook of Hydrology. *McGraw-Hill. 1400 pp.*
- Mendez, J., Hinzman, L.D. and Kane, D.L.** (1998): Evapotranspiration from a Wetland Complex on the Arctic Coastal Plain of Alaska. *Nordic Hydrology 29(4/5):303-330.*
- McNamara, J.P.** (1997): A nested watershed study in the Kuparuk River basin, Arctic Alaska: stream flow, scaling, and drainage basin structure. *PhD dissertation, University of Alaska, Fairbanks.*
- McNamara, J.P., Kane, D.L. and Hinzman, L.D.** (1998): An Analysis of Streamflow Hydrology in the Kuparuk River Basin, Arctic Alaska: A Nested Watershed Approach. *Journal of Hydrology 206:39-57.*
- Moore, R.D.** (1983): On the use of bulk aerodynamic formulae over melting snow. *Nordic Hydrology 14(4):193-206.*
- Nash, J.E. and Sutcliffe, J.** (1970): River forecasting through conceptual models, Part I: A discussion of principles. *Journal of Hydrology 10:282-290.*
- Nicholls, N. et al** (1996): Observed Climate Variability and Change. *In: Houghton, J.T et al (Eds.): Climate Change 1995. The Science of Climate Change, Contribution of working group I to the second assessment of the Intergovernmental Panel on Climate Change, Chapter 3, Cambridge University Press. 137-192.*
- Nolan, M. and Prokein, P.** (2002): Evaluation of a new DEM of the Putuligayuk Watershed for Arctic hydrological applications. *In: Proceedings of the Eighth International Conference on Permafrost, Zurich, Switzerland. July 21-25, 2003. 833-838.*
- Nuttall, M. (Ed.)** (2005): Encyclopedia of the Arctic. *Routledge. 2278 pp.*
- Ohmura, A.** (1981): Climate and energy balance of the arctic tundra on Axel Heiberg Island. *Water Resources Research 18:291-300.*
- Osterkamp, T.E., Petersen, J.K., Collet, T.S.** (1985): Permafrost thickness in the Oliktok Point, Prudhoe bay and Mikkelson Bay area of Alaska. *Cold regions Science Technology, 11:99-105.*
- Osterkamp, T.E. Viereck, L., Shur, Y., Jorgenson, M., Racine, C., Doyle, A. and Boone, R.** (2000): Observations of thermokarst in boreal forests in Alaska. *Arctic, Antarctic, Alpine Research 32(3):303-315.*
- Oswood, M.W., Everett, K.R. and Schell, D.M.** (1989): Some physical and chemical characteristics of an arctic beaded stream. *Holarctic Ecology 12:290-295.*
- Overpeck, J., Hughen, K., Hardy, D., Bradley, R., Case, R., Douglas, M., Finney, B., Gajewski, K., Jacoby, G., Jennings, A., Lamoureux, S., Lasca, A., MacDonald, G., Moore, J., Retelle, M., Smith, S., Wolfe, A. and Zielinski, G.** (1997): Arctic Environmental Change of the last four centuries. *Science 278:1251-1256.*
- Peterson, B. J., Holmes, R. M., McClelland, J. W., Vörösmarty, C. J., Lammers, R. B., Shiklomanov, A.I., Shiklomanov, I. A. and Rahmstorf, S.** (2002): Increasing river discharge to the Arctic Ocean. *Science 298:2171-2173.*

- Price, A.G., and Dunne, T.** (1976). Energy balance computations of snowmelt in a subarctic area. *Water Resources Research* 12(4):686-694.
- Priestley, C.H.B. and Taylor, R.J.** (1972): On the assessment of Surface Heat Flux and Evaporation Using Large-Scale Parameters. *Monthly Weather Review* 100:81-92.
- Reynolds, J. and Tenhunen, J.D. (Eds.)** (1996): Landscape Function and Disturbance in Arctic Tundra. *Ecological Studies* 120. Springer. 437pp.
- Romanovsky, V., Burgess, M., Smith, S., Yoshikawa, K. and Brown, J.** (2002): Permafrost Temperature Records: Indicators of Climate Change. *EOS, Transactions, American Geophysical Union*. 83(50):589-594.
- Rouse, W.R., Mills, P.F. and Stewart, R.B.** (1977). Evaporation in high latitudes. *Water Resources Research* 13(6):909-914.
- Rovaneck, R.J., Hinzman, L.D. and Kane, D.L.** (1996): Hydrology of a tundra wetland complex on the Alaskan Arctic Coastal Plain. *U.S.A. Arctic and Alpine Research* 28(3):311-317.
- Saha, S. K.** (2005): The influence of an improved Soil Scheme on the Arctic Climate in a RCM. *PhD. Alfred-Wegener-Institut für Meeres- und Polarforschung.*
- Serreze, M.C., Barry, R.G. and Walsh, J.E. (1995)** : Atmospheric Water Vapor Characteristics at 70°N. *Journal of Climate* 8:719-731.
- Serreze, M.C., Wals, I., Chapin, F., Osterkamp, T, Dyurgerov, M, Romanovsky, V., Oechel, W., Morison, J., Zhang, T and Barry, R.** (2000): Observational evidence of recent change in the Northern High-latitude environment. *Climate Change* 46:159-207.
- Stieglitz, M., Hobbie, J., Giblin, A. and Kling, G.** (1999): Hydrologic modeling of an arctic tundra watershed: Toward Pan-Arctic predictions. *Journal of geophysical research* 104(D22):507-518.
- Stieglitz, M., Ducharne, A., Koster, R. and Suarez, M.** (2000a): The impact of detailed snow physics on the simulation of snow cover and subsurface thermodynamics at continental scales. *Journal of Hydrometeorology*. 228-242.
- Stieglitz, M., Giblin, A., Hobbie, J., Williams, M. and Kling G.** (2000b): Simulating the effects of climate change and climate variability on carbon dynamics in Arctic tundra. *Global Biogeochem. Cycles* 14:1123-1136.
- Stieglitz, M., Déry, S., Romanovsky, V. and Osterkamp, T.** (2003): The role of snow cover in the warming of arctic permafrost. *Geophysical research letters* 30(13):54/1-54/4.
- Vörösmarty, C.J., Hinzman, L., Peterson, J., Bromwich, H., Hamilton, L., Morison, J., Romanovsky, V., Sturm, M. and Webb, R.** (2001): The Hydrologic Cycle and its Role in the Arctic and Global Environmental Change: A Rationale and Strategy for Synthesis Study. *Arctic Research Consortium Fairbanks, Alaska*. 84 pp.
- Walker, D., Binnian, E., Evans, B., Lederer, N., Nordstrand, E. and Webber, P.** (1989): Terrain, vegetation and landscape evolution of the R4D research site, Brooks Range Foothills, Alaska. *Holarctic Ecology* 12:283-261.
- Walsh, J.E., Zhou, X., Portis, D. and Serreze, M.** (1994): Atmospheric contribution to Hydrologic Variations in the Arctic. *Atmos-Ocean* 34:733-755.
- Walsh, J.E.** (2000): Global atmospheric circulation patterns and relationships to Arctic freshwater fluxes. p 21-44. *In: Lewis, E.L. (Ed) (2000): The freshwater budget of the Arctic Ocean. Kluwer Academic Publishers, 623 pp.*
- Weller, G. and Holmgren, B.** (1974): The microclimates of the arctic tundra. *Journal of Applied Meteorology* 13:854-862.
- Woo, M.K.** (1983a) Hydrology of a drainage basin in the Canadian high Arctic. *Annals of the Association of American Geographers* 73:577-596.

Woo, M.K., Marsh, P. and Steer, P. (1983b): Basin Water Balance in a continuous permafrost environment. In: *Proceedings Fourth International Conference on Permafrost, Fairbanks, Alaska.* 1407-1411.

Woo, M.K. and Steer, P. (1983c) Slope Hydrology as Influenced by thawing of the Active Layer, *Resolute N.W.T. Canadian Journal of Earth Science* 20(6):978-986.

Woo, M.K. (1990): Response of Soil Moisture Change to Hydrological Processes in a Continuous Permafrost Environment. *Nordic Hydrology* 21:235-252.

Zhang, Z., Kane, D. and Hinzman, L. (2000): Development and application of a spatially-distributed Arctic hydrological and thermal process model (ARHYTHM). *Hydrological Processes* 14:1017-1044.

Internet references:

CALM: Circumpolar Active Layer Monitoring Network.

<http://www.geography.uc.edu/~kenhinke/CALM/sites.html>.

Intermap Technologies: <http://www.intermap.com/>

NSIDC: National Snow and Ice Data Center.

<http://nsidc.org/data/docs/arcss/arcss015/>

RiverTools: <http://www.rivix.com/>

TopoFlow: <http://instaar.colorado.edu/topoflow/>

WERC: Water and Environmental Research Center.

<http://uaf.edu/water>

Appendix A:
List of symbols

Symbol	Meaning	Unit
A	cross-sectional area	m^2
B	projected length on the plane perpendicular to the flow direction	m
C_a	specific heat of air	$J\ kg^{-1}\ ^\circ C^{-1}$
C_p	specific heat of snow	$J\ kg^{-1}\ ^\circ C^{-1}$
C_0	degree-day melt factor	$mm\ day^{-1}\ ^\circ C^{-1}$
D_e	vapor transfer coefficient for neutral stability	$m\ s^{-1}$
D_h	heat transfer coefficient for neutral stability	$m\ s^{-1}$
D_n	bulk exchange coefficient for neutral stability	$m\ s^{-1}$
D_s	heat exchange coefficient for stable conditions	$m\ s^{-1}$
D_u	heat exchange coefficient for unstable conditions	$m\ s^{-1}$
E	saturation vapor pressure	$mbar$
ET	evapotranspiration	mm
K_s	thermal conductivity of the soil	$W\ m^{-1}\ ^\circ C^{-1}$
$K_{F/T/i}$	hydraulic conductivity of frozen soil / unfrozen soil / soil layer i	$m\ s^{-1}$
L_v	latent heat of vaporization	$J\ kg^{-1}$
L_f	latent heat of fusion	$J\ kg^{-1}$
M_{ET}	water loss due to evapotranspiration	$mm\ per\ time\ step$
M_{SM}	water equivalent of snowmelt	$mm\ per\ time\ step$
N	roughness coefficient for overland flow	$s\ m^{-1/3}$
P	precipitation	mm
P_W	wetted perimeter	m
Q	total amount of flow	m^3
Q_{sim}	simulated discharge	$m^3\ s^{-1}$
Q_{obs}	measured discharge	$m^3\ s^{-1}$
Q_a	energy advected by moving water	$W\ m^{-2}$
Q_c	conductive heat flux	$W\ m^{-2}$
Q_{cc}	cold content of the snow pack	$W\ m^{-2}$
Q_e	latent heat flux	$W\ m^{-2}$

Q_{et}	energy utilized for evapotranspiration	$W m^{-2}$
Q_h	sensible heat flux	$W m^{-2}$
Q_m	energy for melting of the snow pack	$W m^{-2}$
Q_{net}	net radiation	$W m^{-2}$
R	runoff	mm
R_H	hydraulic radius	m
R_i	Richardson number	-
ΔS	change of storage	mm
$S_{j/f/0}$	slope of element j / friction / bed	-
$T_{a/s/z/snow}$	temperature of the air / surface / soil / snow	$^{\circ}C$
T_0	temperature of snow for isothermal conditions	$^{\circ}C$
c	Courant condition	-
e_a	air vapor pressure	mbar
e_s	surface vapor pressure	mbar
g	gravitational constant	$m s^{-2}$
h	snow depth	m
p	atmospheric pressure	mbar
q	flow rate	$m^3 s^{-1}$
q_e	flow rate per unit length	$m^3 s^{-1} m^{-1}$
r^2	Nash-Sutcliffe coefficient	-
t	time	s
Δt_{CF}	time increment used for channel flow	s
Δt_{OF}	time increment used for overland flow	s
Δt_{SF}	time increment used for subsurface flow	s
u	wind speed	$m s^{-1}$
v	flow velocity	$m s^{-1}$
Δx	smallest grid scale on an element or channel	m
y	water depth	m
z	height / depth	m
z_0	roughness length	m
α_{PT}	alpha-parameter for the Priestley-Taylor equation	-
α_{TD}	alpha-parameter controlling the thaw depth	-
$\delta_{a/w/s}$	density of air / water / snow	$kg m^{-3}$
κ	von Kármán's constant	-

Appendix B:
Eidesstattliche Erklärung

Hiermit versichere ich an Eides statt, daß die vorliegende Diplomarbeit selbständig abgefaßt wurde und keine anderen als die angegebenen Hilfsmittel verwendet wurden.

Berlin, den 10. April 2005

(Imke Schramm)